

A NEW COMPUTER CODE DEVELOPMENT FOR SOLVING FLUID  
TRANSIENT PROBLEMS IN PRESSURIZED PIPELINES

A THESIS SUBMITTED TO  
THE GRADUATE SCHOOL OF NATURAL AND APPLIED SCIENCES  
OF  
MIDDLE EAST TECHNICAL UNIVERSITY

BY

MURAT CENK UYANIK

IN PARTIAL FULFILLMENT OF THE REQUIREMENTS  
FOR  
THE DEGREE OF MASTER OF SCIENCE  
IN  
CIVIL ENGINEERING

JANUARY 2023



Approval of the thesis:

**A NEW COMPUTER CODE DEVELOPMENT FOR SOLVING FLUID  
TRANSIENT PROBLEMS IN PRESSURIZED PIPELINES**

submitted by **MURAT CENK UYANIK** in partial fulfillment of the requirements  
for the degree of **Master of Science in Civil Engineering, Middle East Technical  
University** by,

Prof. Dr. Halil Kalıpçılar  
Dean, Graduate School of **Natural and Applied Sciences** \_\_\_\_\_

Prof. Dr. Erdem Canbay  
Head of the Department, **Civil Engineering** \_\_\_\_\_

Prof. Dr. Zafer Bozkuş  
Supervisor, **Civil Engineering, METU** \_\_\_\_\_

**Examining Committee Members:**

Prof. Dr. Burcu Altan Sakarya  
Civil Engineering, METU \_\_\_\_\_

Prof. Dr. Zafer Bozkuş  
Civil Engineering, METU \_\_\_\_\_

Assoc. Prof. Dr. Elif Oğuz  
Civil Engineering, METU \_\_\_\_\_

Assoc. Prof. Dr. Ali Ercan  
Civil Engineering, METU \_\_\_\_\_

Assoc. Prof. Dr. Kerem Taştan  
Civil Engineering, Gazi University \_\_\_\_\_

Date: 26.01.2023

**I hereby declare that all information in this document has been obtained and presented in accordance with academic rules and ethical conduct. I also declare that, as required by these rules and conduct, I have fully cited and referenced all material and results that are not original to this work.**

Name Last name : Murat Cenk Uyanık

Signature :

## **ABSTRACT**

### **A NEW COMPUTER CODE DEVELOPMENT FOR SOLVING FLUID TRANSIENT PROBLEMS IN PRESSURIZED PIPELINES**

Uyanık, Murat Cenk  
Master of Science, Civil Engineering  
Supervisor : Prof. Dr. Zafer Bozkuş

January 2023, 177 pages

The water hammer phenomenon, which occurs as a result of changes in the boundary conditions of hydraulic systems, can cause major and dangerous problems. Opening or closing of the valve component, sudden power loss or pump startup, change of water level in the reservoir, etc. can be examples of these boundary condition changes. These problems must be considered at the design stage of hydraulic pipeline systems in order to predict and prevent dangerous results. Since the calculation of water hammer analysis manually is very long and tiring, various software has been developed throughout the world. Within the scope of this study, a computer program has been developed to analyze the time-varying flows in hydraulic systems and to produce solutions to possible problems with the help of simulation. The program, which is coded in the C Sharp programming language, is created in the Visual Studio platform. The primary purpose of the program is to find fast and practical solutions to reduce the negative impact of water hammer phenomena that may occur in hydraulic systems. In this program, the characteristics method is used to solve the equations of time-varying flow. The accuracy and reliability of the program are provided since the results of the sample studies tested on the program are similar to the results in the literature. It is hoped that this program, which is ready to use, would

be improved by becoming more comprehensive with new boundary conditions and additions in the future.

Keywords: Pressurized Pipeline Systems, Fluid Transients, Water Hammer, Boundary Conditions, Software Development

## ÖZ

### **BASINÇLI BORU SİSTEMLERİNDE ZAMANA BAĞLI DEĞİŞEN AKIM PROBLEMLERİNİ ÇÖZMEK İÇİN YENİ BİR BİLGİSAYAR KODU GELİŞTİRİLMESİ**

Uyanık, Murat Cenk  
Yüksek Lisans, İnşaat Mühendisliği  
Tez Yöneticisi: Prof. Dr. Zafer Bozkuş

Ocak 2023, 177 sayfa

Hidrolik sistemlerde, sınır koşullarda meydana gelebilecek değişimler sonucunda ortaya çıkan su darbesi olayı, büyük ve tehlikeli sorunlara yol açabilir. Bu sınır koşullardaki değişikliklere vana elemanının açılma veya kapanma işlemi, pompalarda yaşanabilecek ani güç kaybı, pompaların devreye alınması, rezervuardaki su seviyesinin değişmesi vb. durumlar örnek olarak gösterilebilir. Su darbesi olayının yaratabileceği tehlikeli durumları öngörebilmek ve önlemek için hidrolik boru sistemlerinin tasarım aşamasında bu sorunun dikkate alınması gerekir. Su darbesi analizlerinin el ile hesaplanması çok uzun ve yorucu olduğu için dünyada çeşitli yazılımlar geliştirilmiştir. Bu çalışma kapsamında da hidrolik sistemlerdeki zamana bağlı değişen akışları analiz edebilmek ve simülasyon yardımıyla olası sorunlara çözüm üretebilmek için bir bilgisayar programı geliştirilmiştir. Visual Studio platformunda oluşturulan bu program C Sharp programlama dilinde kodlanmıştır. Programın birincil amacı hidrolik sistemlerde meydana gelebilecek su darbesi olayının olumsuz etkisini azaltabilmek için hızlı ve pratik çözümler bulmaktır. Bu programda zamana bağlı değişen akışın denklemlerinin çözümünde karakteristikler metodu kullanılmıştır. Programın üzerinde test edilmiş olan örnek

alıřma sonularının, literatürdeki sonu deęerlerine benzer olması programın doęruluęunu ve güvenilirlięini göstermektedir. Kullanıma hazır halde olan bu programın, gelecekte yeni sınır kořullar ve eklemeler ile daha kapsamlı bir hale getirilerek geliřtirilebileceęi ümit edilmektedir.

Anahtar Kelimeler: Basınlı Boru Sistemleri, Zamana Baęlı Deęiřen Akım, Su Darbesi, Sınır Kořullar, Yazılım Geliřtirme



To My Niece Beren Temel

## ACKNOWLEDGMENTS

I would like to express my deep and sincere gratitude to my thesis supervisor, Prof. Dr. Zafer Bozkuş, for his support, advice, criticism, and encouragement during this long thesis process. This work could not have been completed without his guidance.

This study is partially funded as a project by Middle East Technical University Office of Scientific Research Projects Coordination under grant number GAP-303-2021-10687. I would also like to thank my teammate in this project Saber Habibi Topraghghaleh for his friendship and support.

In addition, I would like to thank the committee members of this thesis, Prof. Dr. Burcu Altan Sakarya, Assoc. Prof. Dr. Elif Oğuz, Assoc. Prof. Dr. Ali Ercan and Assoc. Prof. Dr. Kerem Taştan for their contributions to improve the quality of the thesis.

Lastly, I would like to thank my parents Sezer and Afer Uyanık, my lovely sister Esra Temel, and my brother-in-law Berkay Temel for supporting me throughout my master's degree period.

## TABLE OF CONTENTS

ABSTRACT.....	v
ÖZ.....	vii
ACKNOWLEDGMENTS .....	x
TABLE OF CONTENTS.....	xi
LIST OF TABLES .....	xv
LIST OF FIGURES .....	xvi
LIST OF SYMBOLS .....	xxii
CHAPTERS	
1 INTRODUCTION .....	1
1.1 General Statements.....	1
1.2 Previous Studies in Literature .....	2
1.3 Objectives of the Thesis .....	6
1.4 Scope of the Thesis .....	8
2 FORMULATION OF TRANSIENT FLOW.....	9
2.1 Concept of Transient Flow .....	9
2.2 Arithmetic Derivation of the Equations of Transient Flow.....	10
2.3 Fundamental Differential Equations for Transient Flow .....	19
2.4 Method of Characteristics .....	21
2.4.1 Characteristics Equations.....	21
2.4.2 Time Discretization of Compatibility Equations .....	25
2.5 Application of Method of Characteristics in Systems.....	28
2.5.1 Handling Single Pipe .....	28

2.6	Handling Pipes Connected in Series in a Pipeline .....	29
3	BOUNDARY CONDITIONS .....	31
3.1	Reservoir at Upstream Boundary .....	32
3.1.1	Reservoir at Upstream with Constant Head .....	32
3.1.2	Reservoir at Upstream with Variable Head .....	33
3.2	Valve Boundary .....	34
3.2.1	Valve at Downstream .....	35
3.2.2	Valve at Interior Point .....	37
3.3	Downstream Dead End Boundary .....	38
3.4	Single Centrifugal Pump Boundary .....	39
3.4.1	Sequence of Events during Power Failure.....	40
3.4.2	Homologous-Dimensionless Turbopump Characteristics .....	41
3.4.3	Transient Equations for Pump Trip .....	45
3.4.4	Equations for Single Pump Boundary .....	50
3.5	Air Chamber with Orifice Entrance Boundary .....	52
3.6	Surge Tank Boundary .....	56
3.6.1	Simple Surge Tank for Rapid Transient .....	56
3.6.2	Simple Surge Tank for Slow Transient .....	58
3.6.3	Surge Tank with Standpipe .....	61
4	THE SOFTWARE PROGRAM .....	65
4.1	Main User Interface .....	65
4.1.1	Main User Interface Tabs .....	66
4.1.2	Design Canvas .....	69
4.1.3	Message Box .....	69

4.1.4	Properties Panel .....	70
4.2	Minor Interface Windows .....	71
4.2.1	Engineering Library Window .....	71
4.2.2	Initial Conditions Window .....	72
4.2.3	Valve Closure Settings Window .....	73
4.2.4	Pump Settings Window .....	74
4.2.5	Wave Speed Calculator Window .....	75
4.2.6	Reynolds Number Calculator Window .....	76
4.2.7	Friction Factor Calculator Window .....	76
4.2.8	Surge Tank Simulator Window .....	77
4.2.9	Tabular and Graphical Results Window .....	78
4.3	Objects and Properties Windows .....	83
4.3.1	Junction Component .....	83
4.3.2	Pipe Component and Properties .....	84
4.3.3	Reservoir Component and Properties .....	85
4.3.4	Valve Component and Properties .....	86
4.3.5	Dead End Component and Properties .....	87
4.3.6	Pump Component and Properties .....	88
4.3.7	Surge Tank Component and Properties .....	89
4.3.8	Air Chamber Component and Properties .....	90
5	VERIFICATION OF THE PROGRAM .....	91
5.1	Verification for Single Pipe Computations .....	91
5.1.1	Case-1: Single Pipe by Wylie & Streeter (1978) Benchmark .....	91
5.1.2	Case-2: Single Pipe by Wood et al. (2005) Benchmark .....	100

5.2	Verification for Pipes Connected in Series .....	107
5.2.1	Case-3: Pipes in Series by Chaudhry (1979) Benchmark .....	107
5.2.2	Case-4: Pipes in Series by Wylie & Streeter (1978) Benchmark ....	118
5.3	Verification for Surge Tanks .....	129
5.3.1	Case-5: Simple Surge Tank by Cofcof (2011) Benchmark.....	129
5.3.2	Case-6: Surge Tank with Standpipe by Cofcof (2011) Benchmark	138
5.4	Verification for Pump Failure.....	145
5.4.1	Case-7: Pump Failure by Wylie et al. (1993) Benchmark.....	145
6	DISCUSSION.....	155
6.1	Computation Time of the Program .....	155
6.2	Advantages and Limitations of the Program .....	156
6.3	Recommendations.....	160
7	CONCLUSION .....	163
	REFERENCES .....	165
	APPENDICES	
A.	USER GUIDE.....	169

## LIST OF TABLES

### TABLES

Table 3.1 Pump operation zones .....	44
Table 5.1 Tabular comparison at the valve-end for Case-1 .....	98
Table 5.2 Tabular valve closure data for Case-2 by Wood et al. (2005) .....	101
Table 5.3 Tabular comparison at the valve-end for Case-2 .....	106
Table 5.4 The known data for the pipes by Chaudhry (1979) in Case-3 .....	109
Table 5.5 Tabular valve closure data by Chaudhry (1979) in Case-3.....	109
Table 5.6 Tabular H comparison at the end of pipes and reservoir of Case-3.....	115
Table 5.7 Tabular Q comparison at the end of pipes and reservoir of Case-3.....	116
Table 5.8 Given data for the pipes by Wylie & Streeter (1978) in Case-4.....	119
Table 5.9 Tabular valve closure data for Case-4 .....	119
Table 5.10 Tabular H value comparison at the end of pipes and the reservoir for Case-4 .....	126
Table 5.11 Tabular Q value comparison at the end of pipes and the reservoir for Case-4 .....	127
Table 5.12 Tabular comparison of $Y_{\max}$ values for Case-5.....	138
Table 5.13 Tabular comparison of $Y_1$ values for Case-5.....	138
Table 5.14 Comparison of the results for Case-6 .....	144
Table 5.15 Given data for Case-7 as used by Wylie et al. (1993) .....	146
Table 5.16 Tabular comparison of H and Q values at the pump and downstream reservoir for the interval [0 - 4.8] sec., Case 7.....	151
Table 5.17 Tabular comparison of the H and Q values at the pump and downstream reservoir for the interval [7.6 - 10.8] sec., Case-7 .....	152
Table 6.1 The run time data of the benchmark studies .....	156
Table 6.2 Comparison table for features .....	157
Table 6.3 Comparison table for boundary conditions.....	159

## LIST OF FIGURES

### FIGURES

Figure 2.1 A frictionless hydraulic pipeline system that has a sudden valve closure case (Wylie & Streeter, 1978) .....	11
Figure 2.2 Application of momentum equation to the control volume at the transient state (Wylie & Streeter, 1978) .....	11
Figure 2.3 Implementation of continuity in a pipe .....	13
Figure 2.4 Forces acting on pipe caused by water hammer .....	16
Figure 2.5 Transient event in a frictionless system for a period $(4L/a)$ after instant valve closure (Wylie & Streeter, 1978) .....	18
Figure 2.6 Control volume for the implementation of equations of motion and continuity (Wylie & Streeter, 1978) .....	19
Figure 2.7 Characteristic lines in x-t plane .....	23
Figure 2.8 Notations for a nodal solution and characteristics lines .....	25
Figure 2.9 Notations for interior points of a single pipe example .....	28
Figure 2.10 Notations for pipes connected in series .....	29
Figure 3.1 Characteristics lines at the endpoints of an example system .....	31
Figure 3.2 Notations of upstream reservoir boundary with constant head .....	33
Figure 3.3 Notations of upstream reservoir boundary with variable head .....	34
Figure 3.4 Downstream valve boundary and notations of the system .....	35
Figure 3.5 Valve at interior points of the system and notations of the system .....	37
Figure 3.6 Dead-end boundary condition and notations .....	39
Figure 3.7 Polar diagram for $v$ and $\alpha$ (Wylie & Streeter, 1978) .....	43
Figure 3.8 Pump characteristics curve (Suter curves) for speed $N_s=35$ rpm .....	45
Figure 3.9 Grids and notation of the pump boundary with a discharge valve .....	46
Figure 3.10 Linear approximation of the WH curve .....	47
Figure 3.11 Air chamber with an orifice .....	53
Figure 3.12 Simple surge tank .....	57
Figure 3.13 Notations of a system that includes simple surge tank .....	59



Figure 3.14 Free-body diagram for the water in the tunnel (Chaudhry, 1979).....	59
Figure 3.15 Surge tank with standpipe and notations .....	61
Figure 3.16 Free body diagram for standpipe .....	63
Figure 4.1 Main user interface .....	65
Figure 4.2 The view of file tab.....	66
Figure 4.3 The view of design tab.....	67
Figure 4.4 The view of analysis tab .....	67
Figure 4.5 The view of calculators tab.....	68
Figure 4.6 The view of view tab .....	68
Figure 4.7 The view of help tab .....	69
Figure 4.8 Design canvas view .....	69
Figure 4.9 Message box .....	70
Figure 4.10 The view of the properties panel (example for a valve component) ...	70
Figure 4.11 The view of the material library .....	71
Figure 4.12 The view of the liquid library .....	72
Figure 4.13 Initial conditions window .....	73
Figure 4.14 The view of the valve closure setting window .....	74
Figure 4.15 The view of the pump setting window .....	75
Figure 4.16 The view of the wave speed calculator window.....	75
Figure 4.17 Reynolds number calculator window .....	76
Figure 4.18 Friction factor calculator window .....	77
Figure 4.19 Simple surge tank simulator window .....	78
Figure 4.20 The view of the steady-state results window.....	79
Figure 4.21 The view of the tables window (pipe-based tab view).....	80
Figure 4.22 The view of the time chart window .....	81
Figure 4.23 The view of the animation chart window .....	81
Figure 4.24 The view of the air chamber simulator window .....	82
Figure 4.25 The view of the surge tank solution window.....	82
Figure 4.26 The view of components.....	83
Figure 4.27 The view of the junction properties panel .....	84

Figure 4.28 The view of the pipe properties panel .....	85
Figure 4.29 The view of the reservoir properties panel.....	86
Figure 4.30 The view of the valve properties panel .....	87
Figure 4.31 The view of the dead end properties panel .....	87
Figure 4.32 The view of the pump properties panel.....	88
Figure 4.33 The view of the surge tank properties panel .....	89
Figure 4.34 The view of the air chamber properties panel.....	90
Figure 5.1 Configuration of Case-1 and notations by Wylie & Streeter (1978) .....	92
Figure 5.2 Visual design of Case-1 in the canvas .....	93
Figure 5.3 Inputs in the reservoir properties panel for Case-1 .....	93
Figure 5.4 Inputs in the pipe properties panel for Case-1 .....	94
Figure 5.5 Inputs in the valve properties panel for Case-1.....	94
Figure 5.6 Inputs in valve closure settings panel for Case-1.....	95
Figure 5.7 Inputs in the initial conditions panel for Case-1 .....	95
Figure 5.8 The view of the tabular results for Case-1 (0-0.3 sec.) .....	96
Figure 5.9 Graphical illustration of obtained results at the valve end for Case-1 ...	97
Figure 5.10 Graphical comparison at the valve-end for Case-1 .....	99
Figure 5.11 Configuration of Case-2 and notations by Wood et al. (2005) .....	100
Figure 5.12 Visual design of Case-2 in canvas .....	101
Figure 5.13 Inputs in the reservoir properties panel for Case-2 .....	102
Figure 5.14 Inputs in the pipe properties panel for Case-2 .....	102
Figure 5.15 Inputs in the valve properties panel for Case-2.....	103
Figure 5.16 Inputs in the valve closure settings panel for Case-2.....	103
Figure 5.17 Inputs in the initial conditions panel for Case-2 .....	104
Figure 5.18 The view of the tabular results for Case-2 .....	105
Figure 5.19 Graphical illustration of the results at the valve-end for Case-2.....	105
Figure 5.20 Graphical comparison at the valve-end section for Case-2.....	106
Figure 5.21 Configuration of Case-3 and notations by Chaudhry (1979).....	108
Figure 5.22 Visual design of Case-3 in canvas .....	110
Figure 5.23 Inputs in the pipe properties panel for the 1 <sup>st</sup> pipe of Case-3 .....	110

Figure 5.24 Inputs in the pipe properties panel for the 2 <sup>nd</sup> pipe of Case-3 .....	111
Figure 5.25 Inputs in the valve properties panel for Case-3 .....	111
Figure 5.26 Inputs in the valve closure settings panel for Case-3 .....	112
Figure 5.27 Inputs in the initial conditions panel for Case-3.....	112
Figure 5.28 The view of tabular results at the upstream reservoir for Case-3 .....	113
Figure 5.29 The view of tabular results at the valve end for Case-3 .....	114
Figure 5.30 Graphical illustration of the results for Case-3.....	114
Figure 5.31 Graphical comparison for the H values at the valve-end of Case-3..	117
Figure 5.32 Graphical comparison for the Q values at the reservoir of Case-3....	117
Figure 5.33 Case-4 as used by Wylie & Streeter (1978) .....	118
Figure 5.34 Visual design of Case-4 in canvas.....	120
Figure 5.35 Inputs in the pipe properties panel for the 1 <sup>st</sup> pipe of Case-4.....	120
Figure 5.36 Inputs in the pipe properties panel for the 2 <sup>nd</sup> pipe of Case-4 .....	121
Figure 5.37 Inputs in the pipe properties panel for the 3 <sup>rd</sup> pipe of Case-4.....	121
Figure 5.38 Inputs in the valve properties panel for Case-4 .....	121
Figure 5.39 Inputs in valve closure settings panel for Case-4 .....	122
Figure 5.40 Inputs in the initial conditions panel for Case-4.....	123
Figure 5.41 The view of tabular results at the upstream reservoir for Case-4.....	124
Figure 5.42 The view of tabular results at the valve end for Case-4 .....	124
Figure 5.43 Graphical illustration of H and Q values at the valve for Case-4.....	125
Figure 5.44 Graphical comparison for the H values at the valve-end of Case-4..	128
Figure 5.45 Graphical comparison for the Q values at the reservoir of Case-4....	128
Figure 5.46 Configuration of Case-5 by Cofcof (2011).....	129
Figure 5.47 The view of the results in the surge tank simulator for Case-5 ( $Q_{\text{tunnel}}=40 \text{ m}^3/\text{s}$ ) .....	131
Figure 5.48 The view of the results in the surge tank simulator for Case-5 ( $Q_{\text{tunnel}}=25 \text{ m}^3/\text{s}$ ) .....	131
Figure 5.49 The view of the results in surge tank simulator for Case-5 ( $Q_{\text{tunnel}}=40$ $\text{m}^3/\text{s}$ ) with frictionless condition .....	132

Figure 5.50 The view of the results in the surge tank simulator for Case-5 ( $Q_{\text{tunnel}}=25 \text{ m}^3/\text{s}$ ) with frictionless condition.....	133
Figure 5.51 The visual design of Case-5 on canvas .....	133
Figure 5.52 Inputs in the reservoir properties panel for the upstream reservoir of Case-5 ( $Q_{\text{tunnel}}=40 \text{ m}^3/\text{s}$ ) .....	134
Figure 5.53 Inputs in the pipe properties panel for the first pipe of Case-5 ( $Q_{\text{tunnel}}=40 \text{ m}^3/\text{s}$ ).....	134
Figure 5.54 Inputs in the pipe properties panel for the second pipe of Case-5 ( $Q_{\text{tunnel}}=40 \text{ m}^3/\text{s}$ ).....	135
Figure 5.55 Inputs in the surge tank properties panel for the surge tank of Case-5 ( $Q_{\text{tunnel}}=40 \text{ m}^3/\text{s}$ ).....	135
Figure 5.56 Inputs in the initial conditions panel for Case-5 ( $Q_{\text{tunnel}}=40 \text{ m}^3/\text{s}$ ).....	136
Figure 5.57 Graphical illustration of water oscillations in the surge tank for Case-5 ( $Q_{\text{tunnel}}=40 \text{ m}^3/\text{s}$ ) .....	136
Figure 5.58 Graphical illustration of water oscillations in the surge tank for Case-5 ( $Q_{\text{tunnel}}=40 \text{ m}^3/\text{s}$ ) for frictionless condition.....	137
Figure 5.59 Case-6 as used by Cofcof (2011) .....	139
Figure 5.60 Visual design of Case-6 in canvas .....	140
Figure 5.61 Inputs in the reservoir properties panel for the upstream reservoir of Case-6 .....	141
Figure 5.62 Inputs in the pipe properties panel for the 1 <sup>st</sup> pipe of Case-6 .....	141
Figure 5.63 Inputs in the pipe properties panel for the 2 <sup>nd</sup> pipe of Case-6.....	142
Figure 5.64 Inputs in the surge tank properties panel for Case-6.....	142
Figure 5.65 Inputs in the initial conditions panel for Case-6 .....	143
Figure 5.66 Graphical illustration of water oscillations in the surge tank for Case-6 .....	143
Figure 5.67 The pump failure scenario presented by Wylie et al. (1993) .....	145
Figure 5.68 Visual design of Case-7 in canvas .....	146
Figure 5.69 The entered inputs in the pump settings panel for Case-7 .....	147
Figure 5.70 Inputs in valve closure settings panel for Case-7.....	148

Figure 5.71 The view of the tabular results at the pump for Case-7 .....	149
Figure 5.72 Graphical illustration of H and Q values at the downstream side of the pump for Case-7.....	149
Figure 5.73 Graphical comparison of H values at the pump for [0-4.8] sec., Case-7 .....	153
Figure 5.74 Graphical comparison of H values at the pump for [7.6-10.8] sec., Case-7 .....	153
Figure 5.75 Graphical comparison of Q values at the pump for [0-4.8] sec., Case-7 .....	154
Figure 5.76 Graphical comparison of Q values at the pump for [7.6-10.8] sec., Case-7 .....	154
Figure A.1 New project dialog window .....	169
Figure A.2 The design component buttons .....	169
Figure A.3 A sample system drawn in the program .....	170
Figure A.4 Properties of the downstream reservoir .....	171
Figure A.5 Properties of the 2 <sup>nd</sup> pipe .....	171
Figure A.6 Pump setting window .....	172
Figure A.7 Properties of the pump component .....	173
Figure A.8 Initial conditions window and selected time options for the case .....	173
Figure A.9 The steady-state results window .....	174
Figure A.10 The informative pop-up window .....	174
Figure A.11 An example for the results of the case in the tables window.....	175
Figure A.12 An example for the results of the case in the time chart window.....	176
Figure A.13 Animation chart for the case study .....	177

## LIST OF SYMBOLS

### SYMBOLS

A	Pipe Area (m <sup>2</sup> )
A <sub>g</sub>	Valve Opening Area (m <sup>2</sup> )
a	Acoustic Wave Speed (m/s)
B	Pipeline Constant (Allievi Constant)
C <sub>D</sub>	Orifice Discharge Coefficient
C <sub>orf</sub>	Orifice Head Loss Coefficient
C <sup>+</sup> , C <sup>-</sup>	Positive and Negative Characteristics Equations
D	Pipe Diameter (m)
E	Modulus of Elasticity of Pipe Material (GPa)
e	Pipe Wall Thickness (mm)
E <sub>m</sub>	Valve Closure Constant
f	Darcy- Weisbach Friction Factor
g	Gravitational Acceleration (m/s <sup>2</sup> )
H	Piezometric Head (m)
H <sub>b</sub>	Barometric Pressure Head (m)
H <sub>R</sub>	Rated Head of Pump (m)
K	Bulk Modulus of Elasticity of Fluid (GPa)
k	Loss Coefficient for Entrance
L	Pipe Length (m)
m	Polytropic Gas Equation Exponent

$N_R$	Rated Rotational Speed of Pump (rpm)
$P$	Pressure (kPa)
$Q$	Discharge ( $m^3/s$ )
$Q_R$	Rated Discharge of Pump ( $m^3/s$ )
$R$	Resistance Coefficient
$T_R$	Rated Torque for Pump (Nm)
$t$	Time (sec)
$t_c$	Closure Time of Valve (sec)
$V$	Velocity (m/s)
$\forall$	Control Volume ( $m^3$ )
WB, WH	Dimensionless pump Characteristics
$WR^2$	Moment of Inertia of Rotating Parts of Pump ( $Nm^2$ )
$z$	Elevation above Datum (m)
$\gamma$	Specific Weight ( $N/m^3$ )
$\mu$	Poisson's Ratio
$\rho$	Fluid Density ( $kg/m^3$ )
$\sigma_1, \sigma_2$	Axial Unit Stress and Lateral Unit Stress (Pa)
$\xi_1, \xi_2$	Axial Unit Strain and Lateral Unit Strain
$\tau$	Dimensionless Valve Opening
$\omega$	Angular Velocity (rad/sec)





# CHAPTER 1

## INTRODUCTION

### 1.1 General Statements

The water hammer phenomenon is an important unsteady problem that is generally observed in hydraulic systems such as pipeline systems used to distribute the water or penstocks used in hydroelectric power plants (HPP), and it is caused by transient flow. The transient flow is a flow type that occurs with a disturbance in the steady flow because of changes that may occur in the components used in a hydraulic system. In other words, it is caused by changes in boundary conditions. The sudden closure of hydraulic system components such as valve or gate, load rejection, pump trips, power failure for the turbine or pump, a malfunction in turbine flow regulation equipment or valves, sudden changes in the water level of the reservoir, etc. can be counted as the changes at boundary conditions that cause the transient event. These changes can create pressure waves that fluctuate back and forth in the system. These fluctuations may produce extremely high or low pressures on the system, which may be dangerous. These possible situations must be considered at the design stage of systems in order to predict and prevent dangerous results that can be created by a water hammer event. Otherwise, this problem may cause great loss of life and property.

There are many examples of accidents that have caused loss of life and finance in the past resulting from the water hammer phenomenon. According to Adamkowski (2001), a major accident occurred due to the improper operation of valves used for a turbine at the Bartlett Dam and Oneida Hydroelectric Power Plant in the United States, resulting in five deaths. Another example can be given as the Oigawa HPP accident that occurred in Japan. The accident, which occurred in 1950, was a penstock burst. This accident was caused by sudden butterfly valve closure and

resulted in three lives lost and \$500 million in damage, according to Lupa et al. (2022).

Moreover, a severe accident occurred in Sayano-Shushenkaya HPP in Russia in 2009. The accident was caused by a sudden closure of a turbine. Severe damages occurred, and 75 people died as a result of this accident (Seleznev et al., 2014).

## **1.2 Previous Studies in Literature**

Transient event and its effects on hydraulic pipeline systems have been a challenging and vital research topic from the past to the present. Historically, various methods have been developed and used to observe the flow and simulation of the transient event or water hammer. These methods can be counted as graphical, arithmetic, characteristics, algebraic, implicit, linear analysis, and other methods. It may be observed that these methods are used in the literature, especially in the last century.

Joukowski (1900, as cited in Ismaier & Schlücker, 2009, and Chaudhry, 2014) published a report that introduced the basic theory of water hammer after he observed the results of extensive experiments started in 1897. This report also includes the formulation of the wave speed considering the elasticity of water and walls of the pipe, a discussion about pressure wave propagation, and its reflection. In addition, he discovered that the maximum pressure rise could be observed when closure time is equal to or smaller than the ' $2L/a$ ' value where ' $L$ ' and ' $a$ ' represent the pipe length and wave speed, respectively (Chaudhry, 2014).

Allievi (1902, 1903, as cited in Saikia & Sarma, 2006, and Chaudhry, 2014) presented the general theory for the water hammer, and he developed analytical and graphical solutions. Similarly, Bergeron (1935, as cited in Saikia & Sarma, 2006) developed a solution by graphical method. The graphical solution method was a useful and practical technique for designing pipeline systems when computers were not in use.

In the final report of the Boulder Canyon Projects (1940), a comparison was made between the obtained test results for water hammer surges occurred in the penstocks and the theoretical information current at that time (Wood, 1970).

Wylie and Streeter (1967, 1978) developed an approach to solve and simplify the transient flow equations, which contain unsteady flow equations. The name of this approach is the characteristics method which is widely used in this research area today. In their published studies, they described the algebraic and graphical solution methods besides the explanation of the principles and application of the characteristics method. In addition, the equations of boundary conditions and protection devices used in the transient solution were presented. Then, they developed computer codes, which are written in FORTRAN programming language, containing the application of the method of characteristics for systems with various boundary conditions.

The main theory of the method of characteristics and applications in hydraulic systems are also explained in the Applied Hydraulic Transients Textbook by Chaudhry (1979). In addition, explanations of various boundary conditions and developed FORTRAN codes were presented. The developed codes can be used to simulate transient events caused by the closure or opening of a valve, power failure for a pump, and to determine water level oscillations in simple surge tanks.

Karney (1984) developed a computer program to observe rapid transient conditions for large water distribution networks by using the method of characteristics. He provided the reliability of the network program by using numerical experiments data. In addition, the network program can simulate transients in hydraulic systems with various boundary conditions.

Thorley (1991, 2004) presented guidance for preventing the harmful effects of a fluid transient event in a closed conduit, and he gave suggestions to control this undesirable transient event with practical methods. He described a variety of protection or control devices. The usage of these devices is recommended according to problem types. These recommendations vary depending on where the transient

event begins and whether there is an increase or decrease in the initial pressure change.

Izquierdo and Iglesias (2002) developed a computer program to analyze and simulate water hammer phenomena in simple water systems by using mathematical modeling. The name of the developed program is 'DYAGATS'. The characteristics method was used to solve partial differential equations, which are continuity and momentum equations.

Koç (2007) developed a computer code to simulate the transient events in hydraulic pipeline systems by using MATLAB 7.1 programming language. Then he converted the developed code to C# programming language to present a program which has a graphical interface for users. In this program, the characteristics method is used for the solution of momentum and continuity equations. The program can also simulate the transient events in pipeline systems which have various boundary conditions. The program has a mechanism to warn the user in case of incorrect operation which makes it user-friendly.

Afshar and Rohani (2008) proposed an implicit characteristics method to observe the hydraulic transient event in pipeline systems. The aim of this study was to find a solution to the limitations and deficiencies of the traditional characteristics method. Element-wise definition is used for the reservoir, valve, pump equipment, and derivation of corresponding equations. As a result, the study validated the accuracy of the method in valve closure and pump failure cases.

Bozkuş (2008) conducted a water hammer analysis for pipelines between Çamlidere Dam and İvedik Treatment Plant by using the characteristics method. These pipelines are formed by a series of connected pipes which have different properties. For this reason, characteristics method equations that include interpolation features were used in this analysis. A modified FORTRAN code is used for the simulations of transient events which may occur by valve closure scenarios in the pipeline systems. As a result, proper valve closure times were determined for safe operations.

Calamak and Bozkuş (2012) studied protective measures and precautions to prevent the undesired effects of water hammer occurring in the penstock of run-of-river hydropower plants. In this study, a water hammer case in a small hydropower plant caused by instant load rejection was analyzed. In order to compare the results, the case was simulated without protection measurements and with a flywheel, pressure-reduced valve (PRV), and safety membrane separately. A computer program developed by Bentley, named HAMMER, was used for the simulation of the cases in this study which applies the characteristics method to solve the transient flow equations.

Dinçer (2013) studied the water hammer problem in pumped-storage hydropower plants. He simulated different water hammer cases such as transients caused by load rejections of turbine and start-up or shut down of pumps for Yahyalı Hybrit Plant. He investigated these cases with and without surge tank protection devices to compare results. In this study, HAMMER software is used for simulations which use the characteristics method to solve nonlinear partial differential equations. In addition, the obtained results are also given for Yahyalı Hybrit Plant in another study presented by Dinçer and Bozkuş (2016).

Dursun (2013) examined the protection measures that can be used against the water hammer phenomenon that may occur in Yeşilvadi Hydroelectric Power Plant (HEPP). HAMMER Software was used for simulations for various scenarios. He also presented a comparison between the obtained results and the values observed during the operation at Yeşilvadi HEPP.

Dalgıç (2017) developed a code called H-Hammer that can simulate transient flow and water hammer phenomenon. This program uses the characteristics method as the solution method for nonlinear partial differential equations of transient flows. H-Hammer program, which can simulate cases including various boundary conditions and protection devices, runs with some system requirements, such as the support of AutoCAD, Visual Basic, and MS Excel programs. The validation of the program

was provided with comparisons between the obtained results and results in the literature

Topraghghaleh (2020) also developed a software computer program called S-Hammer to be used for the simulation of the transient event. The codes of this program were developed in the Visual Studio platform and written in C# programming language. In this software, the method of characteristics is used to solve transient flow equations. This software can analyze case studies involving various boundary conditions. The validation of the program was provided with comparisons between the obtained results and results in the literature.

### **1.3 Objectives of the Thesis**

This study aims to develop a new computer code that can solve time-varying flow problems in pressurized pipeline systems. The computer program created with these codes is developed to simulate the pressure and flow varieties in the hydraulic pipeline systems designed by the users in a time-dependent manner. In this way, it is aimed that the users or engineers can detect and take precautions against possible problems and damages resulting from the water hammer phenomenon. In the developed program, the characteristics method is selected to use for the solution of the transient flow equations. Also, various boundary conditions are added to this program so that the solution for different scenarios can be observed.

There is a large number of computer programs or created codes that were developed to solve transient problems. One of the objectives of the study is to develop new software which is more user-friendly and has more features compared to previous studies such as Dalgıç (2017) and Topraghghaleh (2020). The comparison between the developed program and recent studies is explained in detail in related sections. The developed program has several advantages and disadvantages compared to the programs or codes developed in previous studies.

The drawing area used in hydraulic system design and fields such as tables and text boxes, where related data can be entered, are available in the program. Accordingly, it is ensured that the program is independent and practical without the need for different external programs. This feature provides great convenience for users. The program is designed to display the simulation results as tables, graphs, and animations.

In the program, the steady-state solution of the system, which is analyzed before the transient state, is also presented to users. This feature is not provided in recent studies, so it is added to the program as a novelty. In addition, wave speed, friction factor, Reynolds number calculator windows, and a library window containing specific properties of commonly used fluid or pipe material types in the literature are added to this program. If the mentioned features and contents are considered, it can be inferred that the program is developed as user-friendly and practical as intended.

This study also aims that the developed program can easily detect the order of the components in the drawn hydraulic system. In other words, if the user adds a new object to any point of the system or deletes an existing object from the system, the program will sort the components and provide a solution, taking this into account. This feature is presented as a novelty not found in recent studies in the literature, such as Dalgıç (2017) and Topraghaleh (2020).

The limitations and deficiencies of the thesis are as follows: The program is developed for only pressurized hydraulic pipeline systems with a single pipe or pipes connected in series. This study does not provide solutions for complex pipe networks, branch pipe connections, and pipes connected in parallel. Quasi-steady friction model is used to solve unsteady flow equations. Horizontal pipeline systems with the same elevation are generally used as benchmarks.

The main goal of this study is to create cheap, reliable domestic software that may be considered as an alternative to the existing commercial programs that may be costly. Wanda Transient and Bentley Hammer software can be examples of these commercial programs.

## **1.4 Scope of the Thesis**

This thesis consists of seven chapters, which are the introduction, formulation of the transient flow, boundary conditions, the software program, verification of the program, discussion, and conclusion.

In Chapter 1, the introduction part, the summary and the importance of the thesis subject were explained. The previous studies about the topic, purpose and scope of this thesis were also mentioned.

Chapter 2 provides the derivation of unsteady pipe flow equations for a compressible fluid and their solution by the method of characteristics (MOC), and applications.

Chapter 3 includes general information and equations for the boundary conditions used in this study.

Chapter 4 includes the main contents and abilities of the developed program. In this chapter, the program is presented with the help of figures containing various windows and panel images.

Chapter 5 contains the verification of the program by using proper case studies in the literature as benchmarks.

Chapter 6, the discussion part, contains a discussion about the calculation time of the program for each benchmark. In addition, this section includes the advantages and limitations of the program, along with recommendations for future studies.

Chapter 7, which is the conclusion part of the thesis, includes the summary of this thesis study in general.

Lastly, the user manual is presented in the appendices section, which is Appendix A.



## **CHAPTER 2**

### **FORMULATION OF TRANSIENT FLOW**

In this section, the transient flow expression, the related differential equations with their derivations, and the method of characteristics (MOC), which is the solution technique used for the equations in this study, will be discussed in general.

#### **2.1 Concept of Transient Flow**

Flows may be considered steady or unsteady according to the flow state. In steady flows, conditions of the flow such as velocity, discharge, and pressure observed at a certain point, are always constant; in other words, they are not time-dependent. On the other hand, in unsteady flows, these properties at a certain point may vary depending on time. In addition, steady flow can also be classified as a special state of unsteady flow. It means that unsteady flow equations must also satisfy a steady flow.

The transient flow expression is generally used to represent the intermediate-stage flow of fluids in pipelines. In other words, the transient flow is the flow that has occurred during the time period observed between the initial steady-state flow and another steady-state flow. It is also known that this transition, which is an unsteady state, is caused by the change in boundary conditions and disturbance of steady flow.

The data obtained from steady-state are important to solve transient flow equations. Because in the calculation and analyzing stage of a transient flow, the data known from the steady-state condition of the system are used as initial values. The following sections will describe more details about the formulation of transient flow and the solution technique of related equations.

## 2.2 Arithmetic Derivation of the Equations of Transient Flow

Two fundamental laws of nature are valid for all types of flows. These laws are conservation of mass and conservation of momentum. Based on this information, it can be inferred that transient flow, which shows unsteady flow characteristics, has two basic equations: momentum and continuity. This study focuses on a one-dimensional solution, so the continuity and conservation of momentum equations are derived just for the x-direction. Eqs. (2.1) and (2.2) represent the continuity and conservation of momentum equations for the x-direction, respectively.

$$\frac{d}{dt} \int_{CV} \rho dV + \int_{CS} \rho(\vec{V} \cdot \vec{n}) dA = 0 \quad (2.1)$$

The mass conservation equation represents the summation of the rate of mass change within the control volume, and the net mass flux across the control surface gives a '0' value.

$$\sum F_x = \frac{d}{dt} \int_{CV} V \rho dV + \int_{CS} V \rho(\vec{V} \cdot \vec{n}) dA \quad (2.2)$$

The conservation of momentum represents that the summation of the forces which act on the control volume equals the summation of the time rate of change of the momentum within the control volume and the net momentum flux across the control surface.

Wylie & Streeter (1978) applied Eq. (2.2) to a control volume in a simple frictionless reservoir-pipe-valve case which is illustrated in Figure 2.1 and Figure 2.2. In this simple idealized scenario, the hydraulic pipeline system includes a constant head upstream reservoir and a downstream valve which is instantly closed. A flow towards the downstream is observed in the system with a velocity of  $V_0$ , then a pressure wave generated by this sudden closure of the valve travels towards the upstream direction. The propagated pressure wave is also called as acoustic wave. The speed of this wave is represented by 'a'.

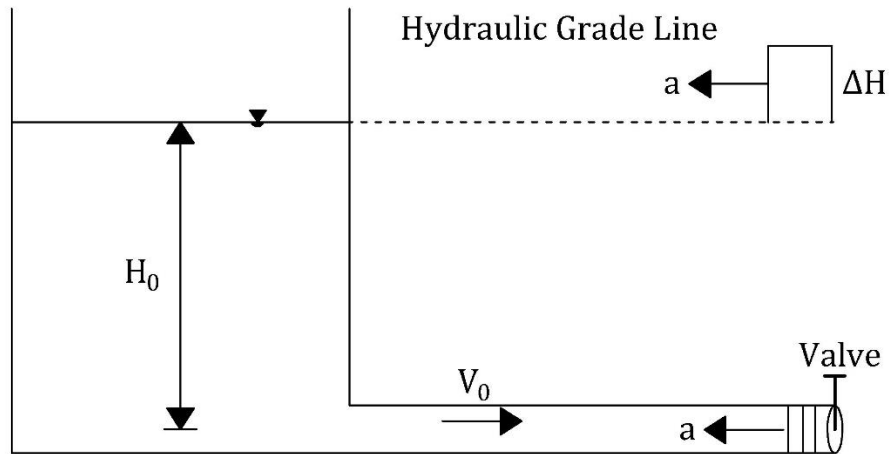


Figure 2.1 A frictionless hydraulic pipeline system that has a sudden valve closure case (Wylie & Streeter, 1978)

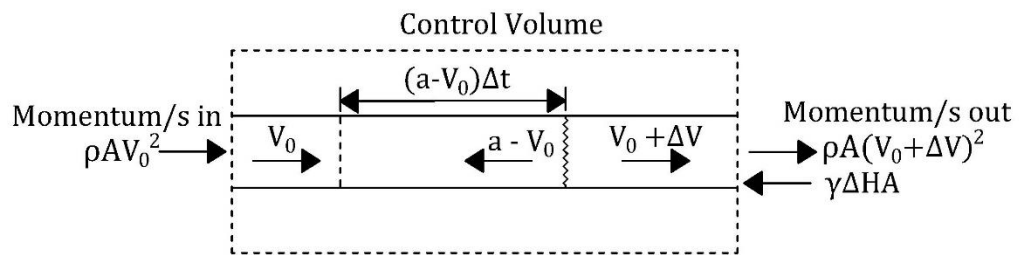


Figure 2.2 Application of momentum equation to the control volume at the transient state (Wylie & Streeter, 1978)

As shown in Figure 2.2, the first term of the momentum equation, which is the change in internal momentum, can be written as;

$$\frac{d}{dt} \int_{CV} V \rho dV = \rho \frac{A(a - V_0)}{\Delta t} \Delta t (V_0 + \Delta V - V_0) \quad (2.3)$$

After the simplification, the final form is written as;

$$\frac{d}{dt} \int_{CV} V \rho dV = \rho A (a - V_0) \Delta V \quad (2.4)$$

Then, from Figure 2.2, the second term of the momentum equation which is the difference between the momentum in and out fluxes (net efflux), can be written as;

$$\int_{CS} V\rho(\vec{V} \cdot \vec{n})dA = \rho A(V_0 - \Delta V)^2 - \rho AV_0^2 \quad (2.5)$$

If Eqs. (2.4) and (2.5) are combined, the general momentum equation can be written as follows.

$$\sum F_x = -\gamma A\Delta H = \rho A(a - V_0)\Delta V + \rho A(V_0 - \Delta V)^2 - \rho AV_0^2 \quad (2.6)$$

where;

A = Area of the pipe (m<sup>2</sup>)

$\gamma$  = Specific weight of the fluid (N/m<sup>3</sup>)

$\rho$  = Fluid density (kg/m<sup>3</sup>)

g = Gravitational acceleration (m/s<sup>2</sup>)

V<sub>0</sub> = Initial velocity of the fluid (m/s)

$\Delta V$  = Change in the velocity (m/s)

a = Acoustic wave speed (m/s)

$\Delta H$  = Change in the head (m)

In Eq. (2.6),  $\rho A(a - V_0)$  term represents the fluid mass, and  $\Delta V$  refers to the change in velocity at one second. It means that the  $\Delta V^2$  term, which has a small value, can be neglected. So, the equation can be simplified as;

$$\Delta H = -\frac{a\Delta V}{g} \left(1 + \frac{V_0}{a}\right) \approx -\frac{a\Delta V}{g} \quad (2.7)$$

As shown in Eq. (2.7), the value of  $V_0/a$  can be ignored since the wave speed has a much higher value than the initial velocity. Moreover, the equation below can be written if there is a condition such that the downstream valve is closed by increments.

$$\Delta H = -\frac{a \sum \Delta V}{g} \quad (2.8)$$

Eq. (2.8) is used for the downstream valve. In order to also consider the upstream gate and make the expression more general, Eq. (2.8) can be rewritten as follows.

$$\Delta H = \pm \frac{a \sum \Delta V}{g} \quad (2.9)$$

If Eq. (2.9) is used for pressure waves moving toward the downstream end, the plus sign must be selected in the equation, and if the equation is used for pressure waves moving toward the upstream end, the minus sign must be chosen in the equation.

Eqs. (2.8) and (2.9) are valid for rapid valve operations, that is, as long as the time duration for the pressure wave to reach the other end of the pipe and come back to the origin of the pressure wave is less than  $2L/a$ .

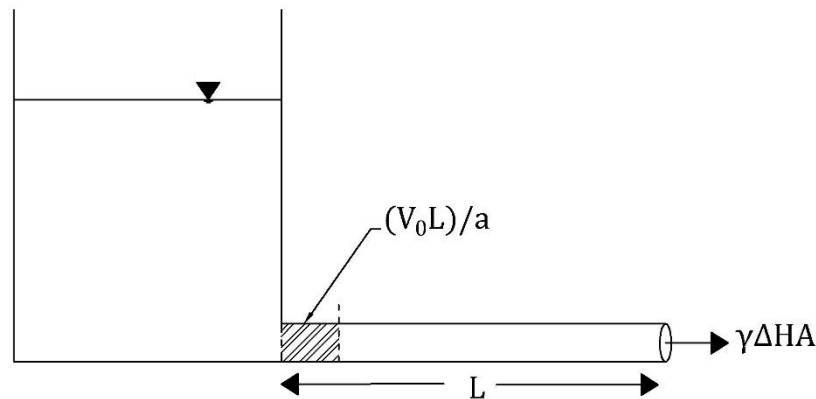


Figure 2.3 Implementation of continuity in a pipe

Next, the pressure wave speed,  $a$  can be calculated using Eq. (2.9) and the continuity concept given in Eq. (2.1). It can be observed in Figure 2.3 that the continuity equation is applied to the pipeline system in Figure 2.1 where the downstream valve is suddenly closed. High pressure changes in the system due to an instant closure of the valve can cause a stretch of  $\Delta s$  in the pipe length. This amount of stretching may

vary depending on the support type of the pipe. If the wave is assumed to travel in  $L/a$  seconds on the pipe of length  $L$  or the velocity is assumed to be  $(a\Delta s)/L$ , then the change in velocity is expressed as  $\Delta V = (a\Delta s/L) - V_0$ . The entered mass during  $L/a$  time is observed as  $\rho AV_0 L/A$ . This expression is equal to the summation of three mass contributions, which are mass stored in increased cross-sectional area, mass occupying the volume expansion caused by the stretch  $\Delta s$ , and mass increase due to compression of the fluid caused by higher pressure. This continuity equation can be expressed mathematically as;

$$\rho AV_0 \frac{L}{A} = \rho L \Delta A + \rho A \Delta s + L A \Delta \rho \quad (2.10)$$

Then, the equation is simplified, and the expression of  $\Delta V = (\Delta s a/L) - V_0$  is used to eliminate the  $V_0$  term.

$$-\frac{\Delta V}{a} = \frac{\Delta A}{A} + \frac{\Delta \rho}{\rho} \quad (2.11)$$

Now, Eq. (2.9) is used for the elimination of the  $\Delta V$  in Eq. (2.11).

$$a^2 = \frac{g\Delta H}{\frac{\Delta A}{A} + \frac{\Delta \rho}{\rho}} \quad (2.12)$$

To rearrange Eq. (2.12), the bulk modulus of elasticity for the fluid is defined as;

$$K = \frac{\Delta P}{\frac{\Delta \rho}{\rho}} = -\frac{\Delta P}{\frac{\Delta V}{V}} \quad (2.13)$$

Then Eq. (2.12) can be rewritten with the combination of Eq. (2.13) as follow;

$$a^2 = \frac{\frac{K}{\rho}}{1 + \left(\frac{K}{A}\right) \left(\frac{\Delta A}{\Delta P}\right)} \quad (2.14)$$

If the wall thickness of the pipe is large enough, the change in pipe area will be quite small, and  $\Delta A/\Delta P$  can be neglected, so the wave speed can be calculated as follows,

$$a \approx \sqrt{\frac{K}{\rho}} \quad (2.15)$$

On the other hand, if the pipe walls are very flexible, the value of 1 in the denominator part of Eq. (2.14) can be neglected, and the expression is written as;

$$a \approx \sqrt{\frac{A \Delta P}{\rho \Delta A}} \quad (2.16)$$

If the pipe wall is thin, three different support situation cases can be observed. Then, the determination of wave speed or  $\Delta A/(A\Delta P)$  changes according to the preferred support condition. According to Wylie and Streeter (1978), these support conditions are stated as;

- Case a: pipe anchored at the upstream end only
- Case b: pipe anchored throughout against axial movements
- Case c: pipe anchored with expansion joints throughout (Wylie & Streeter, 1978)

At first, Poisson's ratio, which is the negative ratio of lateral unit strain to axial unit strain, is expressed mathematically as below.

$$\mu = -\frac{\xi}{\xi_1} \quad (2.17)$$

The change in area is caused by the total change in strains, which are circumferential or lateral,  $\Delta\xi_T$ . The mathematical expression is shown in Eq. (2.18).

$$\Delta A = \Delta\xi_T \frac{D}{2} \pi D = 2A\Delta\xi_T \quad (2.18)$$

where;

$$\xi_T = \xi_2 + \xi = \xi_2 - \mu\xi_1 \quad (2.19)$$

There is a relation between the stress and strain with Young's modulus of elasticity which is E as shown in Eq. (2.20).

$$\xi_1 = \frac{\sigma_1}{E} \quad \xi_2 = \frac{\sigma_2}{E} \quad (2.20)$$

where;

$\sigma_1$  = Axial unit stress

$\sigma_2$  = Lateral unit stress

To determine the expressions for the stresses generated by the transient flow, the circumferential pipe stress forces as shown in Figure 2.4 are used.

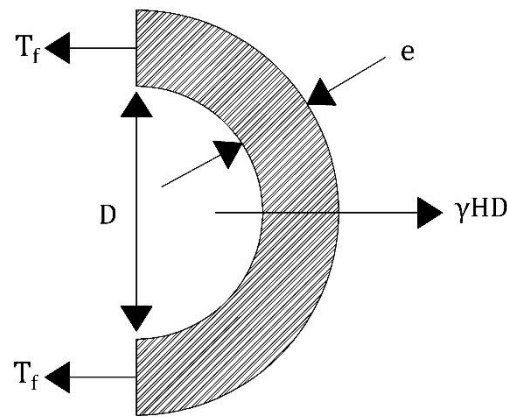


Figure 2.4 Forces acting on pipe caused by water hammer

In Figure 2.4,  $T_f$  and  $e$  represent the circumferential tensile force acting on per unit length of pipe and the thickness of the pipe wall, respectively.

The lateral unit stress expression can be written as;

$$\sigma_2 = \frac{T_f}{e} = \frac{\gamma HD}{2e} \quad (2.21)$$

Then the below equation can be inferred.

$$\Delta\sigma_2 = \frac{\gamma\Delta HD}{2e} = \frac{D\Delta P}{2e} \quad (2.22)$$

The axial unit stress expression can be written as;

$$\sigma_1 = \frac{F}{A} = \frac{P\pi r^2}{2\pi r e} = \frac{DP}{4e} \quad (2.23)$$



Then, the change in the determination of  $\Delta A/(A\Delta P)$  for all three support situation cases can be observed.

- Case a;

$\gamma HA$  is the force acting on the valve which is closed. Then axial tensile stress is determined as;

$$\sigma_1 = \frac{\gamma HA}{\pi De} \quad (2.24)$$

Then, the below equation can be written.

$$\Delta\sigma_1 = \frac{D\Delta P}{4e} \quad (2.25)$$

As a result;

$$\frac{\Delta A}{A\Delta P} = \frac{2\Delta\xi_T}{\Delta P} = \frac{2}{\Delta PE} (\Delta\sigma_2 - \mu\Delta\sigma_1) = \frac{D}{Ee} \left(1 - \frac{\mu}{2}\right) \quad (2.26)$$

- Case b;

$\xi_1=0$  and  $\sigma_1 = \mu\sigma_2$ . Then, simplifications are applied.

$$\frac{\Delta A}{A\Delta P} = \frac{2}{\Delta PE} (\Delta\sigma_2 - \mu^2\Delta\sigma_2) = \frac{D}{Ee} (1 - \mu^2) \quad (2.27)$$

- Case c;

$\sigma_1 = \mu\sigma_2$ . Then;

$$\frac{\Delta A}{A\Delta P} = \frac{2\Delta\sigma_2}{\Delta PE} = \frac{D}{Ee} \quad (2.28)$$

So, the final expression of the wave speed can be rearranged as:

$$a = \frac{\sqrt{(K/\rho)}}{\sqrt{1 + \left(\frac{KD}{Ee}\right) c_1}} \quad (2.29)$$

where  $c_1$  is an expression that will change according to the support condition of the pipe in the system.  $c_1$  expressions are listed below accordingly for the above cases;

- For case a;  $c_1 = 1 - \mu/2$
- For case b;  $c_1 = 1 - \mu^2$
- For case c;  $c_1 = 1$

Figure 2.5 represents a sequence of events of a system which has an upstream reservoir at a constant head, a suddenly closed downstream valve, and a single pipe with the length  $L$ . In addition, friction and minor losses are neglected in this pipeline system. After the sudden valve closure, a wave is propagated toward the upstream end of the pipe. The time required for the wave to reach the upstream end of the system is  $L/a$  second, and the wave can reach the downstream valve again in total  $2L/a$  seconds. At time 0 and  $4L/a$ , the conditions of the system are similar. Then it can be said that the process shown in Figure 2.5 is repeated every  $4L/a$  (Wylie & Streeter, 1978).

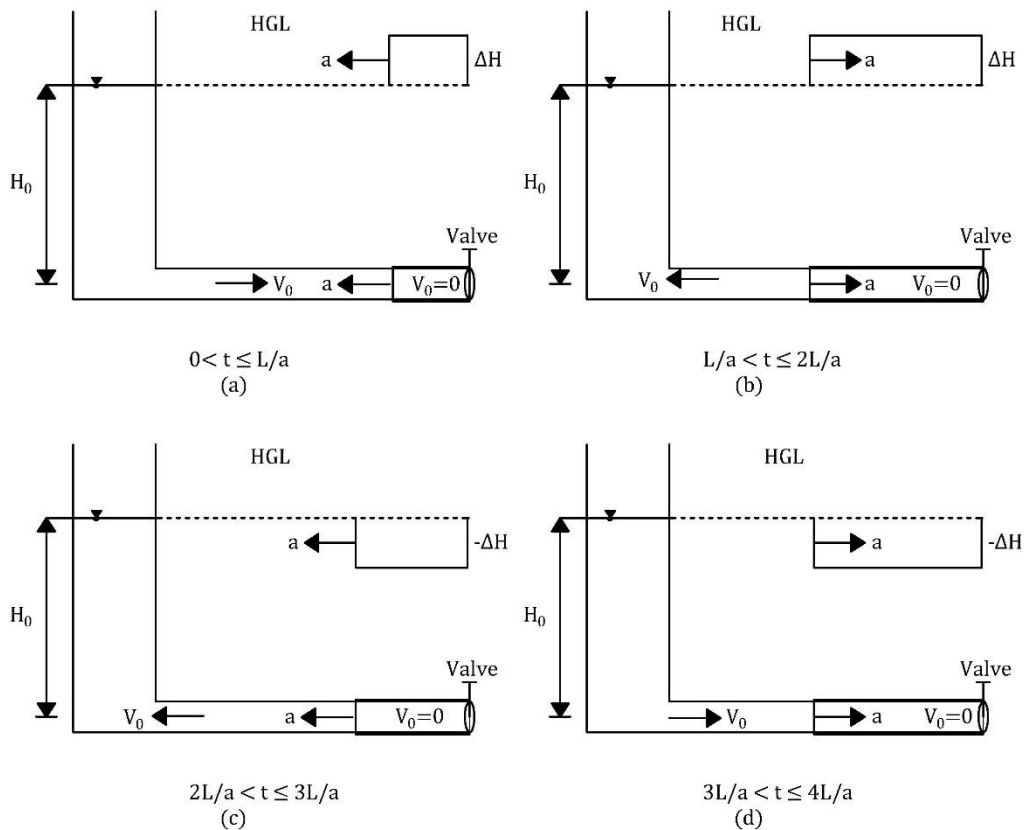


Figure 2.5 Transient event in a frictionless system for a period ( $4L/a$ ) after instant valve closure (Wylie & Streeter, 1978)

### 2.3 Fundamental Differential Equations for Transient Flow

The main purpose of the transient flow or water hammer analysis is to be able to observe the fluid behavior during the transition event at a certain point and in a certain time interval. In order to achieve the stated purpose, the conservation of mass and momentum laws must first be applied to a defined control volume. These laws and their equations are represented in Section 2.2. This process is important for deriving partial differential equations that can be used in water hammer solutions. The parameters and forces which are used for the derivation of continuity and momentum equations are illustrated in Figure 2.6.

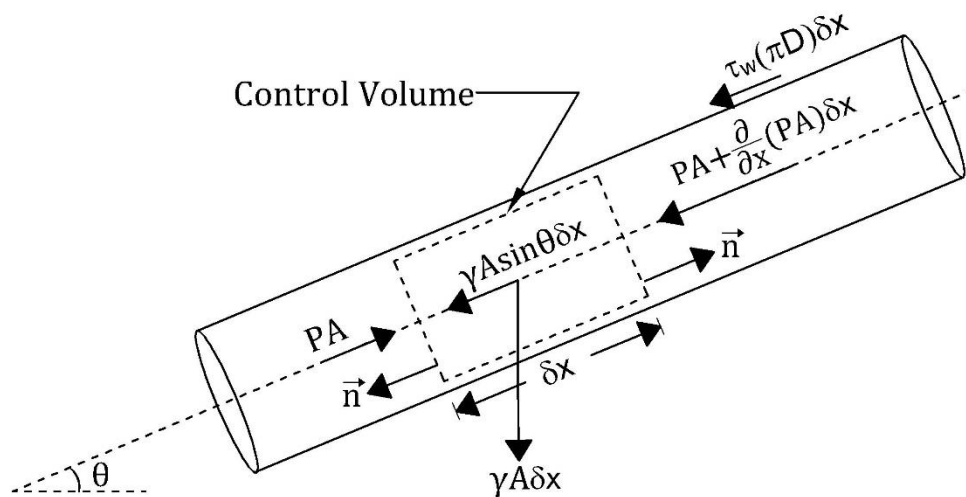


Figure 2.6 Control volume for the implementation of equations of motion and continuity (Wylie & Streeter, 1978)

Before applying the continuity and momentum equations, four assumptions are made for the system. These assumptions are:

- Flow and wave movements are one dimensional
- Control volume is fixed
- Cross section of the conduit is constant, and the conduit wall is elastic
- The fluid in the conduit is slightly compressible

After the application of the conservation of momentum and mass laws, and simplifications, the continuity equation and momentum equation are derived in terms of partial differential equations as expressed in Eqs. (2.30) and (2.31), respectively. Here, P and V are the dependent variables, x and t are the independent variables.

$$\frac{\partial P}{\partial t} + V \frac{\partial P}{\partial x} + \rho a^2 \frac{\partial V}{\partial x} = 0 \quad (2.30)$$

$$V \frac{\partial V}{\partial x} + \frac{\partial V}{\partial t} + \frac{1}{\rho} \frac{\partial P}{\partial x} + \left( g \sin \theta + \frac{4\tau_w}{\rho D} \right) = 0 \quad (2.31)$$

where;

D = Pipe diameter (m)

P = Pressure (N/m<sup>2</sup>)

$\rho$  = Fluid density (kg/m<sup>3</sup>)

g = Gravitational acceleration (m/s<sup>2</sup>)

V = Velocity of the fluid (m/s)

a = Acoustic wave speed (m/s)

$\tau_w$  = Wall shear stress (N/m<sup>2</sup>)

In the solution process of momentum and continuity equations, velocity and pressure values must be obtained at each time step and distance interval. Therefore, it is quite difficult to solve the equations which are given in the closed form. In order to solve the equations, different types of solution techniques such as arithmetic, graphical, algebraic, and linear analysis can be used. In this study, the characteristics method is used to solve the transient flow equations and perform water hammer analyses.

## 2.4 Method of Characteristics

Method of Characteristics is a widely used mathematical method which is employed to transform partial differential equations into ordinary differential equations. These equations can then be integrated to obtain the finite difference equations (Wylie & Streeter, 1978).

This section includes the transforming of the transient flow equations into solvable form by using the method of characteristics.

### 2.4.1 Characteristics Equations

The momentum and continuity equations, which are derived in Section 2.3, are nonlinear, hyperbolic, partial differential equations. As shown in Eqs. (2.30) and (2.31), these equations have two dependent variables, which are pressure (P) and velocity (V), and two independent variables, which are the distance (x) along the pipe and time (t).

Momentum and continuity equations can be transformed into four ordinary differential equations by the method of characteristics. At first, 'L<sub>1</sub>' and 'L<sub>2</sub>' are used as labels for Eqs. (2.30) and (2.31), respectively, as shown below.

$$L_1 = \frac{\partial P}{\partial t} + V \frac{\partial P}{\partial x} + \rho a^2 \frac{\partial V}{\partial x} = 0 \quad (2.32)$$

$$L_2 = V \frac{\partial V}{\partial x} + \frac{\partial V}{\partial t} + \frac{1}{\rho} \frac{\partial P}{\partial x} + g \sin \theta + \frac{4\tau_w}{\rho D} = 0 \quad (2.33)$$

Since Eqs. (2.32) and (2.33) are both equal to zero; linear combinations of L<sub>1</sub> and L<sub>2</sub> must be equal to zero. Then the combination of these equations with an unknown multiplier  $\lambda$  is provided as expressed in Eq. (2.34), where F refers to  $(g \sin \theta + 4\tau_w/\rho D)$ .

$$L_1 + \lambda L_2 = \left( \frac{\partial P}{\partial t} + V \frac{\partial P}{\partial x} + \rho a^2 \frac{\partial V}{\partial x} \right) + \lambda \left( V \frac{\partial V}{\partial x} + \frac{\partial V}{\partial t} + \frac{1}{\rho} \frac{\partial P}{\partial x} + F \right) = 0 \quad (2.34)$$

Then, the equation is rearranged as follows;

$$\left[ \frac{\partial P}{\partial t} + \left( V + \frac{\lambda}{\rho} \right) \frac{\partial P}{\partial x} \right] + \lambda \left[ \left( V + \frac{\rho a^2}{\lambda} \right) \frac{\partial V}{\partial x} + \frac{\partial V}{\partial t} \right] + \lambda F = 0 \quad (2.35)$$

It is known that velocity (V) and pressure (P) terms are functions dependent on distance (x) and time (t). Then, the chain rule from calculus is used to rearrange the terms.

$$\frac{dV}{dt} = \frac{\partial V}{\partial t} + \frac{\partial V}{\partial x} \frac{dx}{dt} \quad (2.36)$$

where;

$$\frac{dx}{dt} = V + \frac{\rho a^2}{\lambda} \quad (2.37)$$

and

$$\frac{dP}{dt} = \frac{\partial P}{\partial t} + \frac{\partial P}{\partial x} \frac{dx}{dt} \quad (2.38)$$

where;

$$\frac{dx}{dt} = \left( V + \frac{\lambda}{\rho} \right) \quad (2.39)$$

Then, Eq. (2.35) can be rearranged as;

$$\frac{dP}{dt} + \lambda \frac{dV}{dt} + \lambda F = 0 \quad (2.40)$$

To provide the validation of the chain rule, dx/dt values, which are in Eqs. (2.37) and (2.39), must be the same. Then, this expression can be written as;

$$\frac{dx}{dt} = \left( V + \frac{\lambda}{\rho} \right) = V + \frac{\rho a^2}{\lambda} \quad (2.41)$$

From Eq 2.41, the unknown multiplier  $\lambda$  can be determined with the cancelation of V parameters. So,

$$\lambda = \pm \rho a \quad (2.42)$$

Then, Eq. (2.41) is expressed as in Eq. (2.43) by substituting  $\lambda$ . When the magnitudes of the acoustic wave speed (a) and the flow velocity (V) are compared,

it is observed that the magnitude of the flow velocity is negligible compared to the wave speed. Therefore, the  $V$  term can be dropped from the equation.

$$\frac{dx}{dt} = V \pm a \cong \pm a \quad (2.43)$$

Now that value of  $\lambda$  is known, Eqs. (2.40) and (2.41) take the following forms:

$$C^+ \text{ or } C^- \begin{cases} \pm \frac{1}{\rho} \frac{dP}{dt} + a \frac{dV}{dt} + aF = 0 \\ \frac{dx}{dt} \cong \pm a \end{cases} \quad (2.44)$$

In this equation set, if  $\lambda$  value is  $+pa$ , the equation set is named as  $C^+$  equation. Similarly, if  $\lambda$  value is  $-pa$ , the equation set is called as  $C^-$  equation. So, it can be observed that two partial differential equations turned into four ordinary differential equations along with Eq. (2.43), which are expressed together in Eq. (2.44). The upper part of these equations is called compatibility equations, and they are valid along the corresponding lower part of the equations called characteristic lines. A visualization of the characteristic lines on the  $x$ - $t$  plane is shown in Figure 2.7.

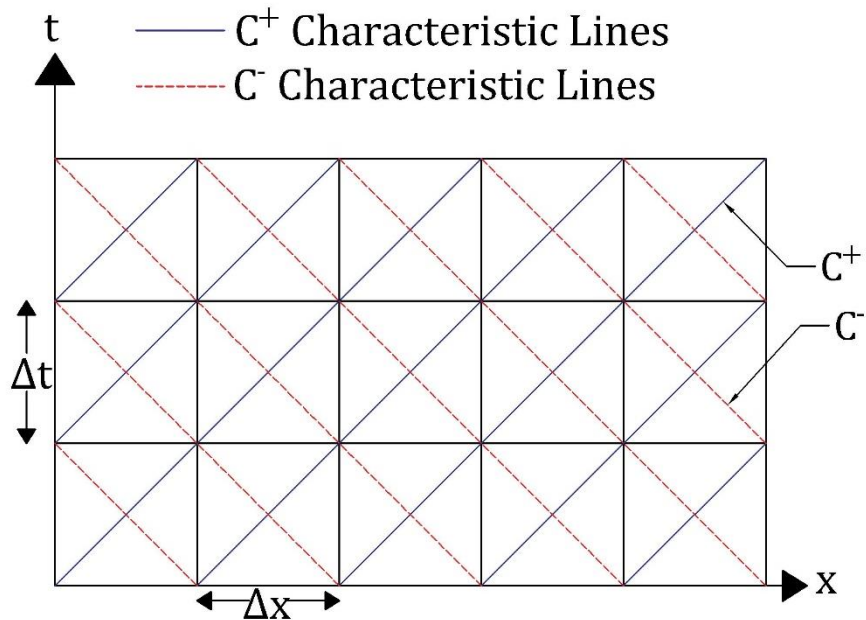


Figure 2.7 Characteristic lines in  $x$ - $t$  plane

In addition, Courant condition must be checked and satisfied to obtain accurate results and to ensure convergence. Courant condition is expressed as;

$$\frac{\Delta x}{\Delta t} \leq a \quad (2.45)$$

If it is assumed that the system has quasi-steady friction, the shear stress defined by Darcy - Weisbach can be applied to the compatibility equations.

$$\frac{4\tau_w}{\rho D} = f \frac{V|V|}{2D} \quad (2.46)$$

Then;

$$F = g \sin \theta + f \frac{V|V|}{2D} \quad (2.47)$$

Finally, Eq. (2.44) can be rearranged in terms of velocity (V) and head (H) as expressed in Eqs. (2.48) and (2.49).

$$C^+ \left\{ \begin{array}{l} + \frac{g}{a} \frac{dH}{dt} + \frac{dV}{dt} + f \frac{V|V|}{2D} = 0 \\ \frac{dx}{dt} = a \end{array} \right. \quad (2.48)$$

$$C^- \left\{ \begin{array}{l} - \frac{g}{a} \frac{dH}{dt} + \frac{dV}{dt} + f \frac{V|V|}{2D} = 0 \\ \frac{dx}{dt} = -a \end{array} \right. \quad (2.49)$$

In the differential equations, which are stated in Eqs. (2.48) and (2.49), piezometric head ( $H=z+P/\gamma$ ) and flow velocity (V) are the unknown parameters. According to Wylie and Streeter (1978), first order finite difference approximation can be used to solve these differential equations simultaneously due to the selected time increments has generally small values. But in the cases, which have considerably large friction losses, usage of a second order finite difference approximation is more proper to prevent instability of the finite-difference scheme. It is also known that the selection of a small value for time increment makes the transient analysis more computational but more accurate.



## 2.4.2 Time Discretization of Compatibility Equations

In this subsection, the compatibility equations mentioned in Eqs. (2.48) and (2.49) will be discretized in x-t plate with the finite difference approximation. The main purpose is to solve the characteristics equations for each node and time in the pipeline. At first, the pipeline in the hydraulic system must be divided into N sections, and the length of these sections is symbolized as  $\Delta x$  with a proper time-step value,  $\Delta t$ , as shown in Figure 2.8. Therefore, the node number of the pipeline is represented as N+1. The time increment value can be determined with the consideration of Courant condition, i.e. Eq. (2.45). It is generally preferred to set equal to  $\Delta t = \Delta x/a$ .

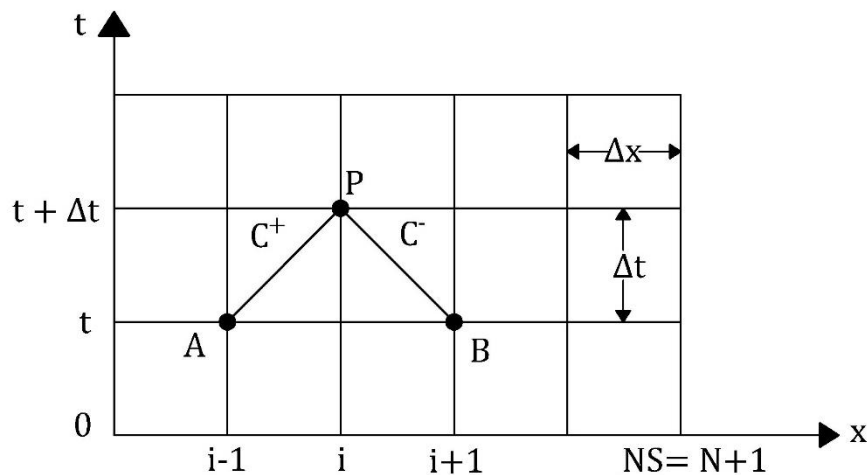


Figure 2.8 Notations for a nodal solution and characteristics lines

According to Figure 2.8, AP and BP lines represent the  $C^+$  and  $C^-$  characteristics lines, respectively. If the head (H) and velocity (V) values, which are dependent variables, are known at point A, the compatibility equation expressed in Eq. (2.48) can be integrated along the AP line. In this equation, there are 2 unknown variables which are H and V values at point P.

As it is mentioned in Eq. (2.45), the equality  $adt=dx$  can be written. Then, Eqs. (2.48) and (2.49) are multiplied by the 'adt' term and divided by the 'g' term to simplify

and convert the equations to integration form. Lastly, the expression is written in terms of flow discharge (Q) instead of V as;

$$\int_{H_A}^{H_P} dH + \frac{a}{gA} \int_{Q_A}^{Q_P} dQ + \frac{f}{2gDA^2} \int_{x_A}^{x_P} Q|Q|dx = 0 \quad (2.50)$$

Similarly, if head and velocity values are known at point B, the compatibility equation that is expressed in Eq. (2.49) can be integrated along the BP line. In the second equation, the unknown variables are exactly the same in Eq. (2.50) which are the H and Q variables at point P. So the same procedure is applied to the second equation.

$$\int_{H_B}^{H_P} dH - \frac{a}{gA} \int_{Q_B}^{Q_P} dQ - \frac{f}{2gDA^2} \int_{x_B}^{x_P} Q|Q|dx = 0 \quad (2.51)$$

As a result, two equations with two unknowns were obtained. The integrals which have the variation of flow discharge (Q) with x in the last term of Eqs. (2.50) and (2.51) are unknowns a priori. So, first order approximation, which is satisfying most problems except the problems dominated by friction, is introduced in these evaluations (Wylie & Streeter, 1978). Then, the following equations are obtained for C<sup>+</sup> and C<sup>-</sup> respectively as follows;

$$H_P - H_A + \frac{a}{gA} (Q_P - Q_A) + \frac{f\Delta x}{2gDA^2} Q_A|Q_A| = 0 \quad (2.52)$$

$$H_P - H_B - \frac{a}{gA} (Q_P - Q_B) - \frac{f\Delta x}{2gDA^2} Q_B|Q_B| = 0 \quad (2.53)$$

Eqs. (2.52) and (2.53) represent the basic mathematical relations which describe the discharge and head propagation in a pipeline in transient phenomena.

B and R variables are defined to simplify and shorten these equations as;

$$B = \frac{a}{gA} \quad R = \frac{f\Delta x}{2gDA^2} \quad (2.54)$$

Then, these compatibility equations are rewritten as follows, which are solved for H<sub>p</sub>.

$$C^+: H_P = H_A - B(Q_P - Q_A) - RQ_A|Q_A| \quad (2.55)$$

$$C^-: H_P = H_B + B(Q_P - Q_B) + RQ_B|Q_B| \quad (2.56)$$

Then, Eqs. (2.55) and (2.56) are expressed in nodal notation form with some simplifications by defining  $C_P$  and  $C_M$  terms as follows.

$$C^+: H_{P_i} = C_P - BQ_{P_i} \quad (2.57)$$

$$C^-: H_{P_i} = C_M + BQ_{P_i} \quad (2.58)$$

where;

$$C_P = H_{i-1} + BQ_{i-1} - RQ_{i-1}|Q_{i-1}| \quad (2.59)$$

$$C_M = H_{i+1} - BQ_{i+1} + RQ_{i+1}|Q_{i+1}| \quad (2.60)$$

It should be noted that these equations and procedures are also proper to apply in the steady-state condition, which is a special case of unsteady-state.

For each interior node in the pipeline, these compatibility equations can be solved simultaneously to find unknown H and Q values at the node. The H variable at point P can be determined by the elimination of Q parameters from Eqs. (2.57) and (2.58) as;

$$H_{P_i} = (C_P + C_M)/2 \quad (2.61)$$

Then, the unknown discharge value at point P can be calculated by using the calculated H value in Eqs. (2.57) or (2.58).

This procedure can be repeated for each interior node in a pipeline. If the initial time has the notation of  $t = t_0$ , in the next step, the calculated H and Q values at  $t_0$  are used as new initial inputs for the next iteration, which is  $t + \Delta t$ .

In addition, for some points, such as the upstream end and downstream end of the system, only one characteristic line may be valid. Also, additional equations may be needed at some interior junctions where include extra components in the pipeline system. This situation and boundary conditions are explained in the next chapter.

## 2.5 Application of Method of Characteristics in Systems

Pipelines may contain more than one pipe with different or same properties. These pipeline systems are called complex systems. Series pipe connection, branch connection, and parallel pipelines can be given as examples of these systems. In this thesis, single pipe and pipe connected in series systems are focused and studied.

### 2.5.1 Handling Single Pipe

In pipe segment, the head and flow rate values can be obtained for each interior node in the pipe by using characteristic equations, which are Eqs. (2.57) and (2.58). If we consider a single constant diameter pipe which has same properties along the pipe, the pressure wave speed has a constant value for each point in the pipe. Then, the characteristic equations can be simplified by considering the notations of the pipe shown in Figure 2.9 as follows;

$$H_{P_i} = \frac{C_P + C_M}{2} \quad (2.62)$$

$$Q_{P_i} = \frac{C_P - H_{P_i}}{B} = \frac{H_{P_i} - C_M}{B} \quad (2.63)$$

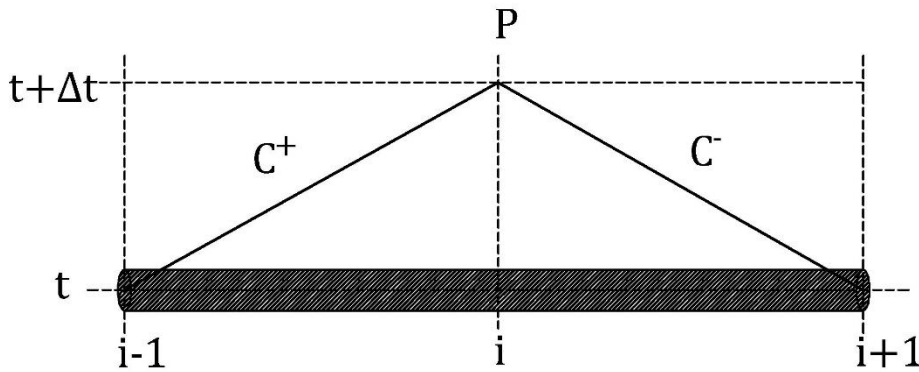


Figure 2.9 Notations for interior points of a single pipe example

Eqs. (2.62) and (2.63) can be used to calculate head and discharge values in interior points of the pipe, respectively, as also mentioned in subsection 2.4.2.

## 2.6 Handling Pipes Connected in Series in a Pipeline

If the hydraulic system contains a series of pipes connected with each other one after another and having different properties such as diameter, thickness, and material type, they should be handled carefully. The difference in properties of pipes causes a difference in the magnitude of pressure wave speed for each pipe. Then, the transient solution must be calculated separately. For this reason, a double subscription, which includes the pipe name and node number, is used in the equations. The notations in pipes connected in series boundaries, such as the name and node number of pipes, are illustrated in Figure 2.10.

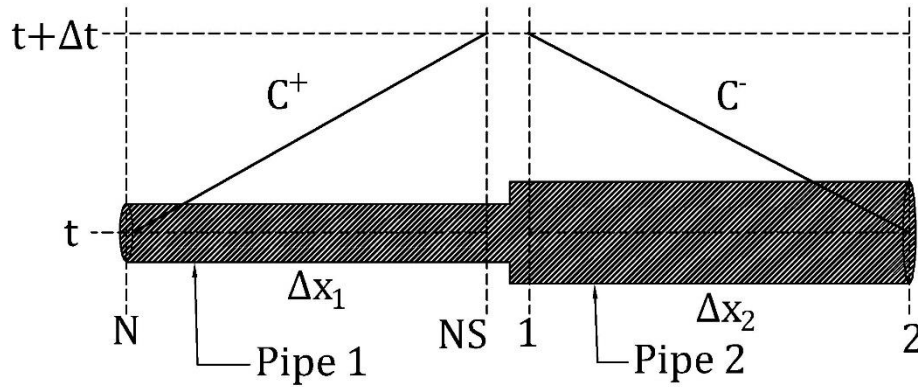


Figure 2.10 Notations for pipes connected in series

As shown in Figure 2.10, the last node of Pipe 1 and the first node of Pipe 2 are connected. If minor losses at this junction are neglected, two equations can be written by using continuity expression and the logic of common piezometric head existence at the junction as follows;

$$H_{P_{1,NS}} = H_{P_{2,1}} \quad (2.64)$$

$$Q_{P_{1,NS}} = Q_{P_{2,1}} \quad (2.65)$$

where;

The first and second subscripts represent the pipe and node numbers, respectively.

Then, the characteristic equations, which are Eqs. (2.57) and (2.58) can be solved simultaneously by using Eqs. (2.64) and (2.65). The new equation is expressed as;

$$Q_{P_{2,1}} = Q_{P_{1,NS}} = \frac{C_{P_1} - C_{M_2}}{B_1 + B_2} \quad (2.66)$$

where;

$$B_1 = \frac{a_1}{gA_1} \text{ and } B_2 = \frac{a_2}{gA_2} \quad (2.67)$$

Finally, the unknown piezometric head,  $H_P$  can be obtained by Eqs. (2.57) and (2.58) by using the calculated value of  $Q_{P_{2,1}}$  in Eq. (2.66).

## CHAPTER 3

### BOUNDARY CONDITIONS

In Chapter 2, details and the formulation of transient equations were explained. In the simulation of a transient event, the head and discharge values can be calculated by using two compatibility equations for each nodal point in the pipeline with respect to specific time and space in the interior domain.

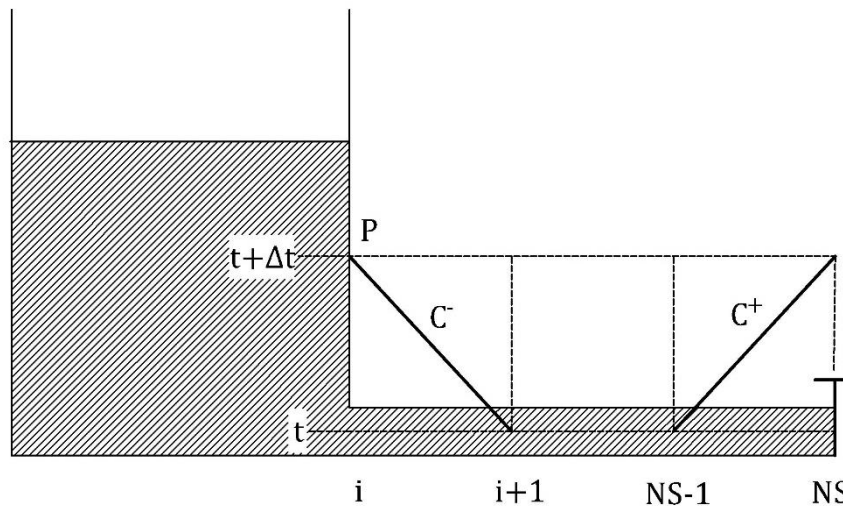


Figure 3.1 Characteristics lines at the endpoints of an example system

At the endpoints of the system, there exists only one characteristic line, either  $C^-$  or  $C^+$  as shown in Figure 3.1. This means we have only one compatibility equation despite two unknowns to be solved,  $Q$  and  $H$ , at the boundary. Therefore, we need an additional equation or a value for one of the unknowns. This could be an expression relating some behavior of one of the unknowns at the end boundary, such as a constant head reservoir or a closing valve, etc.

In the code that is developed in the present study, some important boundary conditions are selected. They are the most widely used boundaries that may be found in most transient events. These boundary conditions are listed as follows;

- Reservoir at the Upstream with Constant Head
- Downstream Reservoir with Constant Head
- Reservoir at the Upstream with Variable Head
- Valve at the Downstream and In-line
- Downstream Dead-end
- Single Centrifugal Pump
- Air Chamber with Orifice
- Simple Surge Tank
- Surge Tank with Standpipe

In this chapter, general information, equations, and formulation steps for these listed boundary conditions will be explained.

### **3.1 Reservoir at Upstream Boundary**

If there is a reservoir at the upstream end of the hydraulic system, upstream reservoir boundary conditions must be considered. Upstream reservoir boundary can be examined in two groups which are upstream reservoir with constant head and upstream reservoir with variable head.

#### **3.1.1 Reservoir at Upstream with Constant Head**

The reservoir, which is located at upstream of the system, is generally large, then it can be assumed that the elevation of the water surface does not change in a rapid transient event. In other words, the reservoir has a constant head. The first node of the pipe, which is connected to the upstream reservoir, has the same head values with the reservoir. So, the mathematical expression can be written as;

$$H_{P_i} = H_R \quad (3.1)$$

where;

$H_R$  = Upstream reservoir head, which is constant (m).



In boundary conditions at the upstream end of the system, only one of the compatibility equations, which is the negative characteristic equation ( $C^-$ ) can be used. The illustration of an upstream reservoir with constant head boundary condition and notations of the nodes and times are shown in Figure 3.2.

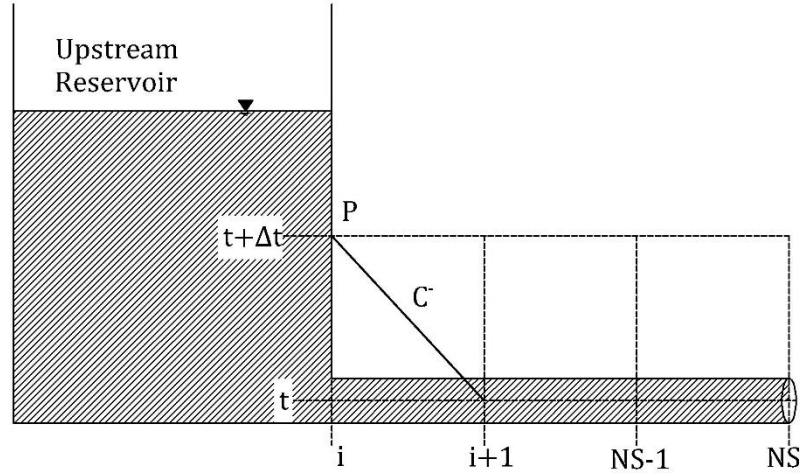


Figure 3.2 Notations of upstream reservoir boundary with constant head

So, the discharge which flows through the pipeline from the upstream reservoir can be obtained by using Eq. (2.58) for each time. So;

$$Q_{P_i} = \frac{H_{P_i} - C_M}{B} \quad (3.2)$$

It must also be mentioned that the similar procedure can be applied for downstream reservoir with a constant head boundary. In that case, Eq. (2.57), which is the positive characteristic equation ( $C^+$ ) can be used to calculate discharge values.

### 3.1.2 Reservoir at Upstream with Variable Head

When a hydraulic system includes a reservoir at the upstream end of the system with a variable head, it is known that the water surface elevation of the reservoir changes in a known manner, such as a sine wave which is used in this study. Then, this change causes variations in heads for each time step. The illustration of an upstream reservoir with variable head boundary conditions and notations of the nodes and times are shown in Figure 3.3.

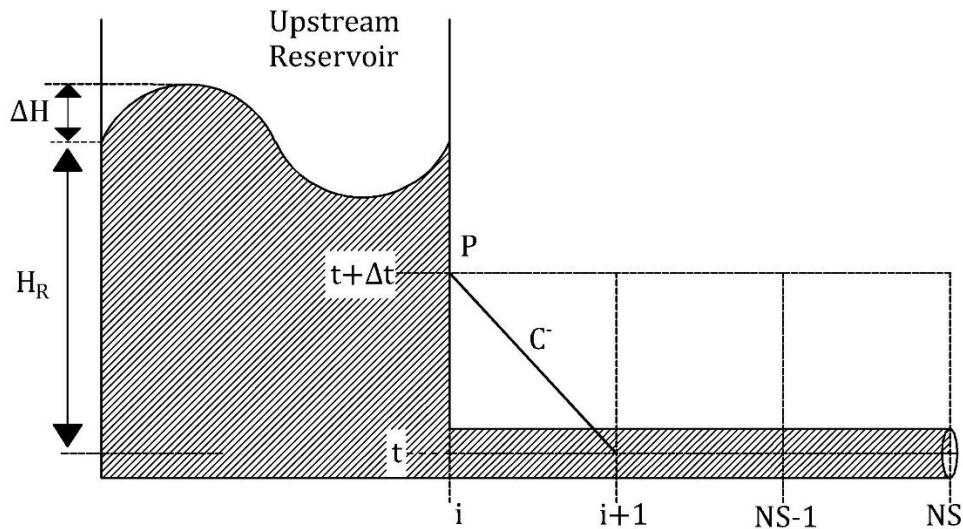


Figure 3.3 Notations of upstream reservoir boundary with variable head

If the notations shown in Figure 3.3 are considered, an auxiliary equation can be defined to obtain head values at each time step. This equation can be expressed as;

$$H_{P_i} = H_R + \Delta H \sin \omega t \quad (3.3)$$

where;

$\omega$  = Circular frequency

$\Delta H$  = Amplitude of the wave in the upstream reservoir (m)

Unknown discharge values at point P for each time step can be determined by using the negative characteristic equation, which is Eq. (2.58), as used in the upstream reservoir with a constant head boundary.

### 3.2 Valve Boundary

Valve is a component used in a pipeline to control the flow passing through the pipeline. In addition, it can be used to protect other devices, such as pumps and turbines, from damage that can be initiated by water hammer phenomena. Valve component may be located at downstream or interior points of the hydraulic system. According to its location, different equations can be obtained and used for the valve boundary condition.

### 3.2.1 Valve at Downstream

If the valve is located at the downstream end of the pipeline, the negative characteristic equation cannot be used. The downstream valve boundary and the notations are shown in Figure 3.4.

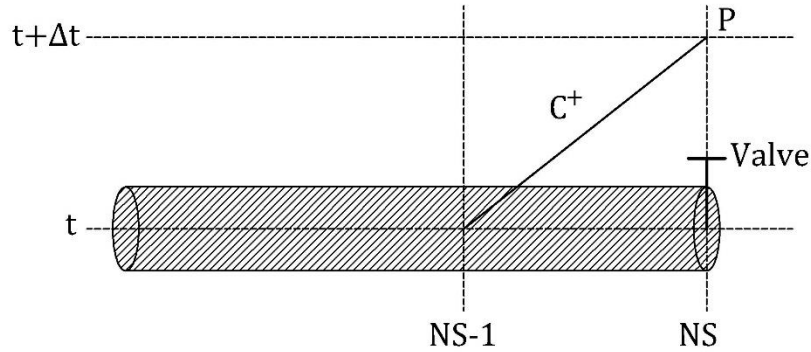


Figure 3.4 Downstream valve boundary and notations of the system

If it is considered the datum for HGL is located at the valve, the orifice equation can be written for the flow through the valve in steady state conditions as follows;

$$Q_0 = (C_d A_g)_0 \sqrt{2gH_0} \quad (3.4)$$

where;

$Q_0$  = Flow in steady state condition ( $m^3/s$ )

$C_d$  = Discharge coefficient

$A_g$  = Effective valve opening area ( $m^2$ )

$H_0$  = Head loss across the valve in steady state (m)

This orifice equation can be written in general form as:

$$Q_P = (C_d A_g) \sqrt{2g\Delta H} \quad (3.5)$$

where;

$\Delta H$  = Instantaneous drop in HGL across the valve (m)

In addition, dimensionless valve opening can be defined as;

$$\tau = \frac{C_d A_g}{(C_d A_g)_0} \quad (3.6)$$

According to the dimensionless valve opening expression,  $\tau = 1$  indicates that the valve is governed with settings at the steady-state condition and  $\tau = 0$  shows the valve is fully closed. ‘ $\tau$ ’ values can also be provided with a tabular valve-closure data or a valve closure formulation which may be expressed as;

$$\tau = \left(1 - \frac{t}{t_c}\right)^{E_m} \quad (3.7)$$

where;

$t$  = Current time (seconds)

$t_c$  = Valve closure time (seconds)

$E_m$  = A constant for valve closure

Then, Eqs. (3.4), (3.5), and (3.6) are used to derive the equation as follows;

$$Q_P = \frac{Q_0}{\sqrt{H_0}} \tau \sqrt{\Delta H} \quad (3.8)$$

Finally, the positive characteristic equation which is Eq. (2.57) and Eq. (3.8) are used to get the discharge equation for the valve boundary. This equation is expressed as;

$$Q_{P_{NS}} = -BC_v \sqrt{(BC_v)^2 + 2C_v C_P} \quad (3.9)$$

where;

$$C_v = \frac{(Q_0 \tau)^2}{2H_0} \quad (3.10)$$

The other unknown which is  $H_{P_{NS}}$  can be calculated by using Eq. (2.57).

### 3.2.2 Valve at Interior Point

If the valve is located at the interior points of the pipeline, the orifice equation needs to be used for the end boundary conditions of each pipe which is located at the right and left of the valve. During a valve closure, pressure rise and pressure drop are observed at the upstream and downstream sides of the valve, respectively. So, the head values of these sides are causally different. The in-line valve boundary and the notations are illustrated in Figure 3.5. Double subscription, which includes pipe name and node number, is used in equations of valve in-line boundary, as shown in Figure 3.5.

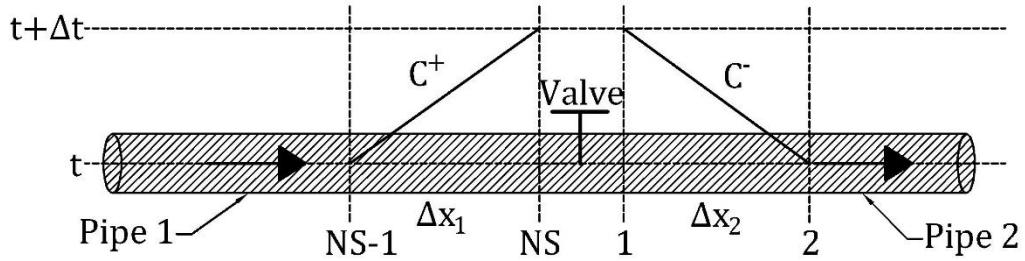


Figure 3.5 Valve at interior points of the system and notations of the system

The steady-state orifice equation is used for the valve. But flow reversal conditions must be considered. So the orifice equation must be expressed for flow in positive and negative directions separately. In addition, the conservation of mass principle is considered, which provides the equality of discharges at upstream and downstream of the valve.

Then, the orifice equation for flow in positive direction can be written as;

$$Q_{P_{1,NS}} = Q_{P_{2,1}} = \frac{Q_0 \tau}{\sqrt{H_0}} \sqrt{H_{P_{1,NS}} - H_{P_{2,1}}} \quad (3.11)$$

And the orifice equation for flow in negative direction can be written as;

$$Q_{P_{1,NS}} = Q_{P_{2,1}} = -\frac{Q_0 \tau}{\sqrt{H_0}} \sqrt{H_{P_{2,1}} - H_{P_{1,NS}}} \quad (3.12)$$

where;

$Q_0$  = Flow in steady state condition ( $m^3/s$ )

$H_0$  = Head loss across the valve in steady state (m)

If the positive characteristic equation, which is Eq. (2.57) for the first pipe, and the negative characteristic equation, which is Eq. (2.58) for the second pipe, are combined with Eq. (3.11), therefore the final equation for positive flow can be written as;

$$Q_{P_{1,NS}} = -C_v(B_1 + B_2) + \sqrt{C_v^2(B_1 + B_2)^2 + 2C_v(C_{P_1} - C_{M_2})} \quad (3.13)$$

As in the procedures applied for positive flow, the positive characteristic equation, which is Eq. (2.57) for the first pipe, and the negative characteristic equation, which is Eq. (2.58) for the second pipe are combined with Eq. (3.12) for negative flow as follows;

$$Q_{P_{1,NS}} = C_v(B_1 + B_2) + \sqrt{C_v^2(B_1 + B_2)^2 - 2C_v(C_{P_1} - C_{M_2})} \quad (3.14)$$

Then, it can be inferred that Eq. (3.13) will be used for positive flow conditions, which provides  $C_{P_1} - C_{M_2} \geq 0$ , and Eq. (3.14) will be used for negative flow conditions, which provides  $C_{P_1} - C_{M_2} < 0$ .

Finally, other unknowns which are  $H_{P_{1,NS}}$  and  $H_{P_{2,1}}$  can be calculated by using Eqs. (2.57) and (2.58), respectively.

### 3.3 Downstream Dead End Boundary

In a hydraulic system, if there is a dead end at the downstream, it can be inferred that there is no liquid flow passing through this boundary. So, it means that  $Q_{P_{NS}}$  value has the value of 0 according to the notations shown in Figure 3.6. In addition,  $H_{P_{NS}}$  can be obtained by using the positive characteristic equation, which is  $C^+$ . A fully closed valve at the downstream of the system can be an example of this situation.

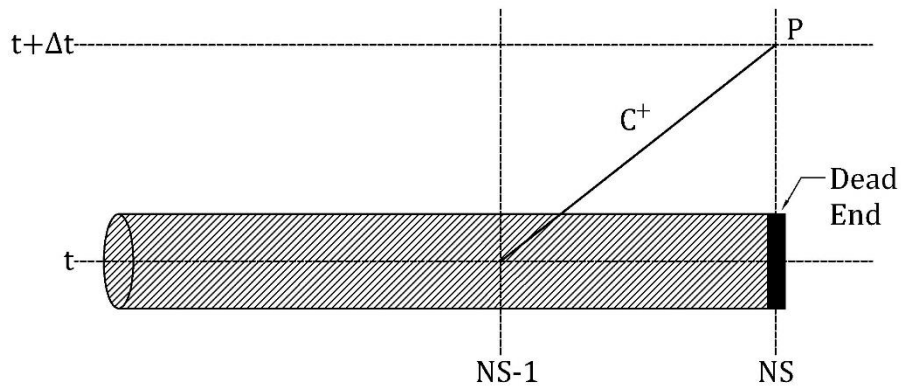


Figure 3.6 Dead-end boundary condition and notations

### 3.4 Single Centrifugal Pump Boundary

Failure of a pump component is one of the common phenomena that causes a transient flow in hydraulic systems. Pump failure or pump trip occurs in cases in which stoppage of the pump inadvertently or sudden closure of the valves that control the pumps. These scenarios can occur during power outages or emergency shutdowns. Additionally, improper pump operation may start a chain reaction of transient events.

The characteristics method is a method that can be used to analyze the transient flow resulting from a pump failure. During the analysis of centrifugal pumps, the two parameters, which are pump head and pump torque, should be combined into the general head and flow equations. Since the values of these parameters change during the transient event, a specific boundary condition must be defined at the point of the pump in the pipeline.

In this subsection, the events that occur on the system as a result of a power failure, the dimensionless pump characteristics with their functional application, and the single pump boundary condition will be examined in the order given. The methodology and equations are taken from Fluid Transients in Systems textbook (Wylie & Streeter, 1978).

### 3.4.1 Sequence of Events during Power Failure

The pump motor exerts a torque on the rotating shaft. The energy which is required for rotation of the impeller is generated by this torque. This rotational movement causes a flow passing through the pump. Then, it develops the total dynamic head (tdh), which increases from the suction flange to the discharge flange. The total dynamic head equals to the increase in the energy per unit weight of the fluid (Wylie & Streeter, 1978). The mathematical expression of tdh can be written as;

$$\text{tdh} = \frac{V_d^2}{2g} + \frac{p_d}{\gamma} + z_d - \left[ \frac{V_s^2}{2g} + \frac{p_s}{\gamma} + z_s \right] \quad (3.15)$$

where;

$V_d$  = Velocity measured in the discharge flange

$V_s$  = Velocity measured in the suction flange

$p_d$  = Pressure in the discharge flange

$p_s$  = Pressure in the suction flange

$z_d$  = Centerline elevation of the discharge flange

$z_s$  = Centerline elevation of the suction flange

When the power supplied to the pump is interrupted, a decrease in the rotational speed of the impeller is observed. This decrease causes the total dynamic head to decrease as well. In addition, this event causes the propagation of positive and negative pressure waves toward the upstream and downstream ends of the system, respectively.

If the fluid in the system is propagated to move from a lower elevation to a higher elevation with the pump operation under normal conditions, after a power failure event, the flow at the pump location becomes in the reverse direction for a while, although the pump impellers continue to rotate in the positive direction. This situation can be called the energy dissipation zone of the pump operation. After a



short time, reverse rotation is observed in the pump impellers. This can be called the turbine zone of the pump operation. The speed of this reverse rotation continues to increase until runaway speed. Because of this speed increment, a decrease is observed in the reverse flow rate coming to the pump due to the choking phenomenon. This situation can be called the reversed speed dissipation zone of the pump operation. As a result of this process, the propagation of negative and positive pressure waves is observed throughout the system. The negative pressure resulting from this instability in the system can cause dangerous problems such as column separation and vapor cavity.

The formulation of these sequences of events can be expressed mathematically with the help of the characteristics method.  $C^+$  and  $C^-$  equations play important roles in transmitting the pump's head and discharge information. In addition, the turbopump characteristics and related equations required to generate the pump boundary condition equations due to pump trip are examined in the next subsections.

### **3.4.2 Homologous-Dimensionless Turbopump Characteristics**

Four quantities which are the total dynamic head 'H', the discharge 'Q', the rotational speed of impellers 'N', and the shaft torque 'T' are used for the pump characteristics during pump operations. According to Wylie & Streeter (1978), two quantities out of these four quantities can be considered as independent, then the rest two quantities are obtained by the known characteristics. In general, N and Q quantities are preliminary determined and regarded as independent. Then, H and T values can be obtained if below two fundamental assumptions are considered as:

1. The steady state characteristics also hold for unsteady-state conditions. Despite the fact that the Q and N values vary over time, these values are used to determine H and T.
2. Homologous relationships are valid.

The equation of the homologous relationship can be represented as; (Wylie & Streeter, 1978)

$$\frac{H_1}{(N_1 D_1)^2} = \frac{H_2}{(N_2 D_2)^2} \quad (3.16)$$

$$\frac{Q_1}{N_1 D_1^3} = \frac{Q_2}{N_2 D_2^3} \quad (3.17)$$

where;

D = Representative linear dimensions for turbomachines

The subscripts used in Eqs. (3.16) and (3.17) describe the two units of centrifugal pumps which have different sizes. If the linear dimensions parameter of the pumps are similar, the equations can be simplified to;

$$\frac{H_1}{N_1^2} = \frac{H_2}{N_2^2} \quad (3.18)$$

$$\frac{Q_1}{N_1} = \frac{Q_2}{N_2} \quad (3.19)$$

One of the assumptions in the homologous theory is that the efficiency does not vary with the size of the unit, accordingly

$$\frac{N_1 T_1}{Q_1 H_1} = \frac{N_2 T_2}{Q_2 H_2} \quad (3.20)$$

Then, Eq. (3.20) is combined with Eqs. (3.18) and (3.19) as;

$$\frac{T_1}{N_1^2} = \frac{T_2}{N_2^2} \quad \frac{H_1}{Q_1^2} = \frac{H_2}{Q_2^2} \quad \frac{T_1}{Q_1^2} = \frac{T_2}{Q_2^2} \quad (3.21)$$

Working with characteristics that have no dimensions is more practical. So the below equations are written as;

$$h = \frac{H}{H_R} \quad \beta = \frac{T}{T_R} \quad u = \frac{Q}{Q_R} \quad \alpha = \frac{N}{N_R} \quad (3.22)$$

Where the subscript 'R' represents the rated values of the quantities. In other words, it represents the value at the best efficiency for H, N, Q, and T.

Then, the homologous relationship can be expressed in non-dimensional form as follows;

$$\frac{h}{\alpha^2} \text{ vs. } \frac{v}{\alpha} \quad \frac{\beta}{\alpha^2} \text{ vs. } \frac{v}{\alpha} \quad \frac{h}{v^2} \text{ vs. } \frac{\alpha}{v} \quad \frac{\beta}{v^2} \text{ vs. } \frac{\alpha}{v} \quad (3.23)$$

According to Wylie & Streeter (1978), in homologous theory, a curve can be plotted with  $v/\alpha$  and  $h/\alpha^2$  of the unit as abscissa and ordinate, respectively, to represent the relationship of head-discharge valid for any speed for that unit. Likewise,  $v/\alpha$  vs.  $\beta/\alpha^2$  can be used as abscissa and ordinate, respectively, to observe the torque relations.

Numerically, it is very difficult to use these relationships and make observations. The reason for this difficulty is that dimensionless characteristics, which are  $h$ ,  $\beta$ ,  $v$ , and  $\alpha$  can change the sign or even become zero during the analysis. Especially, when the alpha value is zero at certain points, some parameters go to infinity, and it causes errors in the results. Marchal, Flesch, and Suter used the following relationship to overcome this problem (Wylie & Streeter, 1978).

$$\frac{h}{\alpha^2 + v^2} \text{ vs. } \tan^{-1} \frac{v}{\alpha} \quad \frac{\beta}{\alpha^2 + v^2} \text{ vs. } \tan^{-1} \frac{v}{\alpha} \quad (3.24)$$

If the  $\theta$  angle is defined as  $\tan^{-1}(v/\alpha)$  the polar diagram of  $v$  and  $\alpha$  is illustrated as shown in Figure 3.7. This diagram helps to obtain the  $v$  and  $\alpha$  signs for four different ranges.

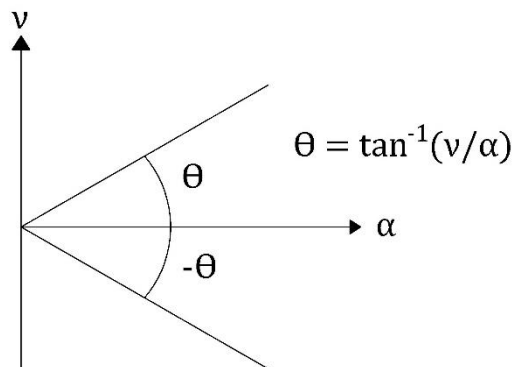


Figure 3.7 Polar diagram for  $v$  and  $\alpha$  (Wylie & Streeter, 1978)

Then, operation zones can be defined in terms of the sign of  $\alpha$  and  $v$ , names, and ranges, as shown in Table 3.1.

Table 3.1 Pump operation zones

Zone Name	$v$	$\alpha$	Region
Turbine	$\leq 0$	$< 0$	$0 - \pi/2$
Dissipation	$< 0$	$\geq 0$	$\pi$
Normal	$\geq 0$	$\geq 0$	$\pi - 3\pi/2$
Reversed Speed	$> 0$	$< 0$	$3\pi/2 - 2\pi$

With using the relationships in Eq. (3.24), two closed curves, which are a polar diagram of  $\theta = \tan^{-1}(v/\alpha)$  vs.  $r=h/(\alpha^2+v^2)$  and  $\theta = \tan^{-1}(v/\alpha)$  vs.  $r= \beta/(\alpha^2+v^2)$  can be obtained as complete pump characteristics. These two curves are formulated as;

$$\begin{aligned} WH(x) &= \frac{h}{\alpha^2 + v^2} & WB(x) &= \frac{\beta}{\alpha^2 + v^2} \\ \theta = x &= \pi + \tan^{-1} \frac{v}{\alpha} \end{aligned} \quad (3.25)$$

The angle  $x$  is used for plotting abscissa against  $WH(x)$  and  $WB(x)$  to represent the relationship of the head and torque of the pump unit, respectively. Then, the rectangular coordinates can be plotted as shown example curves in Figure 3.8.

In solution and analysis of a transient phenomenon that occurs after a pump failure, the complete pump characteristics data sets must be used. The manufacturers provide these data sets to customers. But, generally, these data sets are not simple to obtain. So, available data or curves in the literature are preferred to use for similar pumps.

The program developed in this study has the pump characteristics curve data for three speeds that are  $N_s= 35$  (in Figure 3.8),  $N_s= 147$ , and  $N_s= 261$  rpm in SI units.

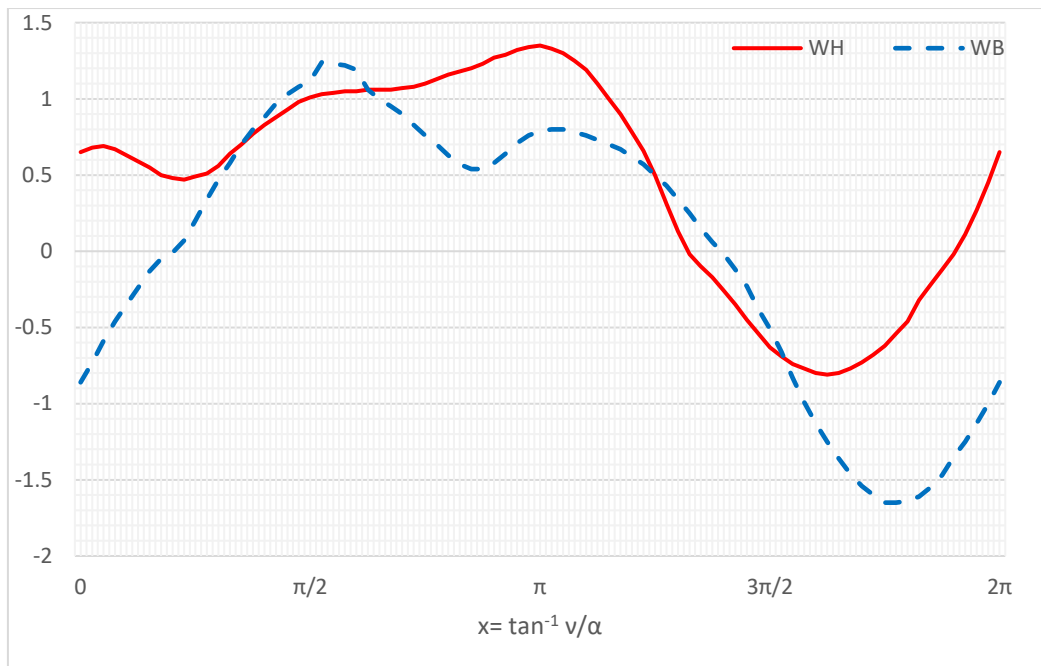


Figure 3.8 Pump characteristics curve (Suter curves) for speed  $N_s=35$  rpm

### 3.4.3 Transient Equations for Pump Trip

In pump trip scenarios, two equations are solved concurrently for each time increment  $\Delta t$  used for the characteristics method. These equations can be listed as;

- Head-balance equation along the pump and discharge valve, if it exists
- Torque-angular deceleration equation for rotating masses such as impeller.

#### 3.4.3.1 Equations of Head Balance

In the pump boundary condition, the head balance equation has three components that are piezometric head value at the suction ( $H_s$ ), valve head loss (vhl), and total dynamic head (tdh). This equation comes from the energy equation.

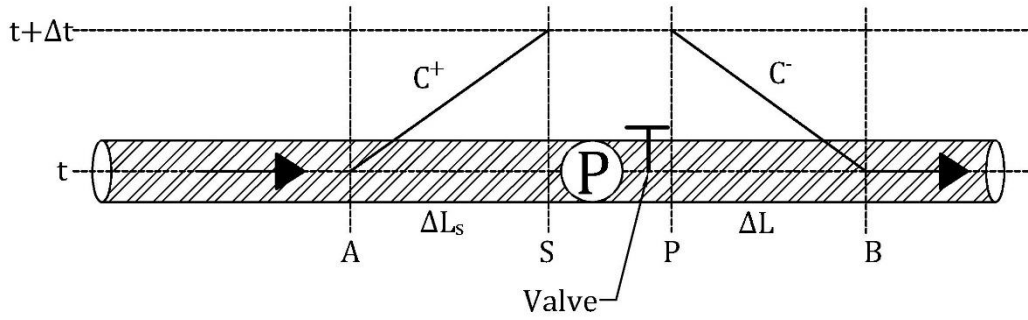


Figure 3.9 Grids and notation of the pump boundary with a discharge valve

According to the notations in Figure 3.9, the equation of head balance may be written as;

$$H_P = H_S + (tdh) - (vhl) \quad (3.26)$$

where;

$H_P$  = Piezometric head at point P

If it is assumed that NS is the last section of the suction pipe and NS1 represents NS+1, the  $C^+$  equations are expressed as both Eqs. (3.27) and (3.28) for the NS1.

$$H_{SP_{NS1}} = H_{S_{NS}} + B_S(Q_{SP_{NS1}} - Q_{S_{NS}}) - R_S Q_{S_{NS}} |Q_{S_{NS}}| \quad (3.27)$$

Or

$$H_{SP_{NS1}} = H_{CP} - B_S Q_{SP_{NS1}} \quad (3.28)$$

where;

$B_S$  = B value for suction pipe =  $a_s/gA_s$

$R_S$  = Frictional resistance for suction pipe =  $(f_s \Delta x_S)/(2gD_S A_S^2)$

If it is assumed that points (1) and (2) are the first and second sections of the discharge pipe, respectively, the  $C^-$  equations are expressed as both Eqs. (3.29) and (3.30) for Point 1.

$$H_{P_1} = H_2 + B(Q_{P_1} - Q_2) + RQ_2 |Q_2| \quad (3.29)$$

Or

$$H_{P_1} = HCM + BQ_{P_1} \quad (3.30)$$

Then, the continuity equation is applied as;

$$Q_{SP_{NS1}} = Q_{P_1} \quad (3.31)$$

The total dynamic head can be written as Eq. (3.32) with using the form of the non-dimensional homologous relationship, which is given in Eq. (3.25)

$$tdh = H_R h = H_R (\alpha^2 + v^2) WH(x) \quad (3.32)$$

where  $x = \pi + \tan^{-1} (v/\alpha)$

To find the appropriate approximation of  $x = \pi + \tan^{-1} (v/\alpha)$ , it is necessary to convert the  $WH(x)$  curve to a straight line. Obtaining an accurate straight line representing the approximation of the location is possible because of the data stored in small intervals. Therefore, two adjacent data points are used for extrapolation of  $\alpha$  and  $v$  to get the straight line, as shown in Figure 3.10.

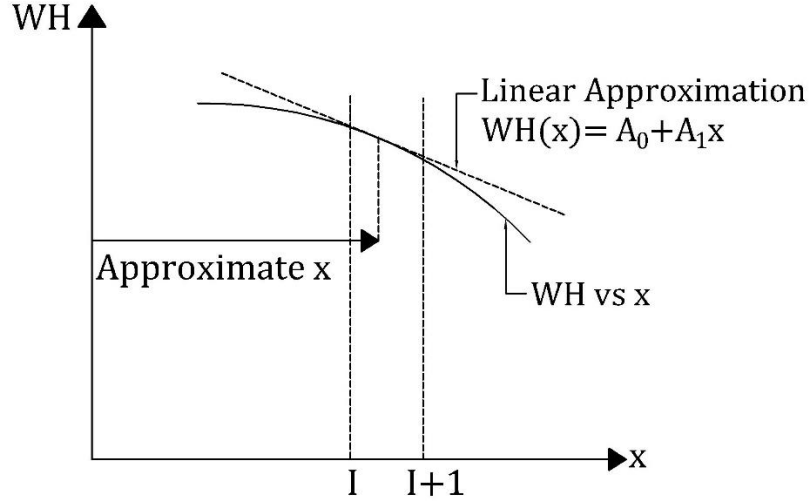


Figure 3.10 Linear approximation of the WH curve

$$I = \frac{x}{\Delta x} + 1 \quad (3.33)$$

where  $I$  is an arithmetic integer term that describes the point of data.

Then the equation of the straight line shown in Figure 3.10 can be expressed as;

$$WH(x) = A_0 + A_1x \quad (3.34)$$

The values of the  $A_1$  and  $A_0$  in Eq. (3.34) can be obtained from the knowledge of geometry as;

$$A_1 = \frac{WH(I+1) - WH(I)}{\Delta x} \quad (3.35)$$

$$A_0 = WH(I+1) - IA_1\Delta x \quad (3.36)$$

If Eqs. (3.32) and (3.34) are combined, then the final expression of the total dynamic head can be written as;

$$tdh = H_R(\alpha^2 + v^2) \left[ A_0 + A_1 \left( \pi + \tan^{-1} \frac{v}{\alpha} \right) \right] \quad (3.37)$$

Valve head loss can be obtained as;

$$vhl = \frac{\Delta H v |v|}{\tau^2} \quad (3.38)$$

where;

$\Delta H$  = Valve head loss value when the discharge is  $Q_R$  and  $\tau$  value is 1.

It is known that the  $\tau$  data is provided in tabular form, which has a fixed time increment.

Then the head balance equation is rewritten as;

$$\begin{aligned} HCP - B_S Q_{P_1} + H_R(\alpha^2 + v^2) \left[ A_0 + A_1 \left( \pi + \tan^{-1} \frac{v}{\alpha} \right) \right] \\ - \frac{\Delta H v |v|}{\tau^2} = HCM + B Q_{P_1} \end{aligned} \quad (3.39)$$

By using the equations of  $HPM = HCP - HCM$ ,  $Q_{P_1} = vQ_R$ , and  $B_S Q = (B_S + B)Q_R$ , Eq. (3.39) can be simplified as;

$$\begin{aligned} F_1 = HPM - B_S Q v + H_R(\alpha^2 + v^2) \left[ A_0 + A_1 \left( \pi + \tan^{-1} \frac{v}{\alpha} \right) \right] \\ - \frac{\Delta H v |v|}{\tau^2} = 0 \end{aligned} \quad (3.40)$$

Where the unknowns are  $\alpha$  and  $v$ . To solve this equation, speed change equations must also be obtained.



### 3.4.3.2 Calculation of Change in Speed

The value of the rotational speed of a pump varies for each time step when a transient phenomenon occurs in a hydraulic system. In other words, the rotational speed changes because of the unbalanced torque applied by the rotating components. This torque equation can be expressed as;

$$T = -\frac{WR_g^2}{g} \frac{d\omega}{dt} \quad (3.41)$$

where;

$W$  = Summation of the weight of rotational parts and entrained liquid

$R_g$  = Radius-of-gyration-of-the rotating mass

$\omega$  = Angular velocity that is in radians/s

$d\omega/dt$  = Angular acceleration

The value of the unbalanced torque mentioned above may be expressed as the average of the two torque values, the initial torque value at the beginning of the time step ( $\Delta t$ ),  $T_0$ , and the unknown torque value at the end of the time step ( $\Delta t$ ),  $T_p$ . Since

$$\omega = N_R \frac{2\pi}{60} \alpha \quad \beta_0 = \frac{T_0}{T_R} \quad \beta = \frac{T_P}{T_R} \quad (3.42)$$

Then, by using Eq. (3.42), Eq. (3.41) can be rewritten as;

$$\beta = \frac{WR_g^2}{g} \frac{N_R}{T_R} \frac{\pi}{15} \frac{(\alpha_0 - \alpha)}{\Delta t} - \beta_0 \quad (3.43)$$

The term  $C_{31}$  is defined as to express Eq. (3.43) in a different form;

$$C_{31} = \frac{WR_g^2}{g} \frac{N_R}{T_R} \frac{\pi}{15\Delta t} \quad (3.44)$$

So Eq. (3.43) is rewritten as;

$$\beta + \beta_0 - C_{31}(\alpha_0 - \alpha) = 0 \quad (3.45)$$

A similar linearization approximation procedure can be applied for the characteristic torque curve, which is  $WB(x)$  as;

$$WB(x) = \frac{\beta}{\alpha^2 + v^2} = B_0 + B_1\left(\pi + \tan^{-1}\frac{v}{\alpha}\right) \quad (3.46)$$

The values of the  $B_1$  and  $B_0$  in Eq. (3.46) can also be determined from the knowledge of geometry as similar in Eqs. (3.35) and (3.36). Then the final expression of the speed change equation can be written as;

$$F_2 = (\alpha^2 + v^2) \left[ B_0 + B_1 \left( \pi + \tan^{-1} \frac{v}{\alpha} \right) \right] + C_{31}(\alpha_0 - \alpha) = 0 \quad (3.47)$$

where;

$\alpha_0$  = Dimensionless speed at the beginning of the time step ( $\Delta t$ )

The unknowns are  $\alpha$  and  $v$  for Eq. (3.47).

### 3.4.3.3 Pumps with Check Valve

Check valves are manually or automatically operated valves which are used to prevent reverse flow toward the pump. If a check valve is used with a pump, it is assumed that the values of the head loss are constant for the flow, which is in the forward direction. Eq. (3.48) can be used to simulate check valve motion.

$$F_3 = H_{CP} - H_{CM} + H_R \alpha^2 WH \left( \frac{\pi}{\Delta X} + 1 \right) \quad (3.48)$$

If the  $F_3 > 0$ , it can be observed that there is a positive flow in the system; otherwise, the  $v$  value will be zero caused by the check valve.

### 3.4.4 Equations for Single Pump Boundary

In previous subsections,  $F_1$  and  $F_2$ , which are head balance and change in speed equations, are determined as Eqs. (3.40) and (3.47), respectively, for a single pump boundary. Then these two transient equations can be solved together mathematically by Newton Raphson Method.

$$F_1 + \frac{\partial F_1}{\partial v} \Delta v + \frac{\partial F_1}{\partial \alpha} \Delta \alpha = 0 \quad (3.49)$$

$$F_2 + \frac{\partial F_2}{\partial v} \Delta v + \frac{\partial F_2}{\partial \alpha} \Delta \alpha = 0 \quad (3.50)$$

At the beginning of any iteration, the initial  $v$  and  $\alpha$  values may be obtained as;

$$v = 2v_0 - v_{00} \quad (3.51)$$

$$\alpha = 2\alpha_0 - \alpha_{00} \quad (3.52)$$

In which  $\alpha_{00}$  and  $v_{00}$  values are one-time step before values for  $\alpha_0$  and  $v_0$ . Then the partial derivative equations may be expressed by using  $\alpha$  and  $v$  parameters as;

$$\frac{\partial F_1}{\partial v} = -B_S Q + H_R \left\{ 2v \left[ A_0 + A_1 \left( \pi + \tan^{-1} \frac{v}{\alpha} \right) \right] + A_1 \alpha \right\} - \frac{2\Delta H|v|}{\tau^2} \quad (3.53)$$

$$\frac{\partial F_1}{\partial \alpha} = H_R \left\{ 2\alpha \left[ A_0 + A_1 \left( \pi + \tan^{-1} \frac{v}{\alpha} \right) \right] - A_1 v \right\} \quad (3.54)$$

$$\frac{\partial F_2}{\partial v} = 2v \left[ B_0 + B_1 \left( \pi + \tan^{-1} \frac{v}{\alpha} \right) \right] - B_1 \alpha \quad (3.55)$$

$$\frac{\partial F_2}{\partial \alpha} = 2\alpha \left[ B_0 + B_1 \left( \pi + \tan^{-1} \frac{v}{\alpha} \right) \right] - B_1 v + C_{31} \quad (3.56)$$

Then, Eqs. (3.49) and (3.50) can be calculated for  $\Delta \alpha$  and  $\Delta v$  ;

$$\Delta \alpha = \frac{\left( \frac{F_2}{\frac{\partial F_2}{\partial v}} - \frac{F_1}{\frac{\partial F_1}{\partial v}} \right)}{\left( \frac{\frac{\partial F_1}{\partial \alpha}}{\frac{\partial F_1}{\partial v}} - \frac{\frac{\partial F_1}{\partial \alpha}}{\frac{\partial F_2}{\partial v}} \right)} \quad (3.57)$$

$$\Delta v = -\frac{F_1}{\frac{\partial F_1}{\partial v}} - \Delta \alpha \left( \frac{\frac{\partial F_1}{\partial \alpha}}{\frac{\partial F_1}{\partial v}} \right) \quad (3.58)$$

After the  $\Delta \alpha$  and  $\Delta v$  values are obtained for an iteration, these values are added to the one step before the iteration values of the  $\alpha$  and  $v$  respectively as;

$$v = v + \Delta v \quad (3.59)$$

$$\alpha = \alpha + \Delta \alpha \quad (3.60)$$

These calculation steps must be repeated until a specific tolerance number which is presented as TOL.

$$|\Delta\alpha| + |v| < \text{TOL} \quad (3.61)$$

where the value of TOL number can be selected as 0.0002 or close to this value. (Wylie & Streeter, 1978)

When the solutions of these equations are found with the completion of the iterations,  $A_0$ ,  $B_0$ ,  $A_1$ , and  $B_1$  values should be confirmed with using the newly determined  $\alpha$  and  $v$ . Then, the resultant integer can be expressed as;

$$\text{II} = \left( \frac{\pi + \tan^{-1} \frac{v}{\alpha}}{\Delta x} \right) + 1 \quad (3.62)$$

Formulation of the value of I is already expressed earlier in Eq. (3.33). Accordingly, when the value of II is equal to I, it can be said that the straight-line segments of WH and WB have the appropriate approximation for this solution. But when this condition is not provided, this process must be repeated by replacing I with II until the condition is satisfied.

### 3.5 Air Chamber with Orifice Entrance Boundary

Air chamber is one of the widely used protection devices to prevent undesirable results of water hammer phenomena. This device includes compressed air and water at its upper and lower parts, respectively. The air chamber device has two functions. These functions are:

- Decreasing the pressure with the inflow of liquid into the chamber during high-pressure increase case in the pipeline
- Increasing the pressure with the outflow of liquid from the chamber during negative pressure or column separation case in the pipeline

An orifice can be provided between the pipeline and the chamber to restrict flow passing through the chamber. If the orifice has a form that produces a different head

loss for each outflow from the chamber and inflow into the chamber scenarios, it is named a differential orifice. Differential orifice provides some advantageous situations. For instance, the inflow into the chamber can be more restricted than the outflow from the chamber in the existence of a significant pressure drop or column separation scenario in the pipeline system. This advantage provides that the flow through the pipeline from the chamber is as unrestricted as possible, and the flow through the chamber is restricted to minimize the size of the chamber, considering the cost.

In the design period of a hydraulic system, the optimal size and location of the air chamber can be determined by trial and error operations. Figure 3.11 shows an air chamber example that is connected to a pipeline with an orifice and its significant member or value notations. The method of characteristics logic will be used for the calculation of air chamber boundary conditions.

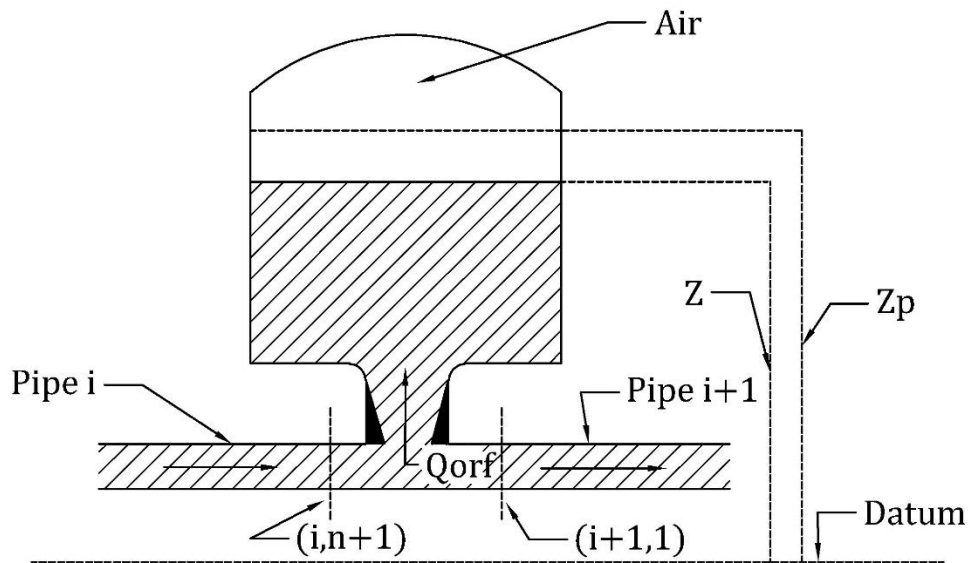


Figure 3.11 Air chamber with an orifice

As shown in Figure 3.11, the characteristics equations which belong to the first node of the pipe (i+1) and the last node of the pipe (i) can be used in calculations. So positive and negative characteristic equations for sections (i, n+1) and (i+1, 1), respectively, can be written as;

$$C^+: H_{P_{i,n+1}} = C_p - B_i Q_{P_{i,n+1}} \quad (3.63)$$

$$C^-: H_{P_{i+1,1}} = C_M + B_{i+1} Q_{P_{i+1,1}} \quad (3.64)$$

If it is provided that the losses at the junction, which connects the pipes, are negligible, head values before and after the junction are equal. Then the energy equation can be written as;

$$H_{P_{i+1,1}} = H_{P_{i,n+1}} \quad (3.65)$$

It is assumed that the flow through the air chamber has a positive sign and the flow out from the air chamber has a negative sign. Then the continuity equation can be written as;

$$Q_{P_{i,n+1}} = Q_{P_{i+1,1}} + Q_{P_{orf}} \quad (3.66)$$

where;

$Q_{P_{orf}}$  = Discharge which flows through the orifice of the air chamber at the end of time step  $\Delta t$ . ( $m^3/s$ )

If it is assumed that the condition of polytropic relation for a perfect gas is true for the air in the chamber. Then;

$$H_{P_{air}}^* V_{P_{air}}^m = C \quad (3.67)$$

where

$H_{P_{air}}^*$  = Absolute pressure head of the air at the end of the time step  $\Delta t$  (m)

$V_{P_{air}}^m$  = Volume of the air at the end of time step  $\Delta t$  ( $m^3$ )

$m$  = Exponent of polytropic gas equation

The polytropic gas equation exponent, which is  $m$ , has a value that is between 1 and 1.4.

$C$  is a constant, and it can be calculated by using the initial steady-state absolute pressure head of air and initial steady-state volume of air.

The absolute pressure head of the air at the end of time step  $\Delta t$  can be expressed as;

$$H_{P_{air}}^* = H_{P_{i,n+1}} + H_b - z_p - h_{P_{orf}} \quad (3.68)$$

where;

$z_p$  = Air chamber water surface elevation at the end of time step  $\Delta t$ . (m)

$H_b$  = Barometric pressure head (m)

$h_{\text{porf}}$  = Orifice head loss for discharge which flows through the orifice of the air chamber at the end of time step  $\Delta t$  (m)

The head loss for the discharge passing through the orifice can be obtained with;

$$h_{\text{porf}} = C_{\text{orf}} Q_{\text{Porf}} |Q_{\text{Porf}}| \quad (3.69)$$

where;

$C_{\text{orf}}$  = Coefficient of orifice losses

If there is a differential orifice, the coefficient of orifice losses has different values for inflow into the chamber and outflow from the chamber periods.

Basically, the changes in water level with respect to time cause changes in air volume in the chamber. Then, the air volume at the end of time step  $\Delta t$  can be expressed as;

$$V_{\text{P}_{\text{air}}} = V_{\text{air}} - A_c(z_p - z) \quad (3.70)$$

where;

$V_{\text{air}}$  = Volume of the air at the beginning of the time step ( $\text{m}^3$ )

$A_c$  = Cross-sectional area of the air chamber ( $\text{m}^2$ )

$z$  = Air chamber water surface elevation at the beginning of time step  $\Delta t$ . (m)

Then, Eq. (3.67) can be rewritten by using Eqs. (3.68), (3.69), and (3.70);

$$C = (H_{\text{P}_{i,n+1}} + H_b - z_p - C_{\text{orf}} Q_{\text{Porf}} |Q_{\text{Porf}}|) (V_{\text{air}} - A_c(z_p - z))^m \quad (3.71)$$

When we consider the conservation of mass law, the water surface elevation at the end of the time step  $\Delta t$  can be calculated as;

$$z_p = z + \frac{0.5(Q_{\text{orf}} + Q_{\text{Porf}})\Delta t}{A_c} \quad (3.72)$$

where;

$Q_{\text{orf}}$  = Discharge which flows through the orifice of the air chamber at the beginning of time step  $\Delta t$ . ( $\text{m}^3/\text{s}$ )

Finally, to simplify the equations, the head value at the end of the time step can be written with using the characteristic, continuity, and energy equations which are Eqs. (3.63), (3.64), (3.65), and (3.66);

$$H_{\text{P}_{i,n+1}} = \frac{B_i C_M + B_{i+1} C_P - B_i B_{i+1} Q_{\text{Porf}}}{B_i + B_{i+1}} \quad (3.73)$$

Now, there are three equations and three unknowns which are Eqs. (3.71), (3.72), and (3.73) and  $z_p$ ,  $Q_{p_{orf}}$ ,  $H_{P_{i,n+1}}$ , respectively. To solve the equations,  $z_p$  and  $H_{P_{i,n+1}}$  unknowns in Eq. (3.71) can be eliminated by using Eqs. (3.72) and (3.73). Then, a nonlinear equation is obtained with the unknown value of  $Q_{p_{orf}}$ . This equation can be solved by Newton- Raphson method. The iteration procedure can be started with using  $Q_{orf}$  as a first estimation.

### **3.6 Surge Tank Boundary**

Surge Tank is one of the widely used protection devices to prevent undesirable results of water hammer phenomena. A surge tank is a tank whose top is usually open to the atmosphere. The main functions of surge tanks are decreasing the head in high-pressure cases and increasing the head in negative-pressure cases by storing and supplying excess water, respectively. It is used to reduce the undesirable effects caused by the operation of turbines, pumps, or control valves. In the design procedure of a surge tank, the diameter and height of the surge tank must be selected properly to prevent overflow risk.

There is a wide variety of surge tanks according to their connection types to the pipeline, such as surge tank orifice, surge tank with standpipe, and shapes such as simple surge tanks, and one-way surge tanks. In this study, simple surge tank type and surge tank with a standpipe type are used as boundary conditions.

#### **3.6.1 Simple Surge Tank for Rapid Transient**

In the simple surge tank type, a direct connection between the pipeline and the tank is considered. There is no additional connection for transition as an orifice or standpipe. In other words, the situation can be accepted as that pipe, which connects a surge tank and pipeline, is too short, and it can be negligible in the calculation. Also, the head losses at junctions are negligible.



In this chapter, the method of characteristics is used for the simple surge tank in a hydraulic system that has a rapid transient event or water hammer. Figure 3.12 shows a simple surge tank illustration that is directly connected to a pipeline and its significant member or value notations.

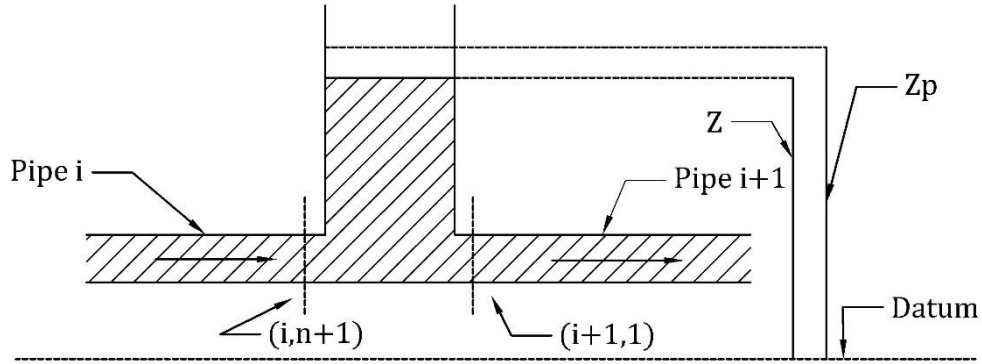


Figure 3.12 Simple surge tank

As shown in Figure 3.12, the characteristics equations, which belong to the first node of the pipe (i+1) and the last node of the pipe (i) can be used in calculations. So positive and negative characteristic equations for sections (i, n+1) and (i+1, 1), respectively, can be written as;

$$C^+: H_{P_{i,n+1}} = C_p - B_i Q_{P_{i,n+1}} \quad (3.74)$$

$$C^-: H_{P_{i+1,1}} = C_M + B_{i+1} Q_{P_{i+1,1}} \quad (3.75)$$

It is assumed that the flow through the surge tank has a positive sign and the flow out from the tank has a negative sign. Then the continuity equation can be written as;

$$Q_{P_{i,n+1}} = Q_{P_{i+1,1}} + Q_{P_{st}} \quad (3.76)$$

$Q_{P_{st}}$  = Inflow through the surge tank at the end of time step  $\Delta t$ . ( $m^3/s$ )

As it is mentioned, the losses at the junction, which connects the pipes, are negligible, so head values before and after the junction are equal. Then the energy equation can be written as;

$$H_{P_{i+1,1}} = H_{P_{i,n+1}} = z_p \quad (3.77)$$

where;

$z_p$  = Surge tank water surface elevation at the end of time step  $\Delta t$ . (m)

If the time step value, which is  $\Delta t$ , is small, the water surface elevation equation can be expressed as;

$$z_p = z + \frac{0.5(Q_{st} + Q_{Pst})\Delta t}{A_{st}} \quad (3.78)$$

where;

$z$  = Surge tank water surface elevation at the end of time step  $\Delta t$ . (m)

$Q_{st}$  = Inflow through the surge tank at the beginning of the time step  $\Delta t$ . ( $m^3/s$ )

$A_{st}$  = Cross-sectional area of the surge tank ( $m^2$ )

Finally, to simplify the equations, the head value at the end of the time step can be written with using the characteristic, continuity, energy, and water level equations which are Eqs. (3.74), (3.75), (3.76), (3.77), and (3.78):

$$H_{P_{i,n+1}} = \frac{B_i C_M + B_{i+1} C_P + B_i B_{i+1} Q_{st} + (2B_i B_{i+1} A_{st} z)/\Delta t}{B_i + B_{i+1} + (2B_i B_{i+1} A_{st})/\Delta t} \quad (3.79)$$

Then, the value of  $H_{P_{i,n+1}}$  is obtained from Eq. (3.79). The other unknown values can be calculated by using Eqs. (3.74), (3.75), (3.76), (3.77), and (3.78) (Chaudhry, 2014).

### 3.6.2 Simple Surge Tank for Slow Transient

In the previous simple surge tank boundary, the method of characteristics is used for rapid transient conditions such as distributed systems. On the other hand, in this boundary condition, the lumped-system approach must be applied in calculations to analyze slow transients. The main reason for using a different method is that oscillations of water level in a simple surge tank are slow. For instance, load change on a turbine can cause water level change in the surge tank, and the methods used in rapid transient cannot be used in this situation to determine the oscillation of the water. Figure 3.13 illustrates an example of a simple surge tank and some important notations for the tunnel and tank.

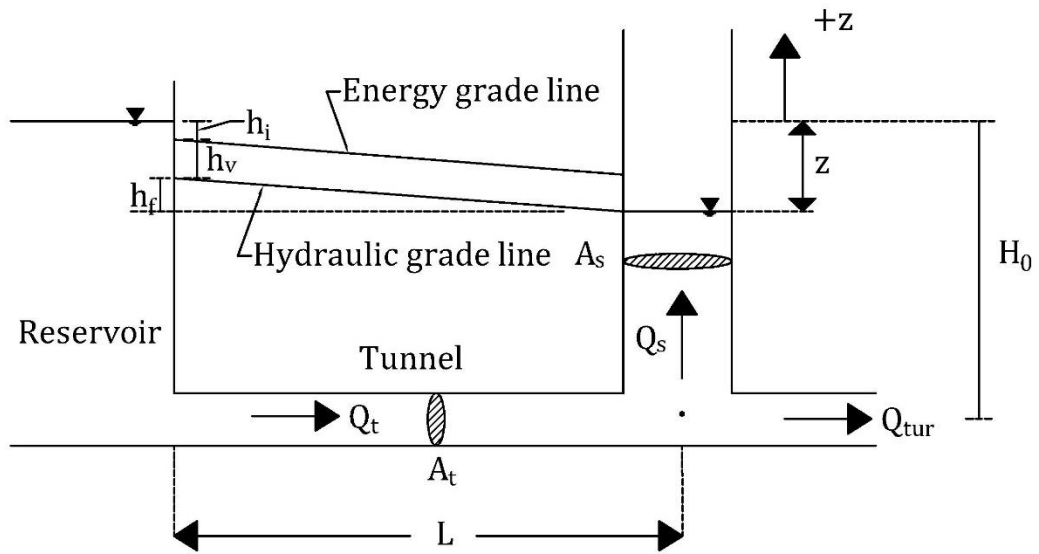


Figure 3.13 Notations of a system that includes simple surge tank

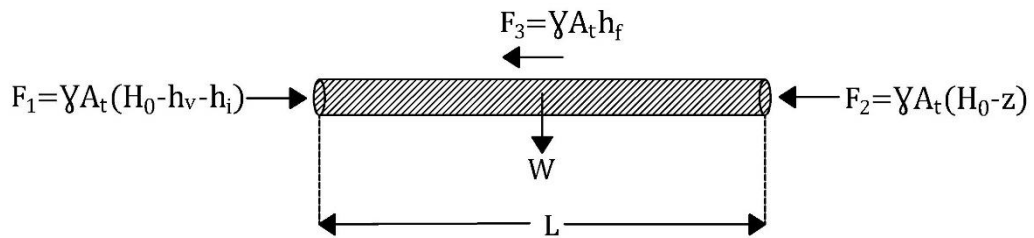


Figure 3.14 Free-body diagram for the water in the tunnel (Chaudhry, 1979)

As shown in the free-body diagram in Figure 3.14, the resultant force acting on the water can be calculated as;

$$F_r = \gamma A_t (-z - h_v - h_i - h_f) \quad (3.80)$$

where;

$A_t$  = Area of the tunnel ( $m^2$ )

$z$  = Water level in the tank above the reservoir level (m)

$h_v$  = Velocity head (m)

$h_i$  = Intake head losses (m)

$h_f$  = Friction and form losses in the tunnel (m)

The resultant force can be equalized with the rate of change of momentum of the water in the tunnel according to Newton's 2<sup>nd</sup> Law. After the simplification, the equation can be written as;

$$\frac{dQ}{dt} = \frac{gA_t}{L} (-z - h_v - h_i - h_f) \quad (3.81)$$

Then,  $h = cQ|Q|$  equality can be used to rewrite Eq. (3.81),

$$\frac{dQ}{dt} = \frac{gA_t}{L} (-z - cQ|Q|) = F_1(Q, z, t) \quad (3.82)$$

where;

$$c = \text{Constant} = \frac{1 + k + \frac{fL}{D_t}}{2g}$$

$k$  = Entrance loss coefficient

$L$  = Length of the tunnel (m)

$D_t$  = Diameter of the tunnel (m)

Finally, Eq. (3.82) is called dynamic equation. In order to obtain continuity equation, the conservation of mass principle is used for the junction which connects the tunnel and the simple surge tank.

$$Q = Q_{st} + Q_{tur} \quad (3.83)$$

where;

$Q_{st}$  = Flow through the simple surge tank ( $m^3/s$ )

$Q_{tur}$  = Turbine flow ( $m^3/s$ )

Due to  $Q_{st} = A_{st}(dz/dt)$ , the continuity equation can be expressed as;

$$\frac{dz}{dt} = \frac{Q - Q_{tur}}{A_{st}} = F_2(Q, z, t) \quad (3.84)$$

where;

$A_{st}$  = Area of the simple surge tank ( $m^2$ )

As a result, both continuity and dynamic equation are functions of  $Q$ ,  $z$ , and  $t$ . Then, time-dependent  $z$  and  $Q$  values are obtained from Eqs. (3.82) and (3.84) by using a numerical method which is the Runge-Kutta method (Chaudhry, 1979).

### 3.6.3 Surge Tank with Standpipe

Surge Tank may be connected to the pipeline with a standpipe. In this type of boundary condition, calculations have different additions relative to other types of surge tanks because of standpipe considerations. Figure 3.15 shows a surge tank illustration that is connected to a pipeline with a standpipe and its significant member or value notations.

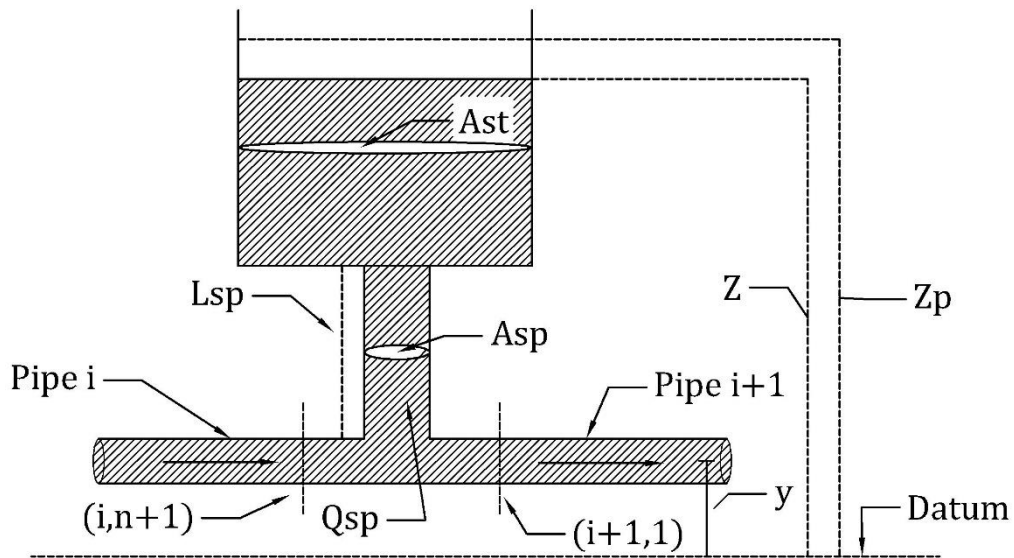


Figure 3.15 Surge tank with standpipe and notations

It is assumed that the flow through the surge tank has a positive sign and the flow out from the tank has a negative sign. Then the continuity equation can be written as;

$$Q_{P_{i,n+1}} = Q_{P_{i+1,1}} + Q_{P_{sp}} \quad (3.85)$$

where;

$Q_{P_{sp}}$  = Inflow through the standpipe at the end of time step  $\Delta t$ . ( $m^3/s$ )

As shown in Figure 3.15, the characteristics equations which belong to first node of the pipe (i+1) and last node of the pipe (i) can be used in calculations. So positive and negative characteristic equations can be written as;

$$C^+: H_{P_{i,n+1}} = C_p - B_i Q_{P_{i,n+1}} \quad (3.86)$$

$$C^-: H_{P_{i+1,1}} = C_M + B_{i+1} Q_{P_{i+1,1}} \quad (3.87)$$

The losses at the junction, which connects the pipes, are negligible, so head values before and after the junction are equal. After the simplification of characteristics equations and continuity equation, the energy equation can be written as;

$$H_{P_{i+1,1}} = H_{P_{i,n+1}} = \frac{B_i C_M + B_{i+1} C_p - B_i B_{i+1} Q_{P_{sp}}}{B_i + B_{i+1}} \quad (3.88)$$

The water surface elevation equation can be expressed as;

$$z_p = z + \frac{0.5 (Q_{sp} + Q_{P_{sp}}) \Delta t}{A_{st}} \quad (3.89)$$

where;

$z_p$  = Surge Tank water surface elevation at the end of time step  $\Delta t$ . (m)

$z$  = Surge tank water surface elevation at the end of time step  $\Delta t$ . (m)

$Q_{sp}$  = Inflow through the standpipe at the beginning of the time step  $\Delta t$ . (m<sup>3</sup>/s)

$A_{st}$  = Cross-sectional area of the surge tank (m<sup>2</sup>)

The length of the standpipe is generally shorter than the pipes in the pipeline. Then it can be considered that the water inside the standpipe is lumped mass (Riasi et al., 2010). The weight of the water in the standpipe can be calculated as;

$$W = \gamma A_{sp} L_{sp} \quad (3.90)$$

where;

$A_{sp}$  = Cross-sectional area of the standpipe (m<sup>2</sup>)

$L_{sp}$  = Length of the standpipe (m)

The friction force can be expressed as;

$$F_f = \frac{f \gamma A_{sp} L_{sp} Q_{sp} |Q_{sp}|}{2g D_{sp} A_{sp}^2} \quad (3.91)$$

where;

$f$  = Friction factor of standpipe

$D_{sp}$  = Diameter of the standpipe (m)

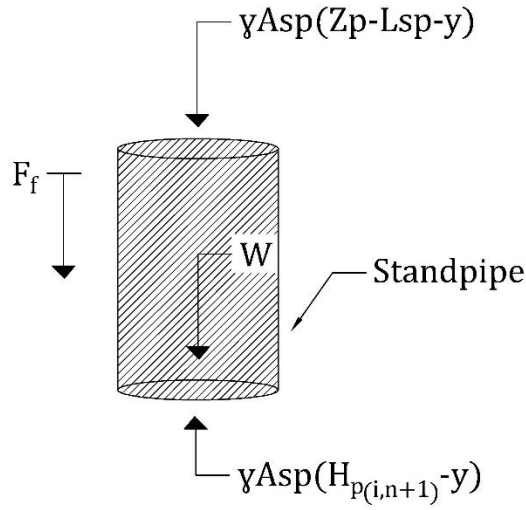


Figure 3.16 Free body diagram for standpipe

If the free body diagram of the standpipe is considered as shown in Figure 3.16 with using the acceleration of the flow in the standpipe, the below equation can be written;

$$\gamma A_{sp} \frac{L_{sp}}{g A_{sp}} \frac{dQ_{sp}}{dt} = \gamma A_{sp} (H_{P_{i,n+1}} - (z_p - L_{sp})) - W - F_f \quad (3.92)$$

After the simplification of the equation, it can be expressed as;

$$Q_{P_{sp}} = \frac{g \Delta t A_{sp}}{L_{sp}} (H_{P_{i,n+1}} - z_p - F_f) + Q_{sp} \quad (3.93)$$

Eq. (3.93) can be rewritten by using Eqs. (3.88), (3.89), (3.91), and (3.87). Then,  $Q_{P_{sp}}$  can be obtained.





## CHAPTER 4

### THE SOFTWARE PROGRAM

In this chapter, the software program that is developed in the study, its main contents, and its abilities will be presented. The program is introduced as three main parts, which are the main user interface, minor windows, and objects with their properties windows.

#### 4.1 Main User Interface

In the main user interface that appears with the program's opening, there are different tabs, a design area (canvas), a message box, and a panel where the properties of objects in the system can be entered.

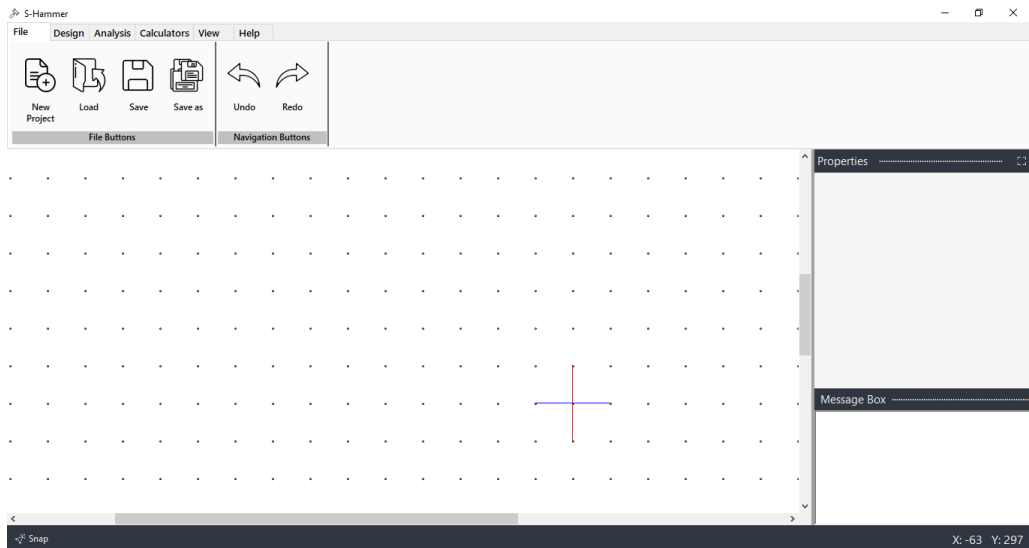


Figure 4.1 Main user interface

As shown in Figure 4.1, the main interface window has six tabs which are file, design, analysis, calculators, view, and help tabs. These tabs contain different options and buttons that can be used for various functions.

## 4.1.1 Main User Interface Tabs

### 4.1.1.1 File Tab

When the program is opened, the file tab appears as automatically selected in the main form. This tab includes file and navigation buttons. File buttons can be listed as ‘New Project,’ ‘Load,’ ‘Save,’ and ‘Save as’ buttons, as shown in Figure 4.2. These buttons are used to create and save a new project or open an existing project.

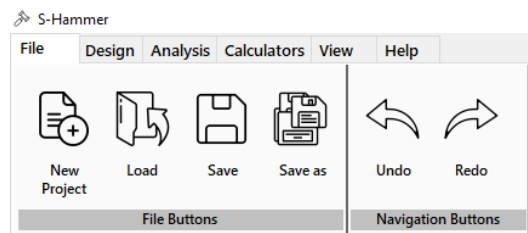


Figure 4.2 The view of file tab

### 4.1.1.2 Design Tab

The design tab contains design components, initial settings, and engineering settings buttons as shown in Figure 4.3. The design components buttons are used to draw selected items on the canvas, thereby visualizing the hydraulic system. These buttons are ‘Pipe,’ ‘Reservoir,’ ‘Valve,’ and ‘Dead-End,’ ‘Pump,’ ‘Turbine,’ ‘Junction,’ ‘Air Chamber,’ ‘Surge Tank’ component buttons.

In this tab, it is also provided that the user can edit valve closure settings, pump settings, initial conditions, and analysis options. In addition, this tab includes the engineering library button, which opens the engineering library form that will be explained in subsection 4.2.1.

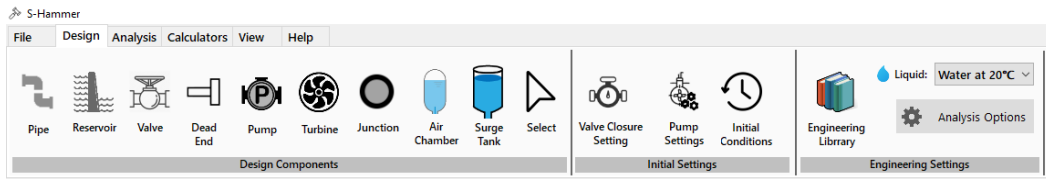


Figure 4.3 The view of design tab

#### 4.1.1.3 Analysis Tab

The analysis tab contains two types of button sets which are run selection buttons and simulation results buttons, as shown in Figure 4.4. Run selection buttons set has the computation of steady-state button, transient state computation button, and a button to stop analyzing. In this tab, there are also various simulation result buttons, which are activated after the computations are completed. Simulation forms will be explained in subsection 4.2.9.

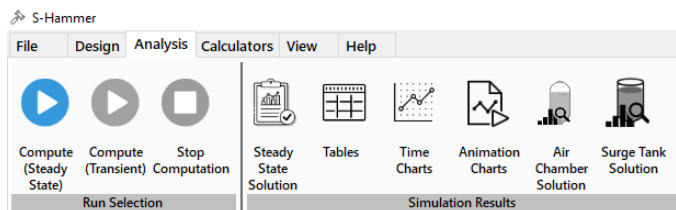


Figure 4.4 The view of analysis tab

#### 4.1.1.4 Calculators Tab

In the calculators tab, there are wave speed, Reynolds number, and friction factor calculator buttons which are shown in Figure 4.5. Moreover, there is a button that can open the surge tank simulator form explained in subsection 4.2.8.

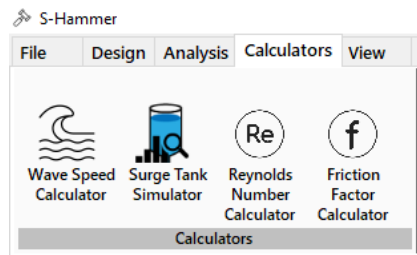


Figure 4.5 The view of calculators tab

#### 4.1.1.5 View Tab

The view tab is the tab that includes visual options and different features for the design canvas. This tab has four main parts: grid options, draw objects, text options, and canvas view options, as shown in Figure 4.6. In the grid option part, the user can change the design canvas's grid type, color, and background color as desired. Draw objects and text options parts can be used to add a line, rectangle, circle items, and text on the design canvas. In addition, the canvas view part includes two buttons that can be used to save the display of the canvas as an image file and for panning the design canvas.

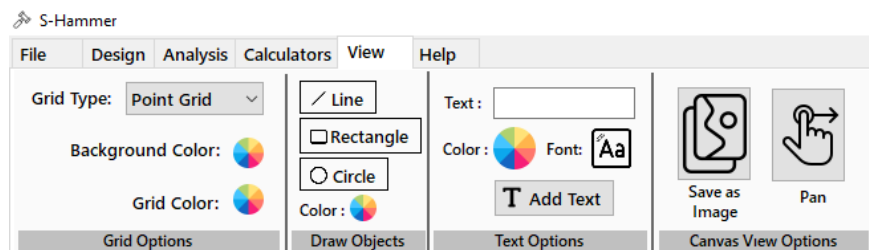


Figure 4.6 The view of view tab

#### 4.1.1.6 Help Tab

The help tab contains the text of the contact information provided to the user for any problem that may occur and a button that can open the quick start user guide document for new users, as shown in Figure 4.7.

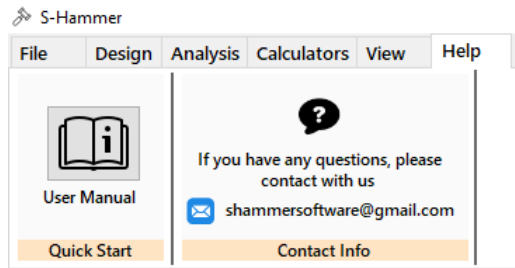


Figure 4.7 The view of help tab

### 4.1.2 Design Canvas

In the main user interface, there is an area where the user can visually design the hydraulic system. This area is called the design canvas. The design canvas has point and grid view options to facilitate the user's drawing. The point-view design canvas is shown in Figure 4.8 with a sample drawing. In addition, snap points are available to easily connect the components that the user will add to the canvas. Objects which can be added to the canvas can be listed as pipe, reservoir, valve, dead end, pump, surge tank, air chamber, and junction. In addition, the user can add various extra shapes and text with the buttons on the view tab.

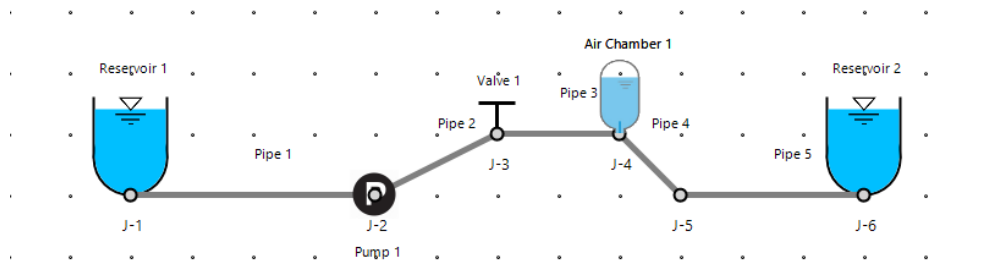


Figure 4.8 Design canvas view

### 4.1.3 Message Box

The message box is located in the main interface's lower right corner, and the view of the box is shown in Figure 4.9. The message box lists and summarizes the actions taken by the user during the design and analysis process.

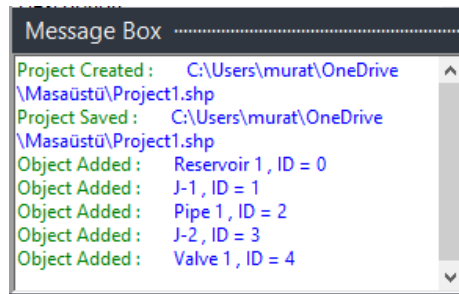


Figure 4.9 Message box

#### 4.1.4 Properties Panel

As shown in Figure 4.1, an empty area for the property panel appears on the right side of the main window. The panel is designed for the user to easily enter the properties and input data of the components in the system. This property panel is designed to automatically display the properties of any component drawn on the canvas when it is selected. The view of the properties panel for a valve component is shown in Figure 4.10 as an example. These properties panels are explained in detail for each component in subsection 4.3.

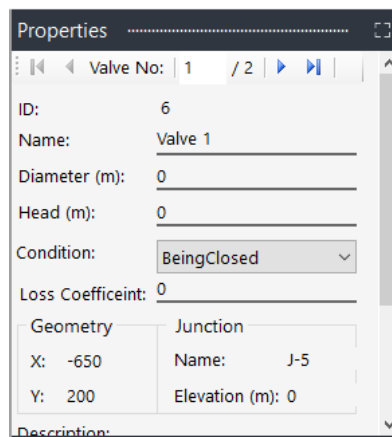


Figure 4.10 The view of the properties panel (example for a valve component)

## 4.2 Minor Interface Windows

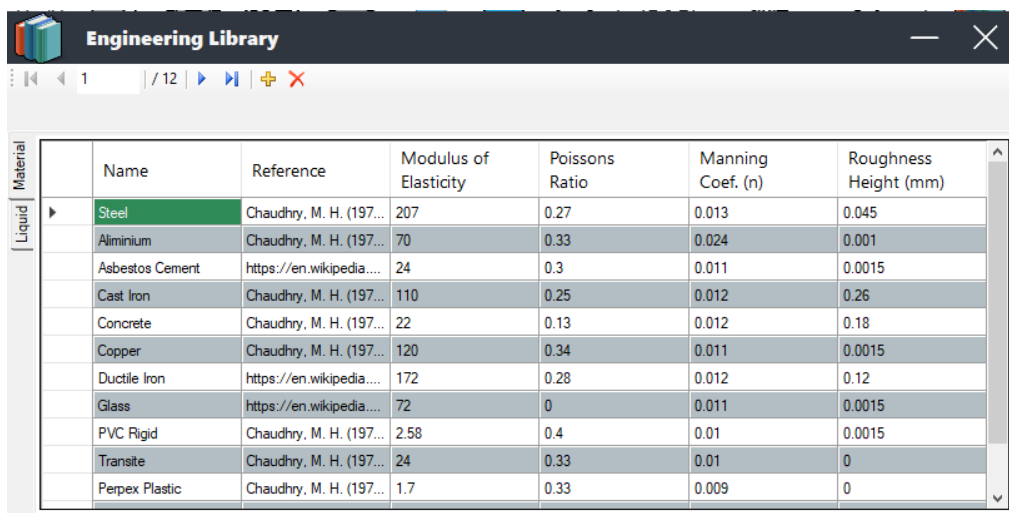
The main window of the program includes different buttons that can open various useful minor pop-up windows. These minor interface windows and their functions will be introduced in this section.

### 4.2.1 Engineering Library Window

The engineering library button in the design tab opens a form where the user can add different types of data and examine the added values. There are two tabs in the engineering library form, which are materials and fluids. These tabs include useful data defined in the material and the liquid library.

#### 4.2.1.1 Material Library

The material library includes various types of pipe materials and their properties that can be used in the proper calculations. These materials and properties are presented and listed in a table, as shown in Figure 4.11.



The screenshot shows a window titled "Engineering Library" with a navigation bar at the top. Below the navigation bar is a table with the following columns: Name, Reference, Modulus of Elasticity, Poissons Ratio, Manning Coef. (n), and Roughness Height (mm). The table lists various materials and their corresponding properties.

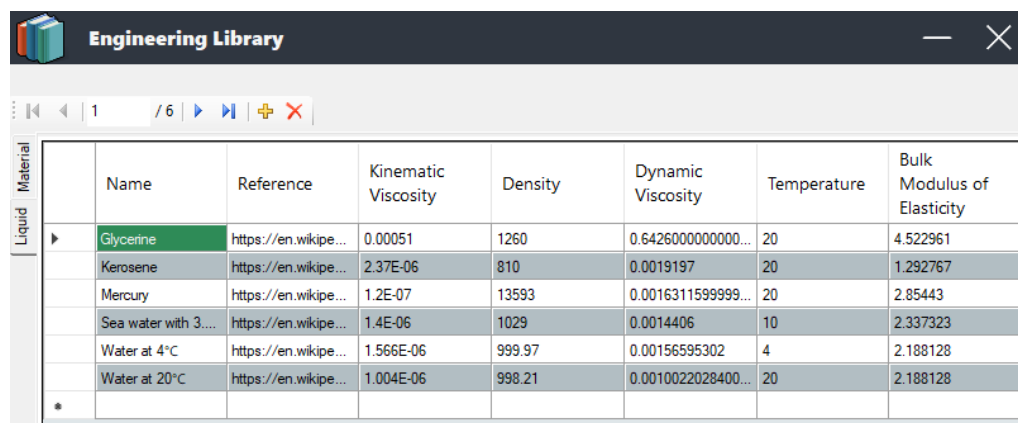
	Name	Reference	Modulus of Elasticity	Poissons Ratio	Manning Coef. (n)	Roughness Height (mm)
Material	Steel	Chaudhry, M. H. (197...	207	0.27	0.013	0.045
Liquid	Aluminium	Chaudhry, M. H. (197...	70	0.33	0.024	0.001
	Asbestos Cement	<a href="https://en.wikipedia...">https://en.wikipedia...</a>	24	0.3	0.011	0.0015
	Cast Iron	Chaudhry, M. H. (197...	110	0.25	0.012	0.26
	Concrete	Chaudhry, M. H. (197...	22	0.13	0.012	0.18
	Copper	Chaudhry, M. H. (197...	120	0.34	0.011	0.0015
	Ductile Iron	<a href="https://en.wikipedia...">https://en.wikipedia...</a>	172	0.28	0.012	0.12
	Glass	<a href="https://en.wikipedia...">https://en.wikipedia...</a>	72	0	0.011	0.0015
	PVC Rigid	Chaudhry, M. H. (197...	2.58	0.4	0.01	0.0015
	Transite	Chaudhry, M. H. (197...	24	0.33	0.01	0
	Perpex Plastic	Chaudhry, M. H. (197...	1.7	0.33	0.009	0

Figure 4.11 The view of the material library

In this tab, users can also add new materials and properties to use in the system. The material's properties can be listed as modulus of elasticity, Poisson's ratio, manning coefficient, and roughness height of materials. It must also be mentioned that the given materials and properties are provided from specific references.

#### 4.2.1.2 Liquid Library

The liquid library includes different types of liquid and their properties that can be used in calculations. These liquids and properties are presented and listed in a table, as shown in Figure 4.12. In this tab, users can also add new liquid types and properties to use in the system. The liquid's properties shown in the table can be listed as bulk modulus of elasticity, kinematic viscosity, dynamic viscosity, density, and temperature of the liquids. The given liquids and properties are provided from specific references.



The screenshot shows a window titled "Engineering Library" with a table of liquid properties. The table has columns for Name, Reference, Kinematic Viscosity, Density, Dynamic Viscosity, Temperature, and Bulk Modulus of Elasticity. The first row is highlighted in green and shows Glycerine with a kinematic viscosity of 0.00051, density of 1260, dynamic viscosity of 0.6426000000000000, temperature of 20, and bulk modulus of elasticity of 4.522961.

Liquid	Name	Reference	Kinematic Viscosity	Density	Dynamic Viscosity	Temperature	Bulk Modulus of Elasticity
	Glycerine	<a href="https://en.wikipe...">https://en.wikipe...</a>	0.00051	1260	0.6426000000000000...	20	4.522961
	Kerosene	<a href="https://en.wikipe...">https://en.wikipe...</a>	2.37E-06	810	0.0019197	20	1.292767
	Mercury	<a href="https://en.wikipe...">https://en.wikipe...</a>	1.2E-07	13593	0.0016311599999...	20	2.85443
	Sea water with 3...	<a href="https://en.wikipe...">https://en.wikipe...</a>	1.4E-06	1029	0.0014406	10	2.337323
	Water at 4°C	<a href="https://en.wikipe...">https://en.wikipe...</a>	1.566E-06	999.97	0.00156595302	4	2.188128
	Water at 20°C	<a href="https://en.wikipe...">https://en.wikipe...</a>	1.004E-06	998.21	0.0010022028400...	20	2.188128
*							

Figure 4.12 The view of the liquid library

#### 4.2.2 Initial Conditions Window

The initial conditions window, which is opened with a button on the design tab, has two sections: time options and hydraulic conditions, as shown in Figure 4.13. In the time options part, the user can define a maximum time and time step interval for the analysis. In addition, the program automatically calculated the maximum allowable



time step that must be selected to provide Courant conditions for the hydraulic system. In the hydraulic conditions part, there are three initial setting types to determine the initial flow for the system. It is ensured that the user can add inputs according to the type of value provided for the hydraulic system to be analyzed.

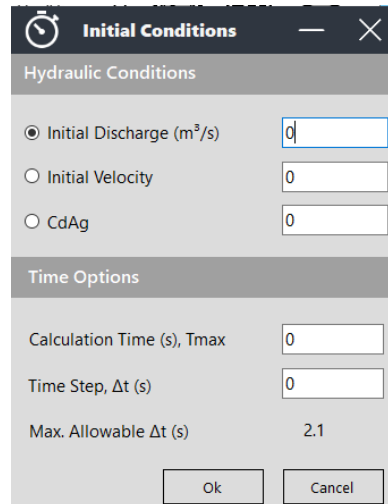


Figure 4.13 Initial conditions window

### 4.2.3 Valve Closure Settings Window

The valve closure settings window is where the user can enter and edit the time-dependent closure data of the valves in the system. In this window, two options, regular closing data and tabular data entries, are provided for the user to determine the valve closure data, as shown in Figure 4.14. If the user selects the regular closure data type, the desired parameters in Eq. (3.7) must be entered as input. On the other hand, if the user wants to enter the data in tabular form, the data can be imported from an excel file or entered manually.

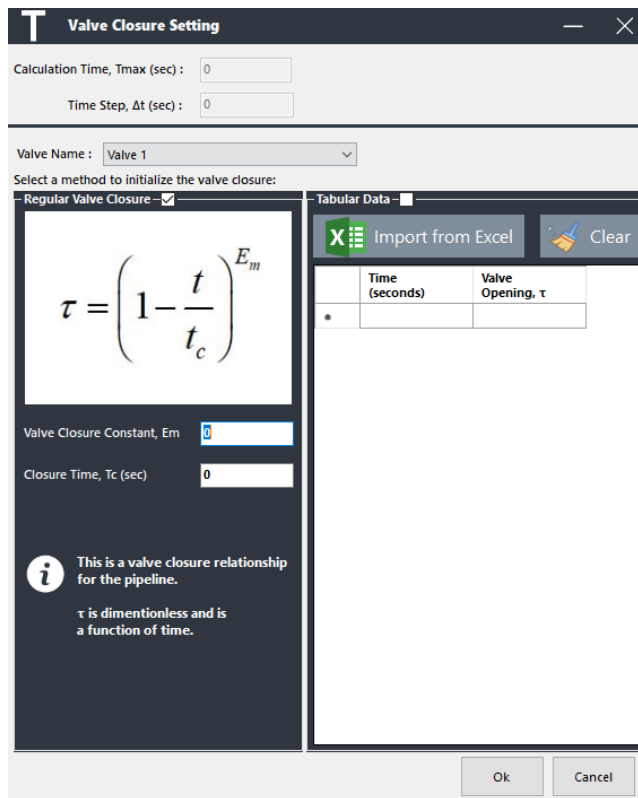


Figure 4.14 The view of the valve closure setting window

#### 4.2.4 Pump Settings Window

The pump setting window is where the user can add and edit pump settings. In this form, it is aimed that the user can create data sets containing rated values and curve data values that can be used for a pump component, as shown in Figure 4.15. In the pump curve data section of this form, three curve data that are available in the literature are given to the user. In addition to these data, an additional option is provided for the user to add different curve data. The additional curve data values can be imported from an excel file or entered manually. Moreover, a chart panel is presented in this form so that the user can visually observe the curve data entered.

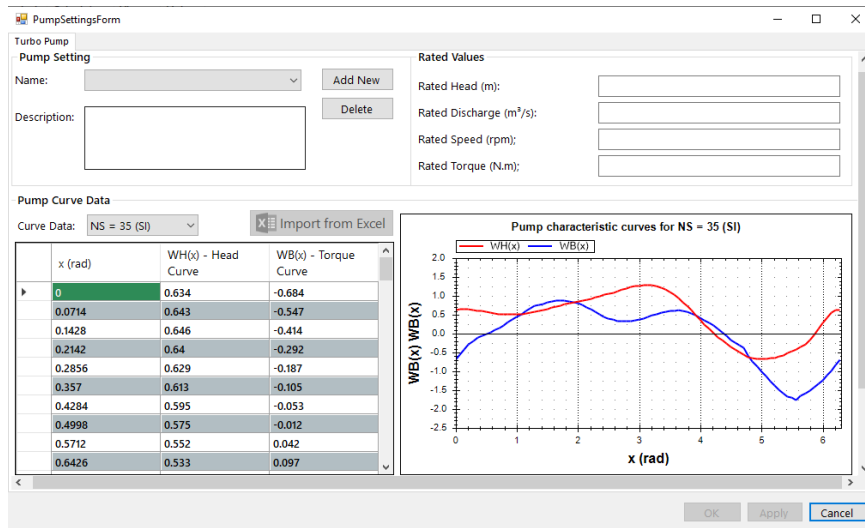


Figure 4.15 The view of the pump setting window

#### 4.2.5 Wave Speed Calculator Window

The wave speed calculator window can be opened with the wave speed calculator button in the calculators tab of the main user window. In this window shown in Figure 4.16, the user can calculate the wave speed using the pipe material properties, diameter, thickness, support situation, and fluid properties data. Eq. (2.29) is used in the program for the calculation of wave speed. Moreover, if there is a defined pipe on the design canvas, the user can select the pipe and add the calculated wave speed value to the proper area of the pipe property panel by using the apply button.

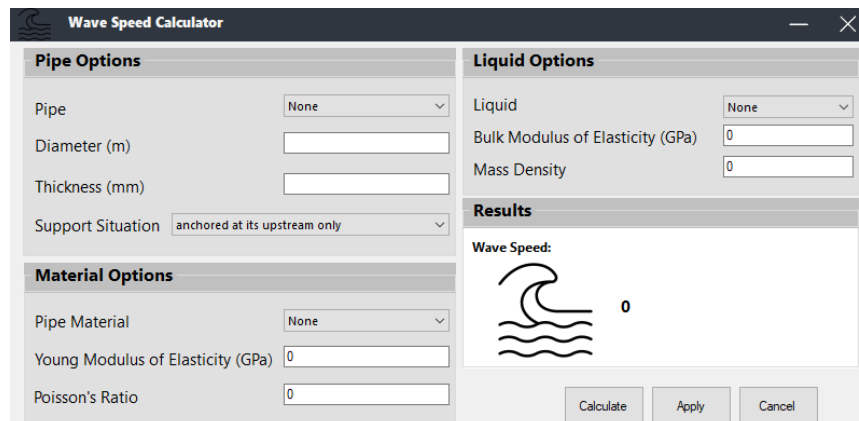


Figure 4.16 The view of the wave speed calculator window

#### 4.2.6 Reynolds Number Calculator Window

The Reynolds number calculator window can be opened with the Reynolds number calculator button in the calculators tab of the main user window. In this window, which is shown in Figure 4.17, the user can calculate the Reynolds number using the diameter of pipe, velocity and kinematic viscosity of the liquid. Eq. (4.1) is used for the program to calculate the Reynolds number. Moreover, suppose there is a defined pipe on the design canvas. In that case, the user can select the pipe and add the calculated Reynolds number value to the proper area of the pipe properties panel by using the apply button.

$$\text{Re} = \frac{\rho V D}{\mu} = \frac{V D}{\nu} \quad (4.1)$$

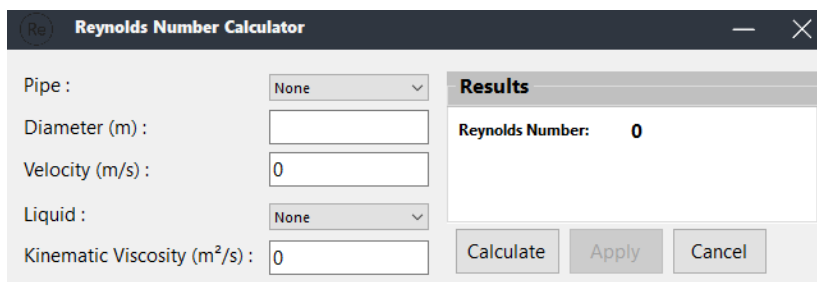


Figure 4.17 Reynolds number calculator window

#### 4.2.7 Friction Factor Calculator Window

The friction factor calculator is a window opened with the friction factor calculator button in the Calculators tab of the main user window. In this window shown in Figure 4.18, the user can calculate the Darcy-Weisbach friction factor using the diameter, roughness height of pipe, and Reynolds number. Moreover, if there is a defined pipe on the design canvas, the user can select the pipe and add the calculated friction factor value to the proper area of the pipe properties panel by using the apply button. Eq. (4.2) and Eq. (4.3) are used for the program to calculate the friction factor.

$$f = \frac{64}{Re} \quad (4.2)$$

Eq. (4.2) is used to calculate the friction factor if  $Re \leq 2000$ , where the flow is laminar.

$$f = \frac{1.325}{\left[ \ln \left( \frac{\epsilon}{3.7D} + \frac{5.74}{Re^{0.9}} \right) \right]^2} \quad (4.3)$$

Eq (4.3) which is the explicit formula developed by Swamee and Jain (1976), is used when  $4000 \leq Re \leq 10^8$  where the flow is in the turbulent flow region and  $10^{-6} \leq \epsilon/D \leq 10^{-2}$ .

In addition, the Moody chart image, which can be used to determine the friction factor for calculations that do not meet the specified conditions mentioned above, is presented to the user in this window.

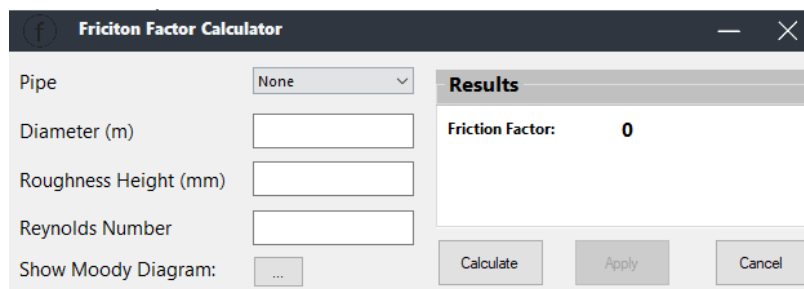


Figure 4.18 Friction factor calculator window

#### 4.2.8 Surge Tank Simulator Window

The calculators tab provides a button for the user to simulate simple systems, which include a simple surge tank. When the user clicks on this button, the surge tank simulator form appears as a minor window, as shown in Figure 4.19. In this window, after the required inputs are entered, the user can simulate the fluctuation height in the surge tank and discharge with respect to time in graphical form. In this simulation and calculation period, Eqs. (3.82) and (3.84) are solved with the Runge-Kutta method. This form also provides option buttons for the user to edit the charts visually.

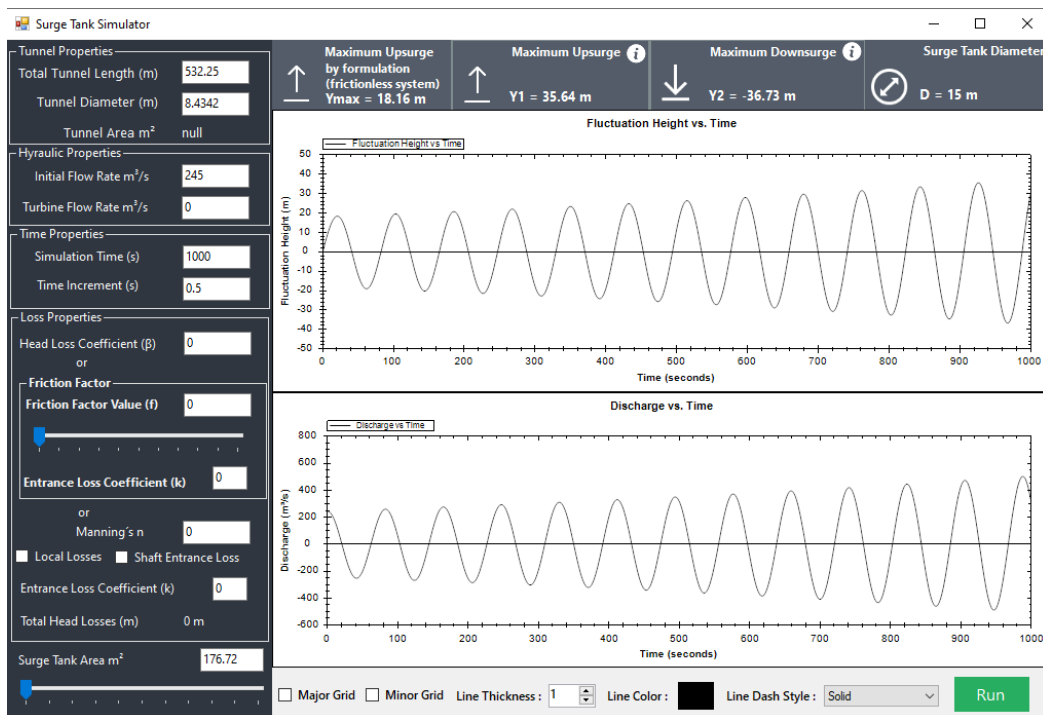


Figure 4.19 Simple surge tank simulator window

## 4.2.9 Tabular and Graphical Results Window

As previously presented in sub-section 4.1.1.3, the analysis tab of the main user interface consists of two parts. Computation can be done with the buttons in the run selection section. In the simulation results section, there are buttons that can open various windows where graphical and tabular results can be observed. This section will examine the general appearance and details of these windows.

### 4.2.9.1 Steady-State Results Window

When the user clicks on ‘compute for steady state’ button, the steady-state results window appears. In this form, the hydraulic grade line (HGL) and the energy grade line (EGL) are presented to users for the steady-state condition of the system. In addition, the initial discharge in the system, the diameter, the length of each pipe, the

elevation of each junction, and the velocity of the fluid passing through each pipe are also summarized in the form as shown in Figure 4.20.

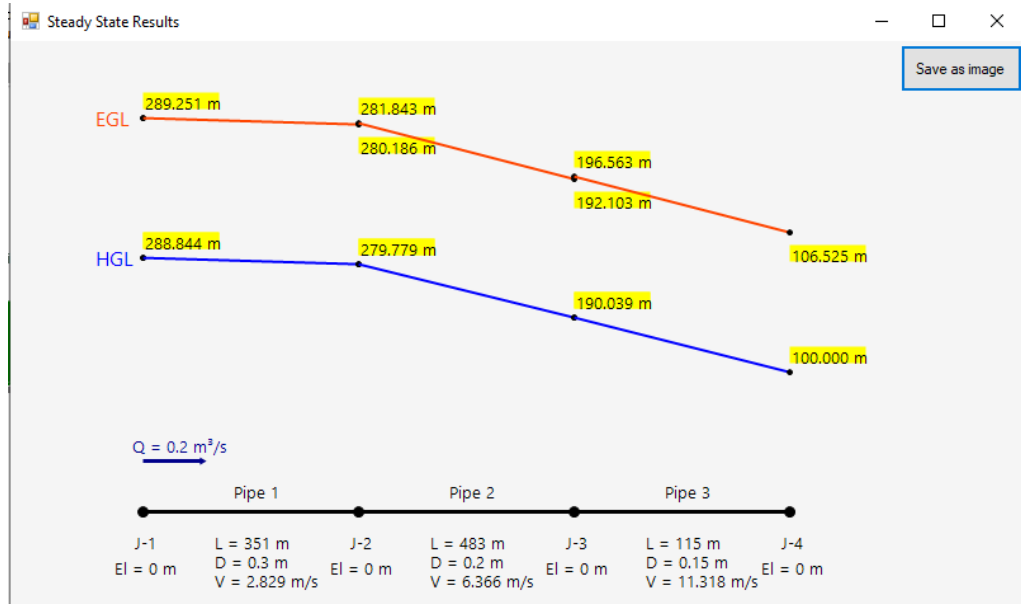


Figure 4.20 The view of the steady-state results window

#### 4.2.9.2 Tabular Transient Solution Window

When the transient computations are done, the tabular results can be obtained in the ‘Tables’ window. This window has three different tabs: time-based, pipe-based, and junction-based. In this panel, the user can view the results according to time, selected pipe, or selected junction in tabular form. Figure 4.21 shows an example result for the pipe-based table. In addition, there are a precision selection box and an ‘export to excel’ button so that the user can observe the results according to the desired decimal number and save the results, respectively.

Tables

Precision: 0,00

Time-Based Pipe-Based Junction-Based

Select a pipe : Pipe 2

Export to Excel Show Table

	Time (sec)	Object Name	Node No.	Distance from Reservoir (m)	Head (m)	Discharge (m <sup>3</sup> /s)	Velocity (m/s)	Pressure (KPa)	Tau
▶	0.00	Pipe 2	1	471.75	257.34	0.2	6.37	2526.09	1
	0.00	Pipe 2	2	592.5	234.91	0.2	6.37	2305.86	1
	0.00	Pipe 2	3	713.25	212.47	0.2	6.37	2085.64	1
	0.00	Pipe 2	4	834	190.04	0.2	6.37	1865.42	1
	0.10	Pipe 2	1	471.75	257.34	0.2	6.37	2526.09	0.87
	0.10	Pipe 2	2	592.5	234.91	0.2	6.37	2305.86	0.87
	0.10	Pipe 2	3	713.25	212.47	0.2	6.37	2085.64	0.87
	0.10	Pipe 2	4	834	190.04	0.2	6.37	1865.42	0.87
	0.20	Pipe 2	1	471.75	257.34	0.2	6.37	2526.09	0.73
	0.20	Pipe 2	2	592.5	234.91	0.2	6.37	2305.86	0.73
	0.20	Pipe 2	3	713.25	212.47	0.2	6.37	2085.64	0.73
	0.20	Pipe 2	4	834	209.13	0.2	6.21	2052.83	0.73
	0.30	Pipe 2	1	471.75	257.34	0.2	6.37	2526.09	0.6
	0.30	Pipe 2	2	592.5	234.91	0.2	6.37	2305.86	0.6
	0.30	Pipe 2	3	713.25	231.03	0.2	6.22	2267.75	0.6
	0.30	Pipe 2	4	834	236.93	0.19	5.98	2325.73	0.6
	0.40	Pipe 2	1	471.75	257.34	0.2	6.37	2526.09	0.47
	0.40	Pipe 2	2	592.5	252.94	0.2	6.22	2482.81	0.47
	0.40	Pipe 2	3	713.25	258.06	0.19	6	2533.16	0.47
	0.40	Pipe 2	4	834	280.17	0.18	5.64	2750.16	0.47
	0.50	Pipe 2	1	471.75	274.86	0.2	6.22	2698.02	0.33

Figure 4.21 The view of the tables window (pipe-based tab view)

### 4.2.9.3 Graphical Transient Solution Windows

When the transient computations are done, the graphical results can be obtained in the time-chart and animation chart windows, as shown in Figures 4.22 and 4.23, respectively. In time chart window, users can view the head, discharges, pressures, and velocity values with respect to time for the selected junction or the pipe node. In addition, there are various buttons to edit the visualization of the charts and lines in the window.

In the time chart window, it is also provided that users can draw two different charts at the same time for easy comparison. Moreover, the maximum and minimum values are provided to users for each chart.





Figure 4.22 The view of the time chart window

In the animation graph, the user can simulate the changes in the head-distance chart over time by pressing the play button. In addition, the user can add maximum envelopes, minimum envelopes, pipeline profiles, and steady-state HGL to the graph for more comprehensive observation. This window also includes various buttons to edit the visualization of the charts.

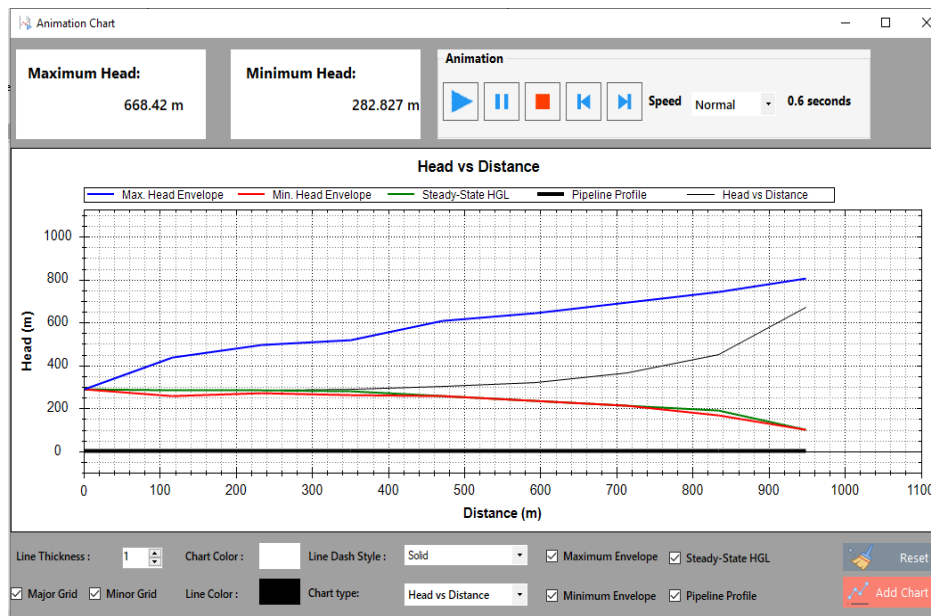


Figure 4.23 The view of the animation chart window

#### 4.2.9.4 Air Chamber and Surge Tank Solution Windows

When the user adds a surge tank or an air chamber component to the hydraulic system, two additional windows can be used to observe charts which are the change of discharge versus time and water elevation in the devices versus time. These windows are shown in Figures 4.24 and 4.25. In these minor interfaces, there are buttons named 'data table' so that the user can observe the results in tabular form. These windows also include various buttons to edit the visualization of the charts.

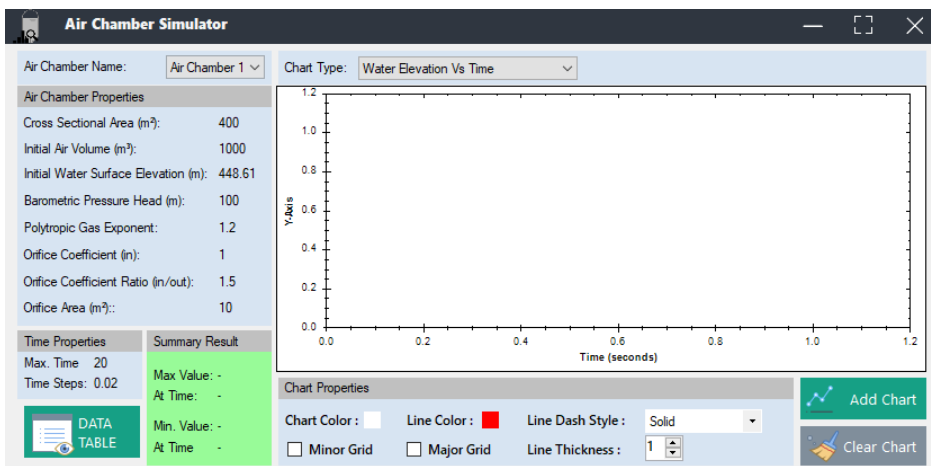


Figure 4.24 The view of the air chamber simulator window

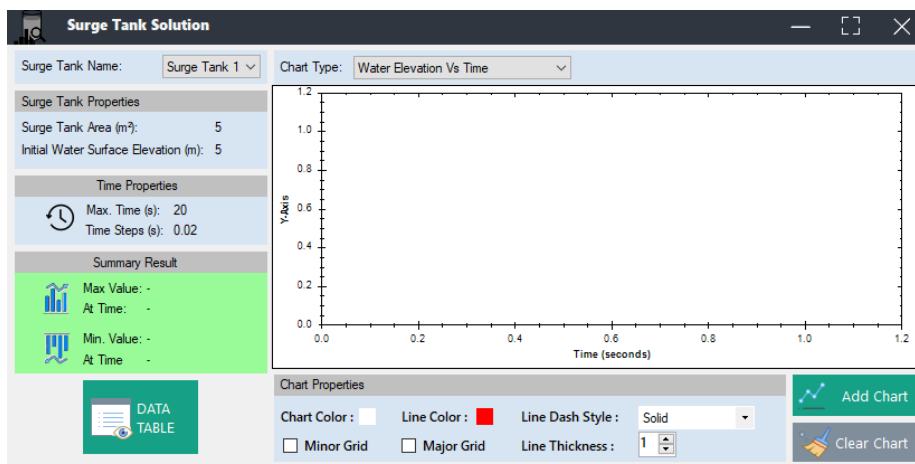


Figure 4.25 The view of the surge tank solution window

### 4.3 Objects and Properties Windows

This section will explain the objects defined in this program that can be used in modeling hydraulic pipeline systems and their property panels. These objects are pipe, reservoir, valve, pump, dead end, surge tank, air chamber, and junction. The images of hydraulic system components drawn on the design canvas are shown in Figure 4.26.

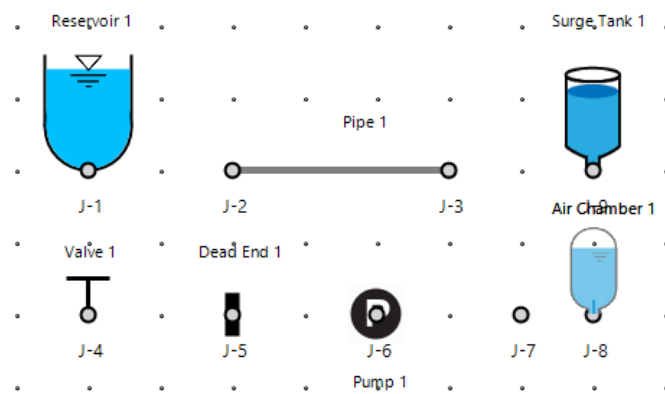


Figure 4.26 The view of components

#### 4.3.1 Junction Component

The junction object is a component used as a connection node to link an object with different objects. The program is designed as each component has a junction. The property panel of the junction component contains text box areas to enter elevation (m) and loss coefficient values, as shown in Figure 4.27. In other words, it is provided that users can enter the elevation value and minor loss coefficient values as inputs into the junction property panel for each junction.

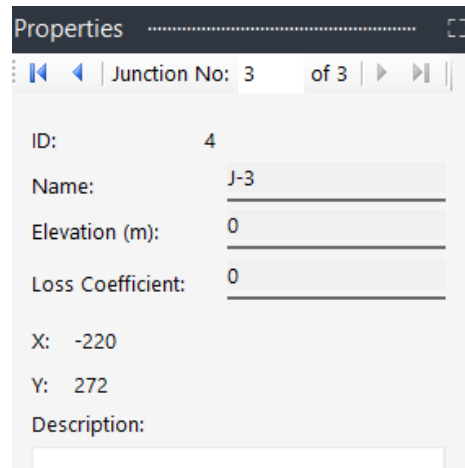


Figure 4.27 The view of the junction properties panel

### 4.3.2 Pipe Component and Properties

The pipe object is a line component that can link two different junctions in a hydraulic pipeline system. Casually, it has two junctions, which are inlet and outlet junctions. Pipe properties can be listed as; length (m), diameter (m), friction factor, roughness height (mm), and wave speed (m/s). In the pipe properties panel, besides the mentioned properties, there are two more sections that can show the pipe area automatically calculated using the entered pipe diameter and the Reynolds number of the flow passing through the pipe after the analysis. This properties panel also contains the connected junction and geometry data, as shown in Figure 4.28.

In addition, the property panel provides a check box called 'is connection pipe' for users. This feature can be used when the users want to add considerably too small pipe elements between two junctions. It provides more straightforward transient computation without affecting the Courant condition in some special cases.

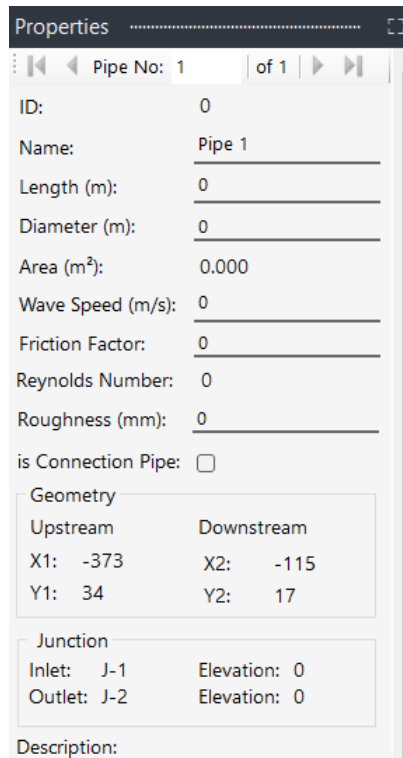


Figure 4.28 The view of the pipe properties panel

### 4.3.3 Reservoir Component and Properties

The reservoir object is a common component used in hydraulic systems. The program contains two types of reservoirs which are upstream and downstream. The reservoir properties panel has the reservoir type selection box and text boxes for reservoir height (m), base elevation (m), and reservoir loss coefficient to enter needed data. In addition, as shown in Figure 4.29, the sinus wave period and wave amplitude (m) text boxes have been added to this panel so that the user can add a sinus wave to the reservoir. In other words, the user can add and define a reservoir with either a constant or a variable head to a system.

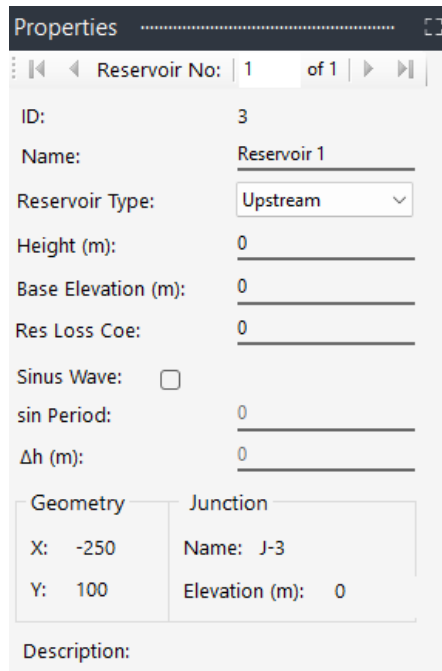


Figure 4.29 The view of the reservoir properties panel

#### 4.3.4 Valve Component and Properties

The valve component can be used to manage the flow in hydraulic systems. This object is included in the program so that users can add it at the downstream end of the hydraulic system or between pipe objects. The valve property panel contains the valve condition type selection box and text boxes for the head (m), diameter (m), and loss coefficient, as shown in Figure 4.30, so that the user can enter the needed data.

In this program, four different condition types can be defined for the valves. These conditions are 'closed', 'open', 'being closed', and 'instant closure'. The valve closure data can be determined by selecting the condition type. If the condition type is selected as 'open',  $\tau$  value is set as '1' for each time step. In 'closed' condition type, the valve acts like a dead end, then there will be no initial flow, and  $\tau$  value is set as '0' for each time step. The selection of 'instant closure' condition represents that the valve is instantly closed. In other words, at the time '0', which is the steady state condition,  $\tau$  is set to 1, and  $\tau$  is considered 0 for the remaining time steps. When

users select the 'being closed' condition type, the closure ( $\tau$ ) data must be entered in the valve closure settings form as explained in subsection 4.2.3.

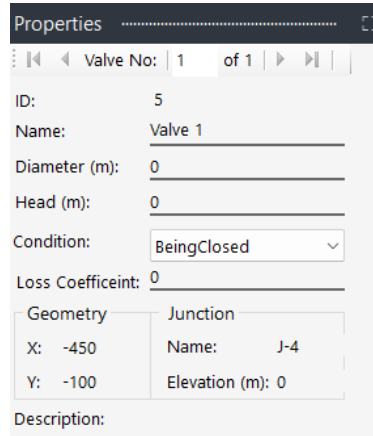


Figure 4.30 The view of the valve properties panel

### 4.3.5 Dead End Component and Properties

The dead-end object is a component used generally in a system's downstream end. The usage of this component also means that there is no flow motion. This component can be used to simulate the transient event when an upstream reservoir has a sinusoidal wave. The dead-end properties panel just contains default information, which is about geometry and junction, and common text boxes, which are for the name and description, as shown in Figure 4.31.

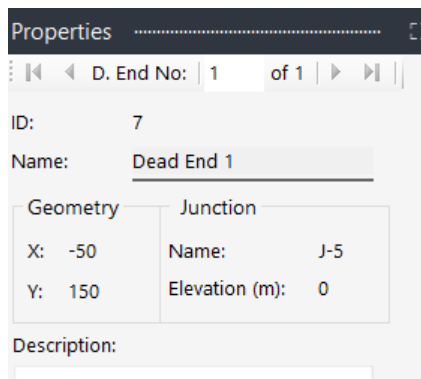


Figure 4.31 The view of the dead end properties panel

### 4.3.6 Pump Component and Properties

The pump object is a point component commonly used in hydraulic systems. Users can place this object between two pipes in the hydraulic pipeline system. The properties of the pump object can be listed as; pump trip time (sec),  $\omega R^2$  value ( $\text{Nm}^2$ ), loss coefficient, rated head (m), rated torque ( $\text{Nm}$ ), rated discharge ( $\text{m}^3/\text{s}$ ), rated rotational speed (rpm), and discharge valve availability.

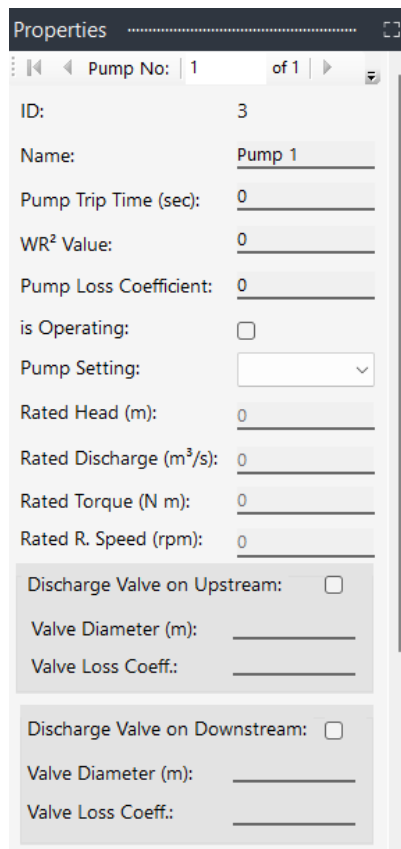


Figure 4.32 The view of the pump properties panel

The pump properties panel includes text boxes for trip time,  $\omega R^2$  value ( $\text{Nm}^2$ ), and loss coefficient, as shown in Figure 4.32. As mentioned in subsection 4.2.4, the pump settings values, the rated values and the pump curve, are defined as data sets with a name in the pump settings form. Users can select these datasets for the pump component from the selection box in the properties panel. In the properties panel, when a pump setting is selected, the rated values update to defined rated values. In



addition, there is 'is Operating' check box in this properties window. The check box can be used to ignore the pump component. In other words, the pump object acts as a junction. This feature is a practical option for the user to compare systems with and without a pump.

Moreover, if a discharge valve is used in the system, the user can define the diameter and loss coefficient for the valve in this properties panel.

### 4.3.7 Surge Tank Component and Properties

In the program, the surge tank component is one of the protection devices used in hydraulic systems. This component can be located between two pipes. As shown in Figure 4.33, the surge tank properties panel contains a selection box to define surge tank type and text boxes for surge tank area ( $m^2$ ) and base elevation (m). In addition, 'is Operating' check box is available in the same manner mentioned in the pump properties panel.

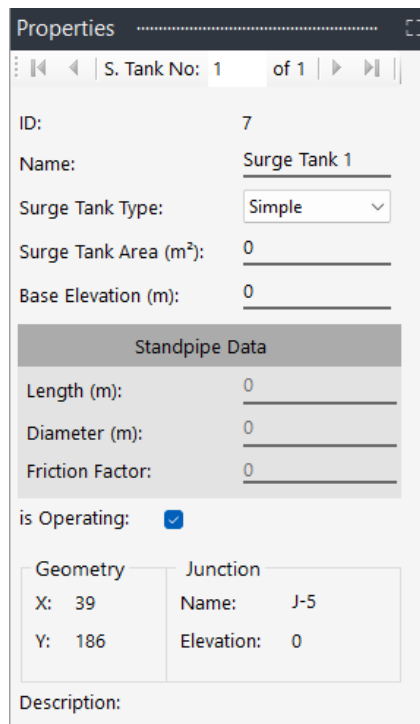


Figure 4.33 The view of the surge tank properties panel

The program includes two types of surge tanks which are the simple surge tank and the surge tank with a standpipe. If the user selects the surge tank type as surge tank with a standpipe, the properties of the standpipe are requested from the user in the properties panel. These required properties are length (m), diameter (m), and friction factor of the standpipe.

#### 4.3.8 Air Chamber Component and Properties

The air chamber component is one of the protection devices that can be used in the program. This component can be located between two pipes. The program includes one type of air chamber component, which is an air chamber with an orifice. As shown in Figure 4.34, the air chamber properties panel contains text boxes to enter values for the cross-sectional area (m<sup>2</sup>), initial air volume (m<sup>3</sup>), polytropic gas equation exponent, base elevation (m), barometric pressure head (m), orifice area (m<sup>2</sup>), orifice loss coefficient for inflow and orifice coefficient ratio. In addition, the ‘is Operating’ check box is available in the same manner mentioned in the pump and surge tank properties panels.

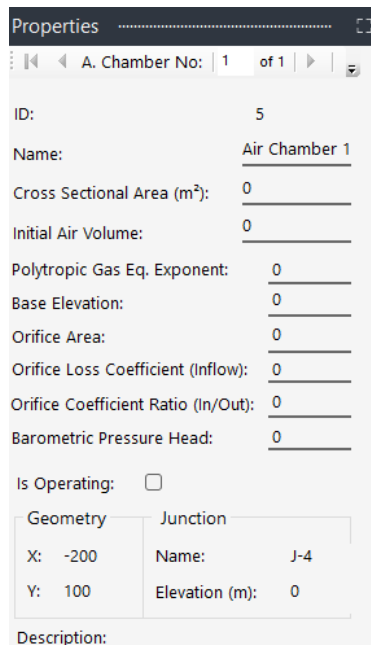


Figure 4.34 The view of the air chamber properties panel

## **CHAPTER 5**

### **VERIFICATION OF THE PROGRAM**

In this study, the program is verified by using proper benchmark cases. These cases are studies on pressurized hydraulic systems, which include the following scenarios; single pipe, pipes connected in series, pump trip due to power loss, and protection with surge tanks.

#### **5.1 Verification for Single Pipe Computations**

In order to verify the software for single pipe scenarios, two different benchmark cases were used to compare their results obtained by the software developed in the present study. The first and second single pipe scenarios are conducted by Wylie & Streeter (1978) and Wood et al. (2005), respectively.

##### **5.1.1 Case-1: Single Pipe by Wylie & Streeter (1978) Benchmark**

In the first scenario for single pipe verification, the hydraulic system includes an upstream reservoir, which has a constant head, single pipe, and a downstream valve. The system is illustrated in Figure 5.1. In this scenario, fluid transient in a regular valve closure case is analyzed.

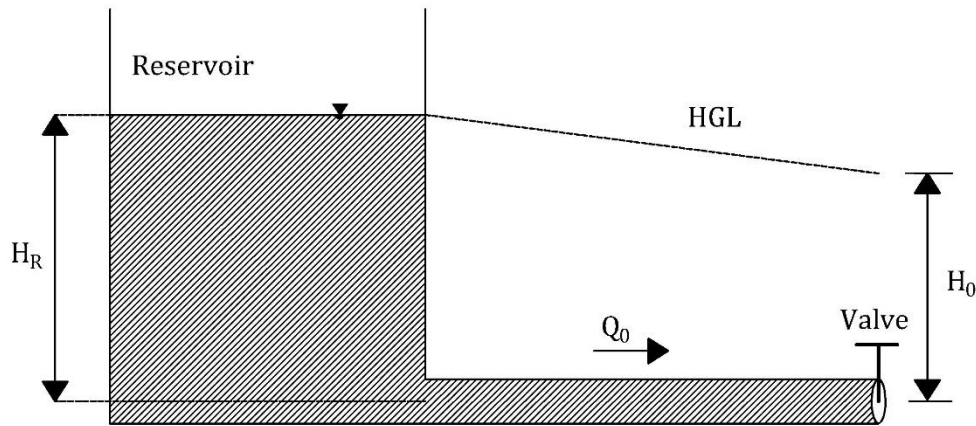


Figure 5.1 Configuration of Case-1 and notations by Wylie & Streeter (1978)

In this case study, the datum is located at the centerline of the pipe. Then,  $H_R$  refers to the elevation of the water surface in the upstream reservoir.  $H_0$  refers to the head value at the valve at the steady-state condition of the system. The difference between  $H_R$  and  $H_0$  can be stated as the head loss along the pipeline due to friction.  $Q_0$  is the initial discharge passing through the pipeline in the steady-state condition.

According to Wylie & Streeter (1978), the known data for the system can be listed as:

- Reservoir head,  $H_R = 150$  m
- Diameter of the pipe,  $D_p = 0.5$  m
- Length of the pipe,  $L_p = 600$  m
- Friction factor for the pipe,  $f = 0.018$
- Wave speed for the pipe,  $a = 1200$  m/s
- Node Count,  $N = 5$
- Valve closure time,  $T_c = 2.1$  s
- Maximum time for the simulation,  $T_{\max} = 4.3$ s
- Constant for valve closure,  $E_m = 1.5$
- Multiplication of discharge coefficient and effective valve opening area for the steady state condition,  $(C_d A_g)_0 = 0.009$

Firstly, Case-1 was visualized in the canvas of the program, as shown in Figure 5.2. In this step, reservoir, pipe, and valve components are added to the system.

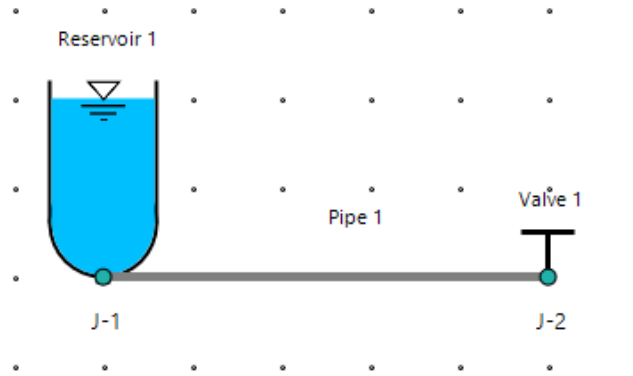


Figure 5.2 Visual design of Case-1 in the canvas

Then, the properties of the upstream reservoir, pipe, and downstream valve components are entered into properties panels in the program, as shown in Figure 5.3, 5.4, and 5.5, respectively.

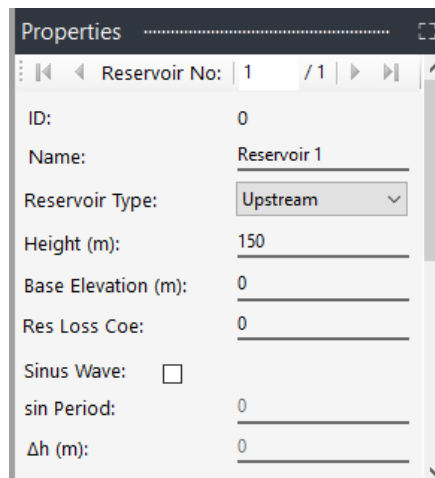


Figure 5.3 Inputs in the reservoir properties panel for Case-1

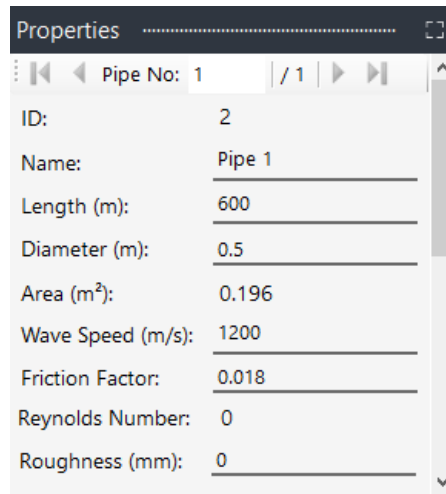


Figure 5.4 Inputs in the pipe properties panel for Case-1

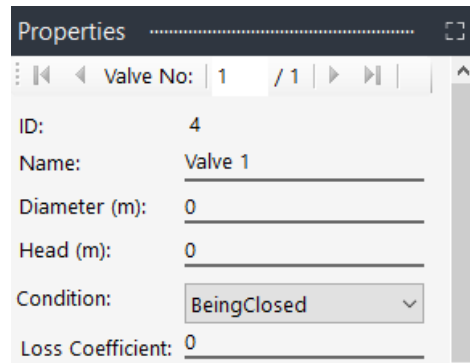


Figure 5.5 Inputs in the valve properties panel for Case-1

Valve closure time and the valve closure constant are defined in the valve closure settings panel for the downstream valve, as shown in Figure 5.6. According to the given data, the regular valve closure formulation is used instead of tabular closure data.

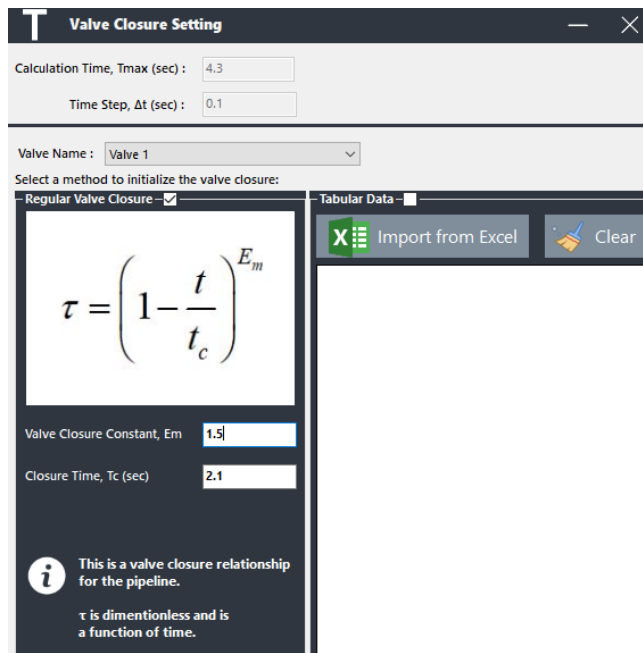


Figure 5.6 Inputs in valve closure settings panel for Case-1

Then, data about the initial conditions for the system are entered into the program, as shown in Figure 5.7. Case-1 has  $(C_d A_g)_0$  value as an input instead of initial discharge or velocity, so initial discharge and velocity values are not inserted as inputs into the program at the beginning.

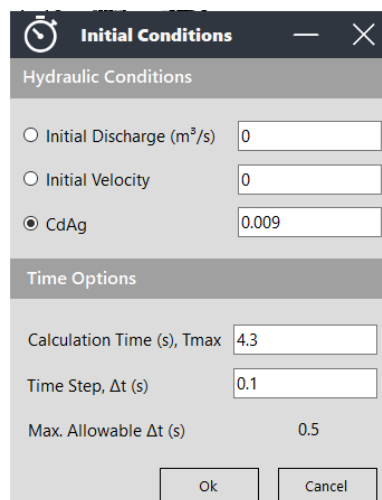


Figure 5.7 Inputs in the initial conditions panel for Case-1

After that, all data are entered into proper panels of the program, transient analyses and simulations can be observed in table, time chart, and animation chart forms. So, the obtained outputs are presented in tabular form and graphical form, as shown in Figure 5.8 and 5.9, respectively.

	Time (sec)	Object Name	Node No.	Distance from Reservoir	Head (m)	Discharge (m <sup>3</sup> /s)	Velocity (m/s)	Pressure (KPa)
▶	0.00	Pipe 1	1	120	148.698	0.477	2.432	1458.129
	0.00	Pipe 1	2	240	147.395	0.477	2.432	1445.358
	0.00	Pipe 1	3	360	146.093	0.477	2.432	1432.588
	0.00	Pipe 1	4	480	144.791	0.477	2.432	1419.817
	0.00	Pipe 1	5	600	143.488	0.477	2.432	1407.046
	0.10	Pipe 1	1	120	148.698	0.477	2.432	1458.129
	0.10	Pipe 1	2	240	147.395	0.477	2.432	1445.358
	0.10	Pipe 1	3	360	146.093	0.477	2.432	1432.588
	0.10	Pipe 1	4	480	144.791	0.477	2.432	1419.817
	0.10	Pipe 1	5	600	154.278	0.46	2.343	1512.849
	0.20	Pipe 1	1	120	148.698	0.477	2.432	1458.129
	0.20	Pipe 1	2	240	147.395	0.477	2.432	1445.358
	0.20	Pipe 1	3	360	146.093	0.477	2.432	1432.588
	0.20	Pipe 1	4	480	155.534	0.46	2.344	1525.165
	0.20	Pipe 1	5	600	165.788	0.442	2.249	1625.714
	0.30	Pipe 1	1	120	148.698	0.477	2.432	1458.129
	0.30	Pipe 1	2	240	147.395	0.477	2.432	1445.358
	0.30	Pipe 1	3	360	156.79	0.46	2.344	1537.483
	0.30	Pipe 1	4	480	166.996	0.442	2.25	1637.563
	0.30	Pipe 1	5	600	178.081	0.422	2.15	1746.258

Figure 5.8 The view of the tabular results for Case-1 (0-0.3 sec.)



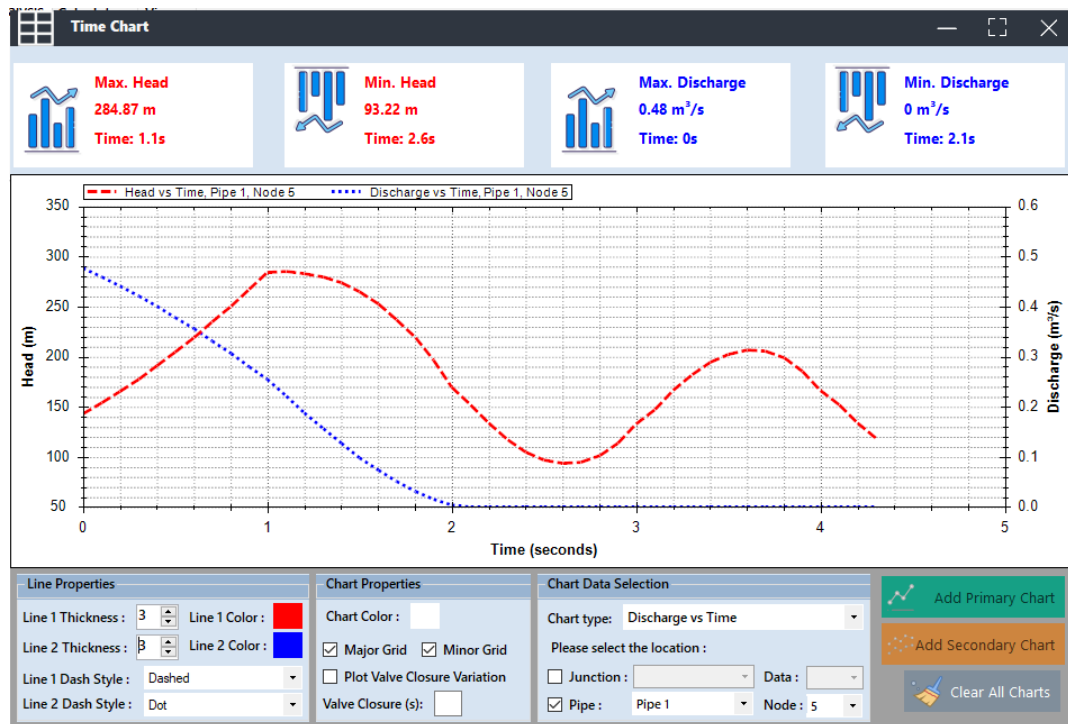


Figure 5.9 Graphical illustration of obtained results at the valve end for Case-1

After the results are obtained in both tabular and graphical form, these results are compared with the results presented by Wylie and Streeter (1978). Wylie and Streeter (1978) also used the method of characteristics to solve this problem. In tabular comparison, head (H) and discharge (Q) values for the valve-end section until 2.6 seconds are compared, as shown in Table 5.1. Moreover, the graphical comparison for the valve-end section is shown in Figure 5.10.

Table 5.1 Tabular comparison at the valve-end for Case-1

Time (sec)	Present Study			Wylie & Streeter (1978)		
	Head (m)	Discharge (m <sup>3</sup> /s)	$\tau$	Head (m)	Discharge (m <sup>3</sup> /s)	$\tau$
0	143.488	0.477	1	143.49	0.477	1
0.1	154.278	0.46	0.929	154.28	0.46	0.929
0.2	165.788	0.442	0.861	165.79	0.442	0.861
0.3	178.081	0.422	0.794	178.08	0.422	0.794
0.4	191.112	0.401	0.728	191.11	0.401	0.728
0.5	204.929	0.379	0.665	204.93	0.379	0.665
0.6	219.461	0.356	0.604	219.46	0.356	0.604
0.7	234.734	0.332	0.544	234.73	0.332	0.544
0.8	250.639	0.307	0.487	250.64	0.307	0.487
0.9	267.174	0.281	0.432	267.17	0.281	0.432
1	284.188	0.255	0.379	284.19	0.255	0.379
1.1	284.87	0.221	0.329	284.87	0.221	0.329
1.2	283.516	0.188	0.281	283.51	0.188	0.281
1.3	279.907	0.157	0.235	279.9	0.157	0.235
1.4	273.744	0.127	0.192	273.74	0.127	0.192
1.5	264.803	0.099	0.153	264.8	0.099	0.153
1.6	252.813	0.074	0.116	252.81	0.074	0.116
1.7	237.566	0.051	0.083	237.56	0.051	0.083
1.8	218.839	0.032	0.054	218.84	0.032	0.054
1.9	196.449	0.016	0.029	196.45	0.016	0.029
2	170.204	0.005	0.01	170.2	0.005	0.01
2.1	152.269	0	0	152.27	0	0
2.2	133.478	0	0	133.48	0	0
2.3	117.66	0	0	117.66	0	0
2.4	105.345	0	0	105.35	0	0
2.5	97.022	0	0	97.02	0	0
2.6	93.217	0	0	93.22	0	0

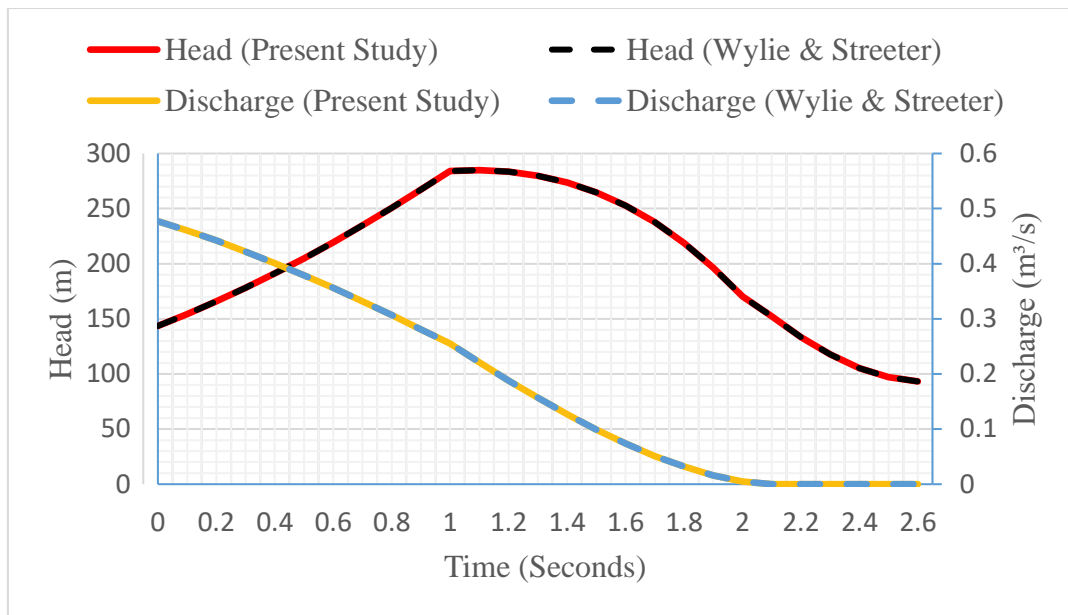


Figure 5.10 Graphical comparison at the valve-end for Case-1

According to the comparison shown in Table 5.1 and Figure 5.10, it is clearly inferred that the obtained results in the present study are highly accurate and very similar to the results presented in Wylie & Streeter (1978). This confirms that the method of characteristics was coded correctly in the software since the benchmark study also used the same method.

### 5.1.2 Case-2: Single Pipe by Wood et al. (2005) Benchmark

In another scenario for single pipe verification, the hydraulic system includes an upstream reservoir that has a constant head, single pipe, and a downstream valve. The system has a similar illustration to the single pipe case in Wylie & Streeter (1978), as shown in Figure 5.11. In this scenario, fluid transients in valve closure case are analyzed considering tabular valve closure data.

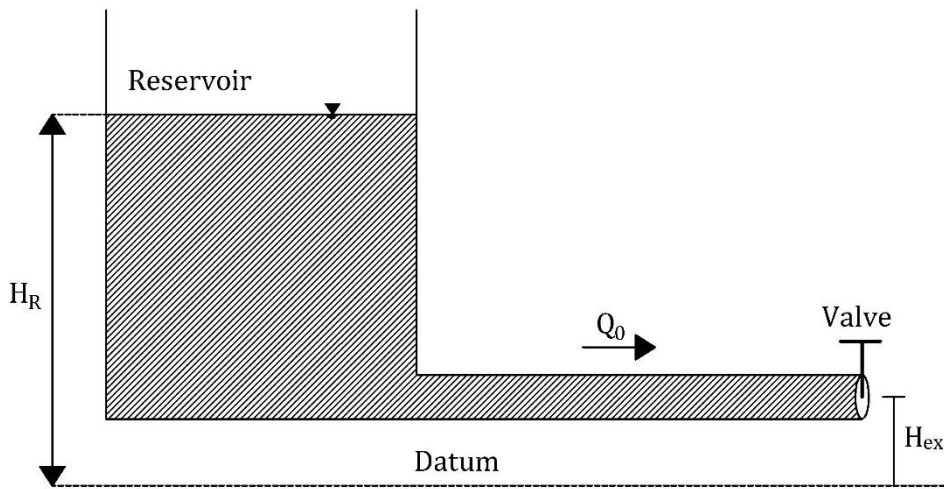


Figure 5.11 Configuration of Case-2 and notations by Wood et al. (2005)

According to Wood et al. (2005), the known data for the system can be listed as:

- Hydraulic grade at the reservoir,  $H_R = 13.72$  m
- Hydraulic grade at the exit of the pipe  $H_{Ex} = 0$  m
- Diameter of the pipe,  $D_p = 0.3$  m
- Length of the pipe,  $L_p = 1098$  m
- Wave speed for the pipe,  $a = 1098$  m/s
- Initial discharge through the pipe,  $Q_0 = 0.085$  m<sup>3</sup>/s
- Valve closure time,  $T_c = 10$  s
- The maximum time for the simulation,  $T_{max} = 10$  s

Valve closure data is given in tabular form for the case, as shown in Table 5.2.

Table 5.2 Tabular valve closure data for Case-2 by Wood et al. (2005)

Time (sec)	$\tau$
0	1
1	0.84
2	0.69
3	0.55
4	0.41
5	0.29
6	0.19
7	0.11
8	0.05
9	0.01
10	0

Firstly, Case-2 was visualized in the canvas of the program, as shown in Figure 5.12. In this step, reservoir, pipe, and valve components are added to the system.

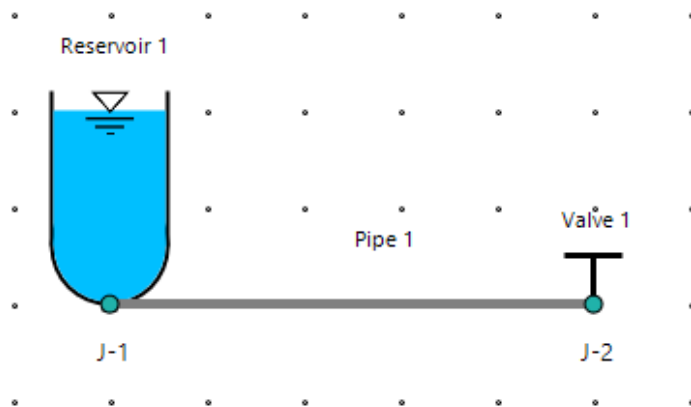


Figure 5.12 Visual design of Case-2 in canvas

Then, the properties of the upstream reservoir, pipe, and downstream valve components are entered into the relevant sections of properties panels in the program, as shown in Figure 5.13, 5.14, and 5.15, respectively.

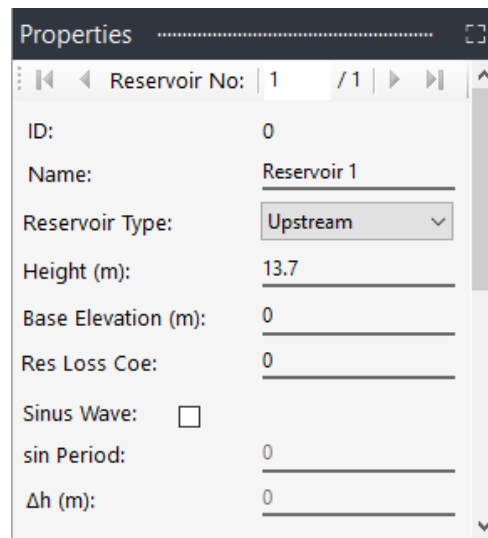


Figure 5.13 Inputs in the reservoir properties panel for Case-2

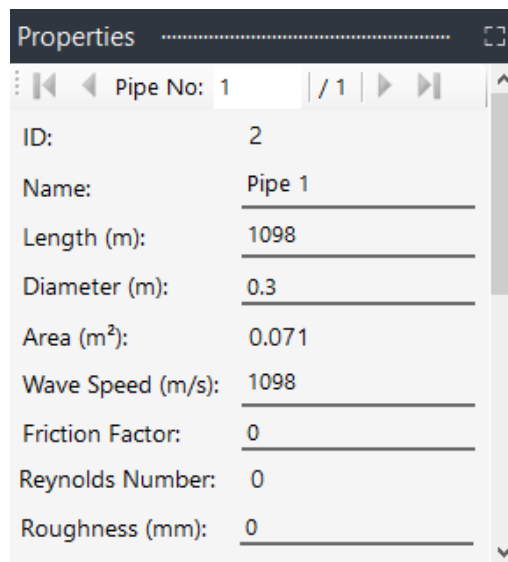


Figure 5.14 Inputs in the pipe properties panel for Case-2

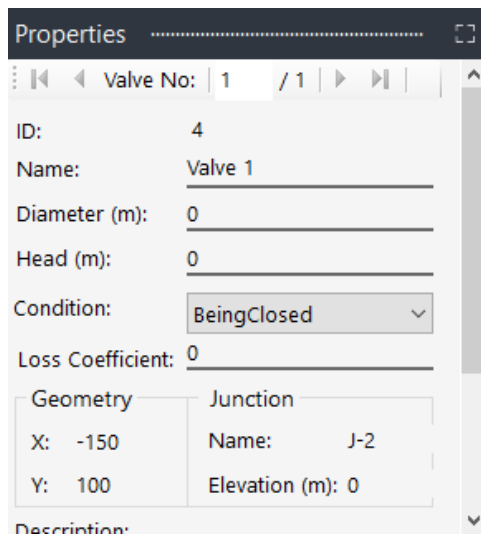


Figure 5.15 Inputs in the valve properties panel for Case-2

Valve closure data are defined in the valve closure settings panel for the downstream valve as shown in Figure 5.16. According to the given data in Table 5.2, tabular closure data is used instead of regular valve closure formulation.

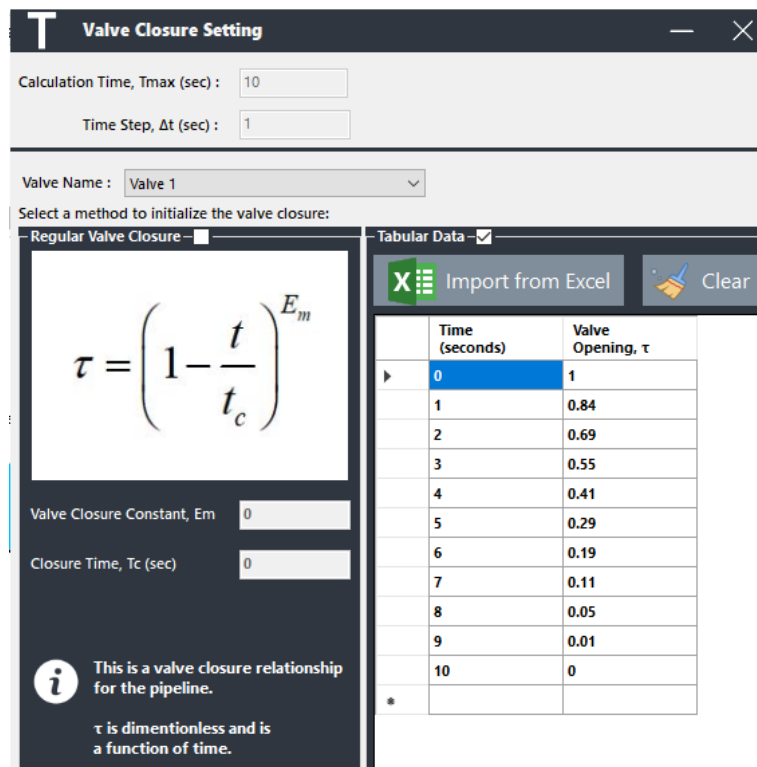


Figure 5.16 Inputs in the valve closure settings panel for Case-2

Then, data about the initial conditions for the system are entered into the program as shown in Figure 5.17. Case-2 has an initial discharge value as an input instead of a value of  $C_dA_g$  or initial velocity, so  $C_dA_g$  and velocity values are not inserted as inputs into the program at the beginning.

The image shows a software dialog box titled "Initial Conditions". It is divided into two main sections: "Hydraulic Conditions" and "Time Options".

**Hydraulic Conditions:**

- Initial Discharge ( $\text{m}^3/\text{s}$ ): 0.085
- Initial Velocity: 0
- $C_dA_g$ : 0

**Time Options:**

- Calculation Time (s),  $T_{\text{max}}$ : 10
- Time Step,  $\Delta t$  (s): 1
- Max. Allowable  $\Delta t$  (s): 1

Buttons: Ok, Cancel

Figure 5.17 Inputs in the initial conditions panel for Case-2

After all data are entered into the proper panels of the program, transient analyses and simulations can be observed in tables, time charts, and animation chart forms. The obtained outputs are presented in tabular form and graphical form, as shown in Figures 5.18 and 5.19, respectively.



	Time (sec)	Object Name	Node No.	Distance from Reservoir	Head (m)	Discharge (m <sup>3</sup> /s)	Velocity (m/s)	Pressure (KPa)
▶	0.00	Pipe 1	1	1098	13.7	0.085	1.203	134.342
	1.00	Pipe 1	1	1098	18.153	0.082	1.163	178.009
	2.00	Pipe 1	1	1098	24.388	0.078	1.107	239.152
	3.00	Pipe 1	1	1098	29.948	0.069	0.978	293.673
	4.00	Pipe 1	1	1098	36.662	0.057	0.807	359.507
	5.00	Pipe 1	1	1098	40.122	0.042	0.597	393.433
	6.00	Pipe 1	1	1098	38.282	0.027	0.382	375.391
	7.00	Pipe 1	1	1098	31.605	0.014	0.201	309.918
	8.00	Pipe 1	1	1098	23.134	0.006	0.078	226.857
	9.00	Pipe 1	1	1098	16.8	0.001	0.013	164.742
	10.00	Pipe 1	1	1098	13.014	0	0	127.616

Figure 5.18 The view of the tabular results for Case-2

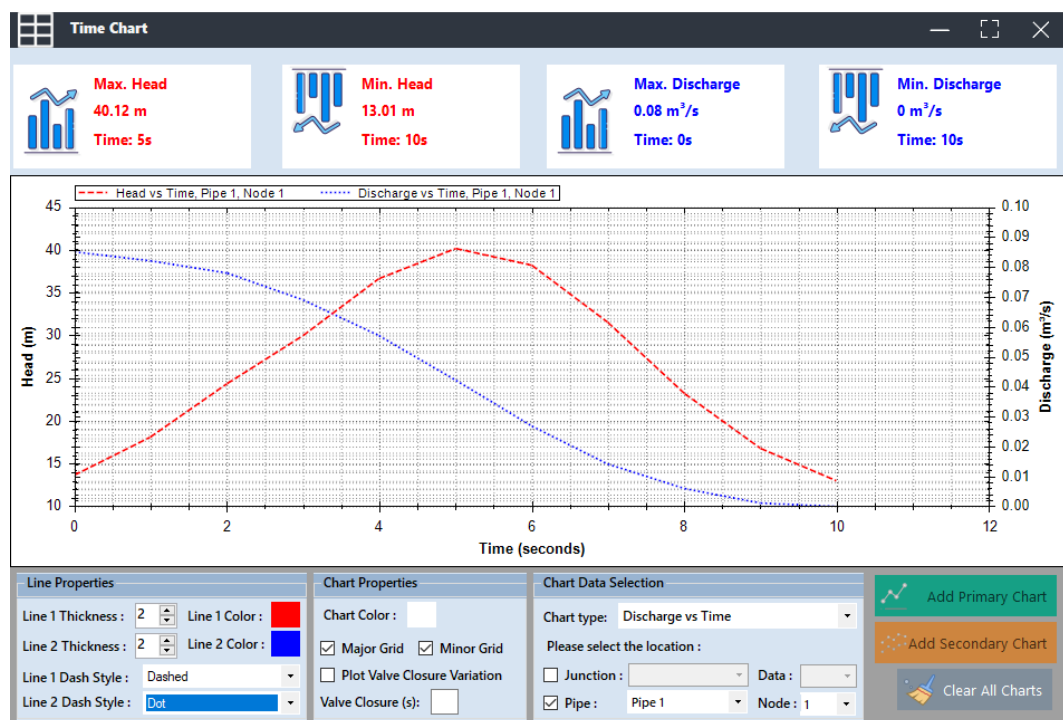


Figure 5.19 Graphical illustration of the results at the valve-end for Case-2

After the results are obtained in both tabular and graphical form, these results are compared with the results presented by Wood et al. (2005). Wood et al. (2005) provide the obtained data by using the Lagrangian wave characteristics methods

(WCM) and the Eulerian method of characteristics (MOC) for this case. To compare the results of the present study, the outputs calculated by the method of characteristics by Wood et al. (2005) will be used. Head (H) and discharge (Q) values for the valve-end section are compared with tabular and graphical forms, as shown in Table 5.3 and Figure 5.20, respectively.

Table 5.3 Tabular comparison at the valve-end for Case-2

Time (sec)	Present Study			Wood et al. (2005)		
	Head (m)	Discharge (m <sup>3</sup> /s)	$\tau$	Head (m)	Discharge (m <sup>3</sup> /s)	$\tau$
0	13.72	0.085	1	13.72	0.085	1
1	18.18	0.082	0.84	18.02	0.082	0.84
2	24.42	0.078	0.69	24.26	0.078	0.69
3	29.98	0.069	0.55	30.06	0.068	0.55
4	36.69	0.057	0.41	35.94	0.057	0.41
5	40.14	0.042	0.29	38.62	0.042	0.29
6	38.29	0.027	0.19	37.33	0.027	0.19
7	31.61	0.014	0.11	31.34	0.014	0.11
8	23.14	0.006	0.05	22.88	0.005	0.05
9	16.82	0.001	0.01	15.82	0.001	0.01
10	13.04	0	0	12.78	0	0

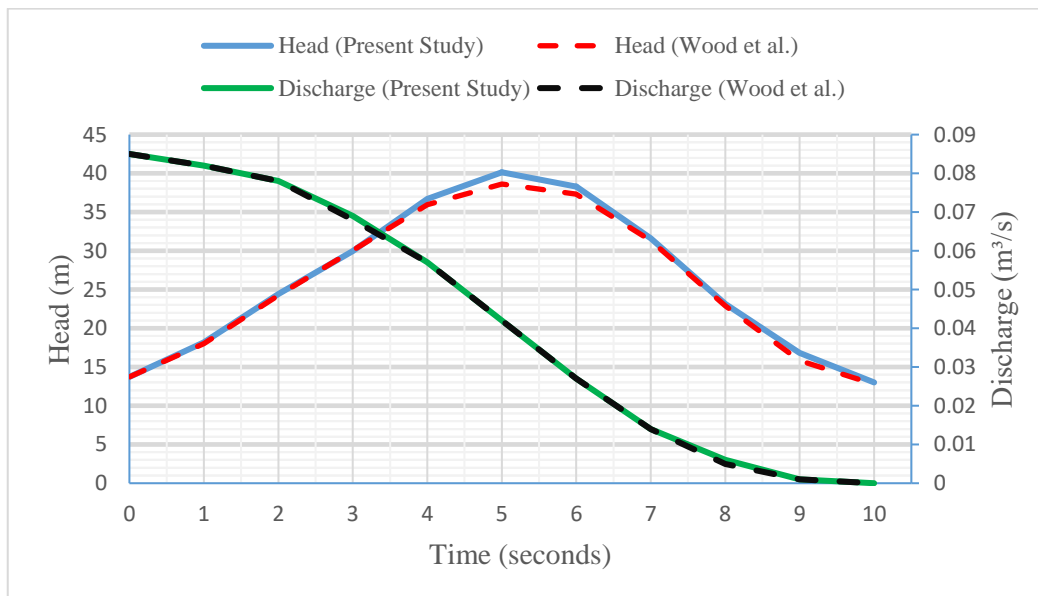


Figure 5.20 Graphical comparison at the valve-end section for Case-2

The comparison, which is made in this section, shows that the calculated results in the present study are highly accurate and very similar to the results of the case presented by Wood et al. (2005), as seen in Table 5.3 and Figure 5.20. The highest difference in this comparison, which is almost 1.5 m, is observed in head values at the fifth second for the valve-end section. This difference may be caused by the use of different assumptions used in the method of characteristics or minor differences in data used. However, this difference is negligible when considering the magnitudes.

## **5.2 Verification for Pipes Connected in Series**

In order to verify the program, two different cases, which contain different numbers of pipes, were used as benchmark cases to compare the results calculated by the program with the results in the literature. The first and second pipes in series scenarios are conducted by Chaudhry (1979) and Wylie & Streeter (1978), respectively.

### **5.2.1 Case-3: Pipes in Series by Chaudhry (1979) Benchmark**

In the first scenario for the verification of pipes connected in series, the hydraulic system includes an upstream reservoir, which has a constant head, two pipes, labeled as ‘Pipe 1’ and ‘Pipe 2’, and a downstream valve. The system and notations are illustrated in Figure 5.21. In this scenario, fluid transients are initiated by the valve closure located at the downstream end of the pipeline.

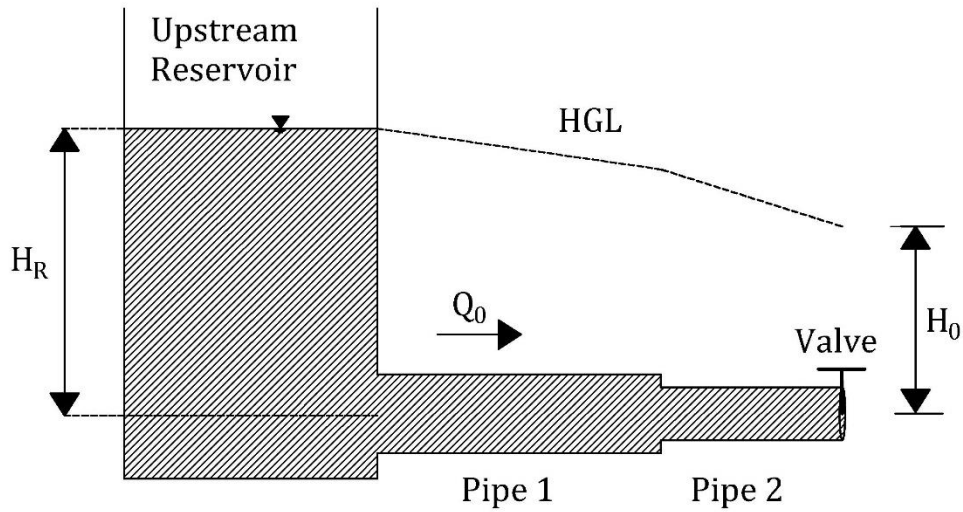


Figure 5.21 Configuration of Case-3 and notations by Chaudhry (1979)

In this case study, the datum is located at the centerline of the pipe. So,  $H_R$  refers to the elevation of the water surface in the upstream reservoir.  $H_0$  refers to the head value at the valve section in the steady-state condition of the system.  $Q_0$  is the initial discharge passing through the pipeline in the steady-state condition.

According to Chaudhry (1979), the known data for the system can be listed as:

- Initial head at the valve-end of the pipeline  $H_0 = 60.05$  m
- Initial discharge through the pipeline,  $Q_0 = 1.0$  m<sup>3</sup>/s
- Valve closure time,  $T_c = 6$  s
- The maximum time for the simulation,  $T_{\max} = 10$  s
- Time step for simulation,  $\Delta t = 0.5$  s

The diameter, length, wave speed, and friction factor values of the first and second pipes are shown in Table 5.4. Valve closure data are given in tabular form for the case, as shown in Table 5.5.

Table 5.4 The known data for the pipes by Chaudhry (1979) in Case-3

<b>Pipe Name</b>	<b>Diameter (m)</b>	<b>Length (m)</b>	<b>Wave Speed (m/s)</b>	<b>Friction Factor</b>
Pipe 1	0.75	550	1100	0.01
Pipe 2	0.6	450	900	0.012

Table 5.5 Tabular valve closure data by Chaudhry (1979) in Case-3

<b>Time (sec)</b>	<b><math>\tau</math></b>
0	1
0.5	0.963
1	0.9
1.5	0.813
2	0.7
2.5	0.6
3	0.5
3.5	0.4
4	0.3
4.5	0.2
5	0.1
5.5	0.038
6	0
6.5	0
7	0
7.5	0
8	0
8.5	0
9	0
9.5	0
10	0

In the first stage, Case-3 was visualized in the canvas of the program, as shown in Figure 5.22. In this step, a reservoir, first pipe, second pipe, and valve components are added to the system.

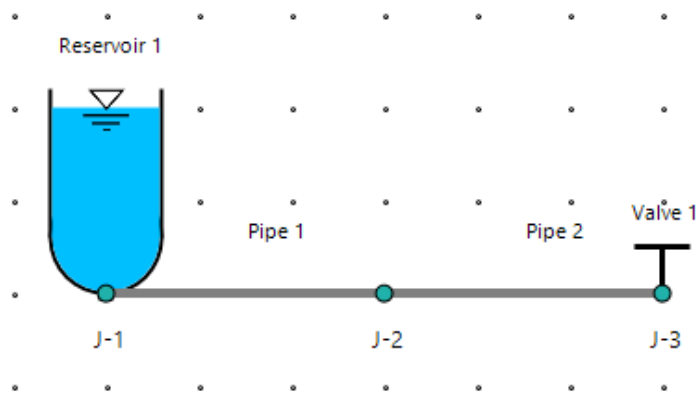


Figure 5.22 Visual design of Case-3 in canvas

Then, the properties of the first pipe, second pipe, and downstream valve components are entered into relevant sections of properties panels in the program, as shown in Figure 5.23, 5.24, and 5.25, respectively.

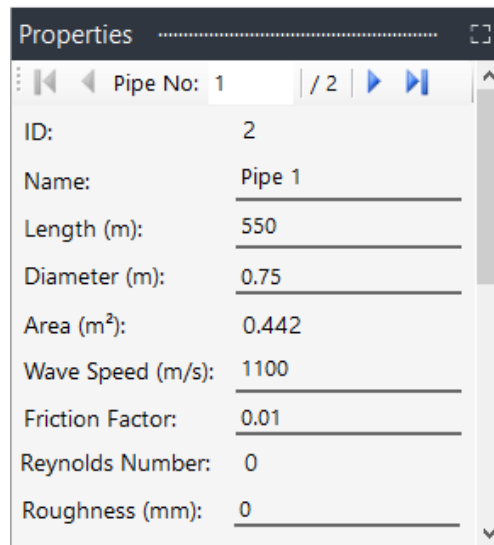


Figure 5.23 Inputs in the pipe properties panel for the 1<sup>st</sup> pipe of Case-3

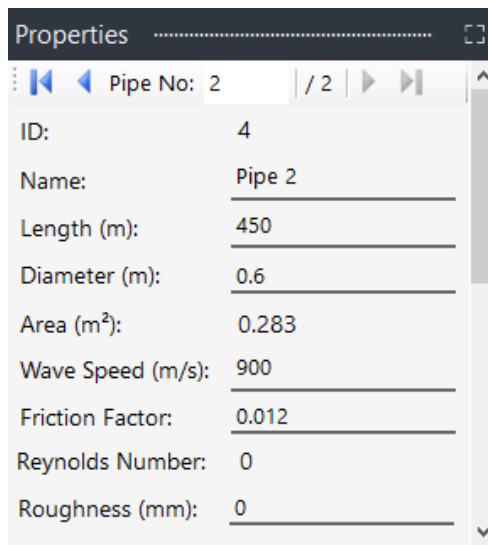


Figure 5.24 Inputs in the pipe properties panel for the 2<sup>nd</sup> pipe of Case-3

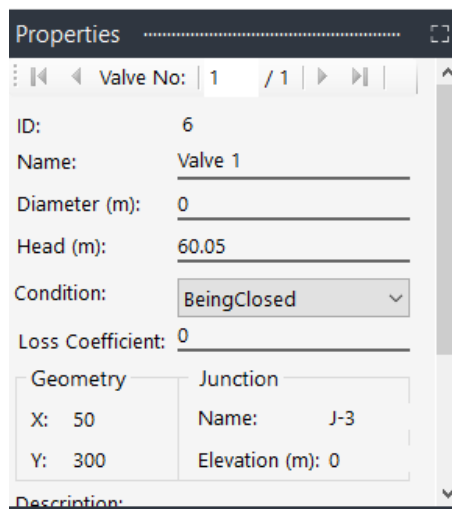


Figure 5.25 Inputs in the valve properties panel for Case-3

Valve closure data are defined in the valve closure settings panel for the downstream valve, as shown in Figure 5.26. According to the given data by Chaudhry (1979) in Table 5.5, tabular closure data is used instead of regular valve closure formulation.

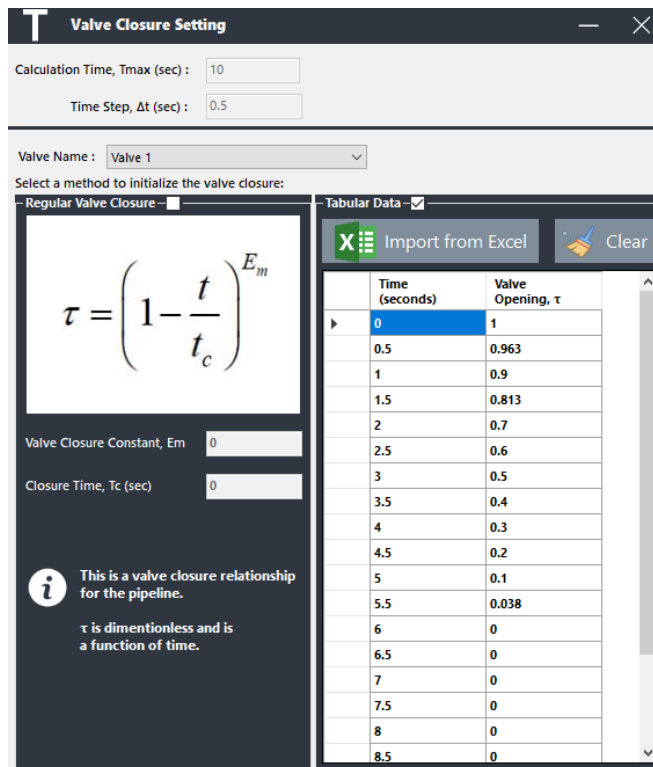


Figure 5.26 Inputs in the valve closure settings panel for Case-3

Then, data about the initial conditions for the system are entered into the program, as shown in Figure 5.27. The maximum allowable time step value is calculated as 0.5 seconds to satisfy the Courant condition. Case-3 has the initial discharge value as an input instead of the value of  $C_d A_g$  or initial velocity.

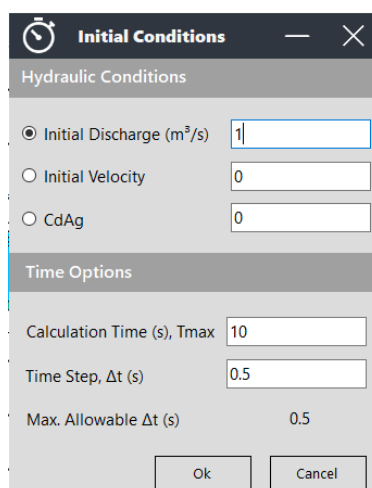


Figure 5.27 Inputs in the initial conditions panel for Case-3.



After all data are entered into the proper panels of the program, transient analyses and simulations can be observed in table, time chart, and animation chart forms. At the beginning of the calculation step, the initial reservoir head value,  $H_R$ , is computed as 67.706 m, then the other computations are made with this initial value. The program calculated all data at each node and junction. The obtained outputs for the upstream reservoir and valve-end are presented in tabular form as shown in Figure 5.28 and 5.29, respectively. The obtained outputs for the discharge at the upstream reservoir and head values at the valve-end of the pipeline are presented in graphical form, as shown in Figure 5.30.

Time (sec)	Object Name	Side	Distance from Reservoir	Head (m)	Discharge (m <sup>3</sup> /s)	Velocity (m/s)	Pressure (KPa)
0.00	J-1	Downstream	0	67.706	1	2.264	663.926
0.50	J-1	Downstream	0	67.706	1	2.264	663.926
1.00	J-1	Downstream	0	67.706	1	2.264	663.926
1.50	J-1	Downstream	0	67.706	0.977	2.212	663.926
2.00	J-1	Downstream	0	67.706	0.934	2.115	663.926
2.50	J-1	Downstream	0	67.706	0.867	1.964	663.926
3.00	J-1	Downstream	0	67.706	0.761	1.722	663.926
3.50	J-1	Downstream	0	67.706	0.643	1.455	663.926
4.00	J-1	Downstream	0	67.706	0.506	1.145	663.926
4.50	J-1	Downstream	0	67.706	0.349	0.79	663.926
5.00	J-1	Downstream	0	67.706	0.183	0.413	663.926
5.50	J-1	Downstream	0	67.706	0.006	0.014	663.926
6.00	J-1	Downstream	0	67.706	-0.174	-0.394	663.926
6.50	J-1	Downstream	0	67.706	-0.215	-0.486	663.926
7.00	J-1	Downstream	0	67.706	-0.14	-0.316	663.926
7.50	J-1	Downstream	0	67.706	0.046	0.104	663.926
8.00	J-1	Downstream	0	67.706	0.208	0.47	663.926
8.50	J-1	Downstream	0	67.706	0.203	0.459	663.926
9.00	J-1	Downstream	0	67.706	0.089	0.201	663.926
9.50	J-1	Downstream	0	67.706	-0.095	-0.215	663.926

Figure 5.28 The view of tabular results at the upstream reservoir for Case-3

Tables

Precision: 0.000

Time-Based Pipe-Based Junction-Based

Select a pipe: Pipe 2

Export to Excel Show Table

	Time (sec)	Object Name	Node No.	Distance from Reservoir	Head (m)	Discharge (m <sup>3</sup> /s)	Velocity (m/s)	Pressure (KPa)
▶	0.00	Pipe 2	1	1000	60.05	1	3.537	588.85
	0.50	Pipe 2	1	1000	63.417	0.99	3.5	621.865
	1.00	Pipe 2	1	1000	69.765	0.97	3.431	684.113
	1.50	Pipe 2	1	1000	79.785	0.937	3.314	782.368
	2.00	Pipe 2	1	1000	95.759	0.884	3.126	939.009
	2.50	Pipe 2	1	1000	110.33	0.813	2.876	1081.892
	3.00	Pipe 2	1	1000	124.951	0.721	2.551	1225.268
	3.50	Pipe 2	1	1000	139.027	0.609	2.153	1363.299
	4.00	Pipe 2	1	1000	148.847	0.472	1.67	1459.598
	4.50	Pipe 2	1	1000	158.276	0.325	1.148	1552.05
	5.00	Pipe 2	1	1000	165.373	0.166	0.587	1621.651
	5.50	Pipe 2	1	1000	149.041	0.06	0.212	1461.501
	6.00	Pipe 2	1	1000	114.306	0	0	1120.883
	6.50	Pipe 2	1	1000	62.024	0	0	608.203
	7.00	Pipe 2	1	1000	12.567	0	0	123.237
	7.50	Pipe 2	1	1000	7.343	0	0	72.004
	8.00	Pipe 2	1	1000	34.687	0	0	340.143
	8.50	Pipe 2	1	1000	88.068	0	0	863.591
	9.00	Pipe 2	1	1000	130.692	0	0	1281.569
	9.50	Pipe 2	1	1000	122.944	0	0	1205.589

Figure 5.29 The view of tabular results at the valve end for Case-3

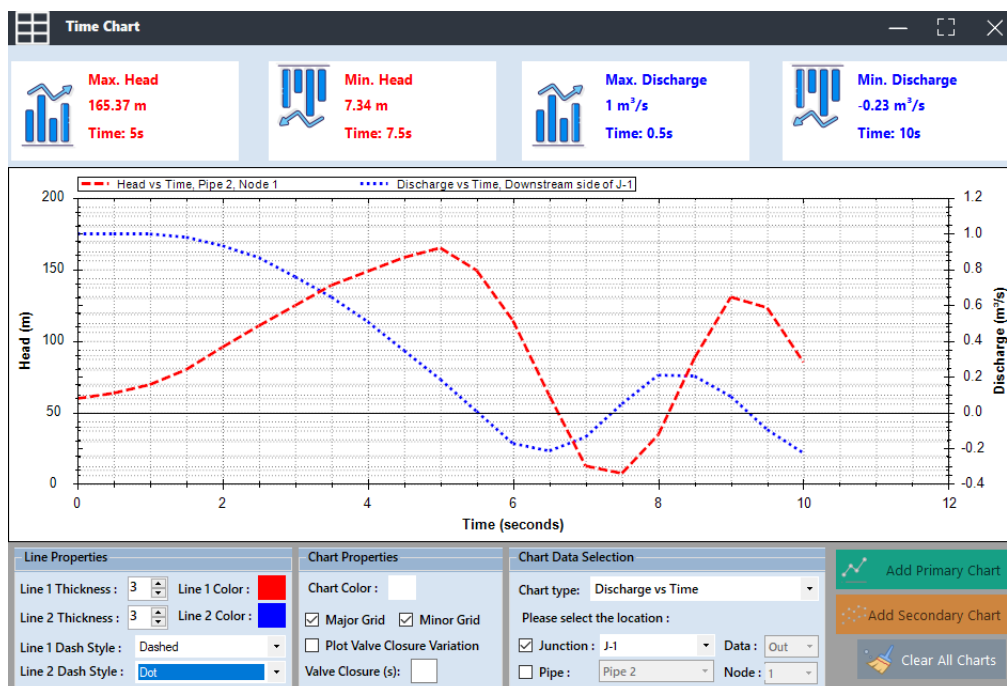


Figure 5.30 Graphical illustration of the results for Case-3

After the results are obtained in both tabular and graphical form, these results are compared with the results presented by Chaudhry (1979). Chaudhry (1979) also used the method of characteristics as a solution technique for this case study. Head (H) and discharge (Q) values for the end section of each pipe and reservoir section are compared in tabular form, as shown in Table 5.6 and Table 5.7, respectively. Then, the graphical comparison is made for head values at the valve-end section and discharge values at the reservoir section, as shown in Figure 5.31 and Figure 5.32, respectively.

Table 5.6 Tabular H comparison at the end of pipes and reservoir of Case-3

		Head Values (m)					
		Present Study			Chaudhry (1979)		
Time (sec)	$\tau$	Reservoir	Pipe 1	Pipe 2	Reservoir	Pipe 1	Pipe 2
0	1	67.7	65.79	60.05	60.7	65.78	60.05
0.5	0.963	67.7	65.79	63.417	60.7	65.78	63.46
1	0.9	67.7	68.694	69.765	60.7	68.73	69.78
1.5	0.813	67.7	74.169	79.785	60.7	74.16	79.88
2	0.7	67.7	79.919	95.759	60.7	79.93	95.83
2.5	0.6	67.7	88.248	110.33	60.7	88.25	110.41
3	0.5	67.7	94.994	124.951	60.7	94.96	125.13
3.5	0.4	67.7	99.139	139.027	60.7	99.19	139.2
4	0.3	67.7	104.335	148.847	60.7	104.41	149.14
4.5	0.2	67.7	108.365	158.276	60.7	108.47	158.61
5	0.1	67.7	111.068	165.373	60.7	111.2	165.65
5.5	0.038	67.7	112.984	149.041	60.7	113.07	149.46
6	0	67.7	95.795	114.306	60.7	96.01	114.27
6.5	0	67.7	63.366	62.024	60.7	63.25	61.79
7	0	67.7	34.663	12.567	60.7	34.25	12.33
7.5	0	67.7	23.631	7.343	60.7	23.55	6.74
8	0	67.7	47.75	34.687	60.7	47.63	34.76
8.5	0	67.7	82.753	88.068	60.7	82.89	88.45
9	0	67.7	105.514	130.692	60.7	105.95	13.93
9.5	0	67.7	107.972	122.944	60.7	108.02	123.44
10	0	67.7	78.4	85.281	60.7	78.39	85.13

Table 5.7 Tabular Q comparison at the end of pipes and reservoir of Case-3

		Discharge Values (m <sup>3</sup> /s)					
		Present Study			Chaudhry (1979)		
Time (sec)	$\tau$	Reservoir	Pipe 1	Pipe 2	Reservoir	Pipe 1	Pipe 2
0	1	1	1	1	1	1	1
0.5	0.963	1	1	0.99	1	1	0.989
1	0.9	1	0.989	0.97	1	0.988	0.97
1.5	0.813	0.977	0.967	0.937	0.977	0.967	0.937
2	0.7	0.934	0.922	0.884	0.935	0.922	0.884
2.5	0.6	0.867	0.847	0.813	0.867	0.847	0.814
3	0.5	0.761	0.754	0.721	0.761	0.755	0.722
3.5	0.4	0.643	0.633	0.609	0.643	0.633	0.609
4	0.3	0.506	0.495	0.472	0.506	0.496	0.473
4.5	0.2	0.349	0.344	0.325	0.35	0.344	0.325
5	0.1	0.183	0.177	0.166	0.183	0.177	0.166
5.5	0.038	0.006	0.004	0.06	0.006	0.004	0.059
6	0	-0.174	-0.104	0	-0.175	-0.106	0
6.5	0	-0.215	-0.157	0	-0.217	-0.157	0
7	0	-0.14	-0.084	0	-0.139	-0.085	0
7.5	0	0.046	0.034	0	0.047	0.035	0
8	0	0.208	0.124	0	0.208	0.126	0
8.5	0	0.203	0.148	0	0.205	0.148	0
9	0	0.089	0.054	0	0.088	0.054	0
9.5	0	-0.095	-0.07	0	-0.097	-0.071	0
10	0	-0.229	-0.137	0	-0.229	-0.139	0

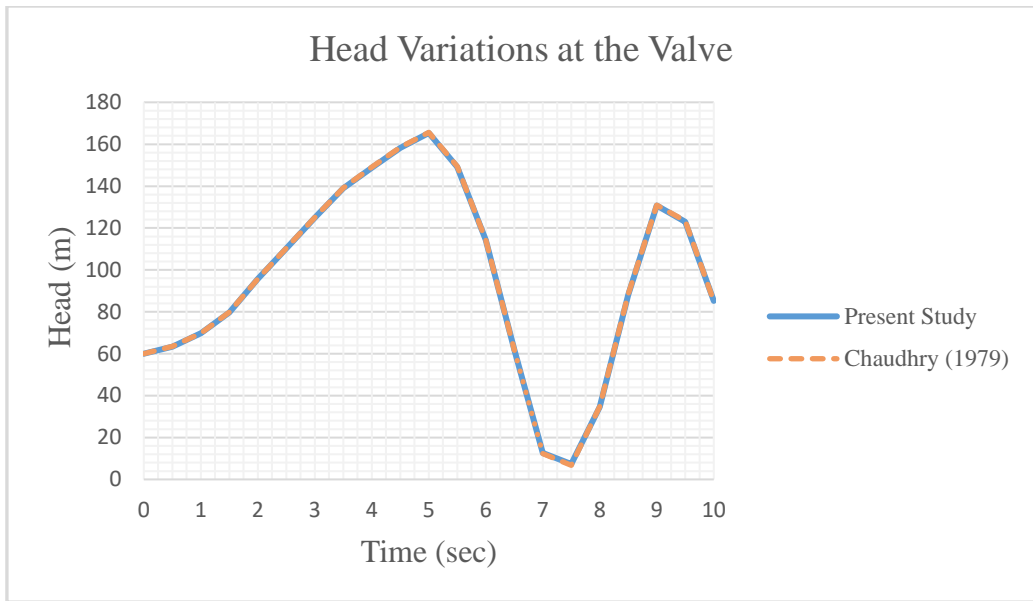


Figure 5.31 Graphical comparison for the H values at the valve-end of Case-3

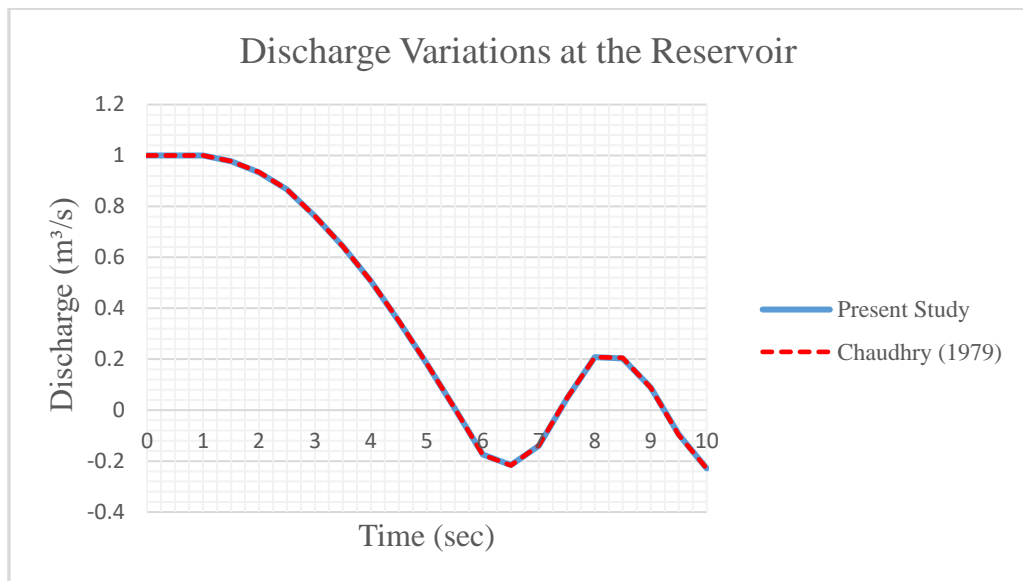


Figure 5.32 Graphical comparison for the Q values at the reservoir of Case-3

According to the comparison shown in Table 5.6, Table 5.7, Figure 5.31, and Figure 5.32, the obtained results in the present study are highly accurate and very similar to the results presented in Chaudhry (1979). This confirms that the method of characteristics was coded correctly in the software for pipes connected in series.

## 5.2.2 Case-4: Pipes in Series by Wylie & Streeter (1978) Benchmark

In another scenario for pipes connected in series verification, the hydraulic system includes an upstream reservoir, which has a constant head, three pipes, labeled as 'Pipe 1', 'Pipe 2' and 'Pipe 3', and a downstream valve. The system and notations are illustrated in Figure 5.33. In this scenario, as previously, fluid transients in the valve closure case are simulated.

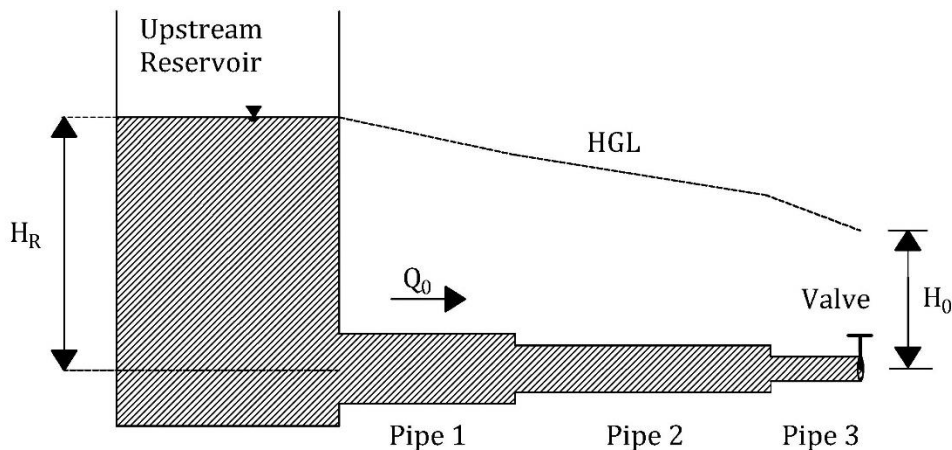


Figure 5.33 Case-4 as used by Wylie & Streeter (1978)

In Case-4, the datum is located at the centerline of the pipe. So,  $H_R$  refers to the elevation of the water surface in the upstream reservoir.  $H_0$  refers to the head value at the valve section in the steady-state condition of the system.  $Q_0$  is the initial discharge passing through the pipeline in the steady-state condition.

According to Wylie & Streeter (1978), the known data for the system can be listed as:

- Initial head at the valve-end of the pipeline,  $H_0 = 100$  m
- Initial discharge through the pipeline,  $Q_0 = 0.2$  m<sup>3</sup>/s
- Valve closure time,  $T_c = 1.8$  s
- Maximum time for the simulation,  $T_{\max} = 2.1$  s
- Time step for simulation,  $\Delta t = 0.1$  s

The diameter, length, wave speed, and friction factor values of the first, second, and third pipes are shown in Table 5.8. Valve closure data by Wylie & Streeter (1978) are given in tabular form for Case-4, as shown in Table 5.9.

Table 5.8 Given data for the pipes by Wylie & Streeter (1978) in Case-4

Pipe Name	Diameter (m)	Length (m)	Wave Speed (m/s)	Friction Factor
Pipe 1	0.3	351	1200	0.019
Pipe 2	0.2	483	1200	0.018
Pipe 3	0.15	115	1200	0.018

Table 5.9 Tabular valve closure data for Case-4

Time (sec)	$\tau$
0	1
0.1	0.867
0.2	0.733
0.3	0.6
0.4	0.467
0.5	0.333
0.6	0.2
0.7	0.183
0.8	0.167
0.9	0.15
1	0.133
1.1	0.117
1.2	0.1
1.3	0.083
1.4	0.067
1.5	0.05
1.6	0.033
1.7	0.017
1.8	0
1.9	0
2	0
2.1	0

In the first stage, Case-4 was visualized in the canvas of the program, as shown in Figure 5.34. In this step, the reservoir, first pipe, second pipe, third pipe, and valve components are added to the system.

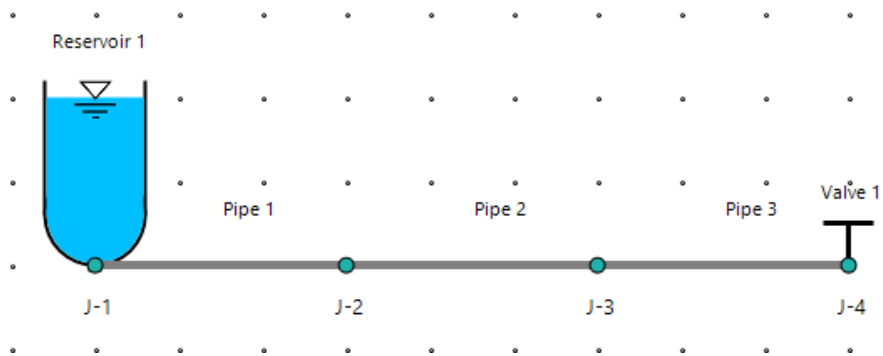


Figure 5.34 Visual design of Case-4 in canvas

Then, the properties of the first pipe, second pipe, third pipe, and downstream valve components are entered into relevant sections of properties panels in the program as shown in Figures 5.35, 5.36, 5.37, and 5.38, respectively.

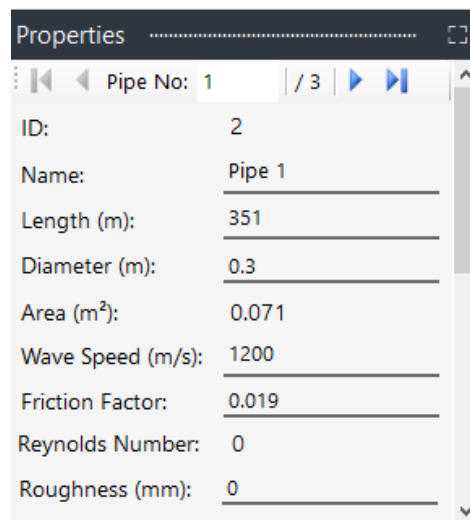


Figure 5.35 Inputs in the pipe properties panel for the 1<sup>st</sup> pipe of Case-4



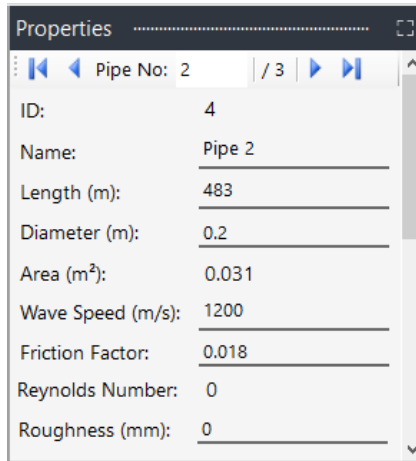


Figure 5.36 Inputs in the pipe properties panel for the 2<sup>nd</sup> pipe of Case-4

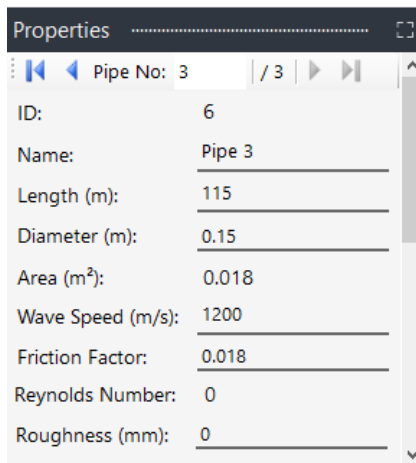


Figure 5.37 Inputs in the pipe properties panel for the 3<sup>rd</sup> pipe of Case-4

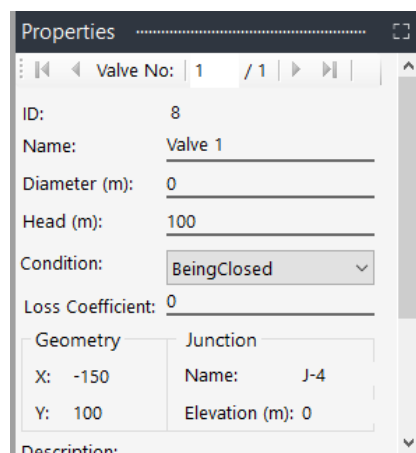


Figure 5.38 Inputs in the valve properties panel for Case-4

Valve closure data are defined in the valve closure settings panel for the downstream valve, as shown in Figure 5.39. According to the given data by Wylie & Streeter (1978) in Table 5.9, tabular closure data is used instead of regular valve closure formulation.

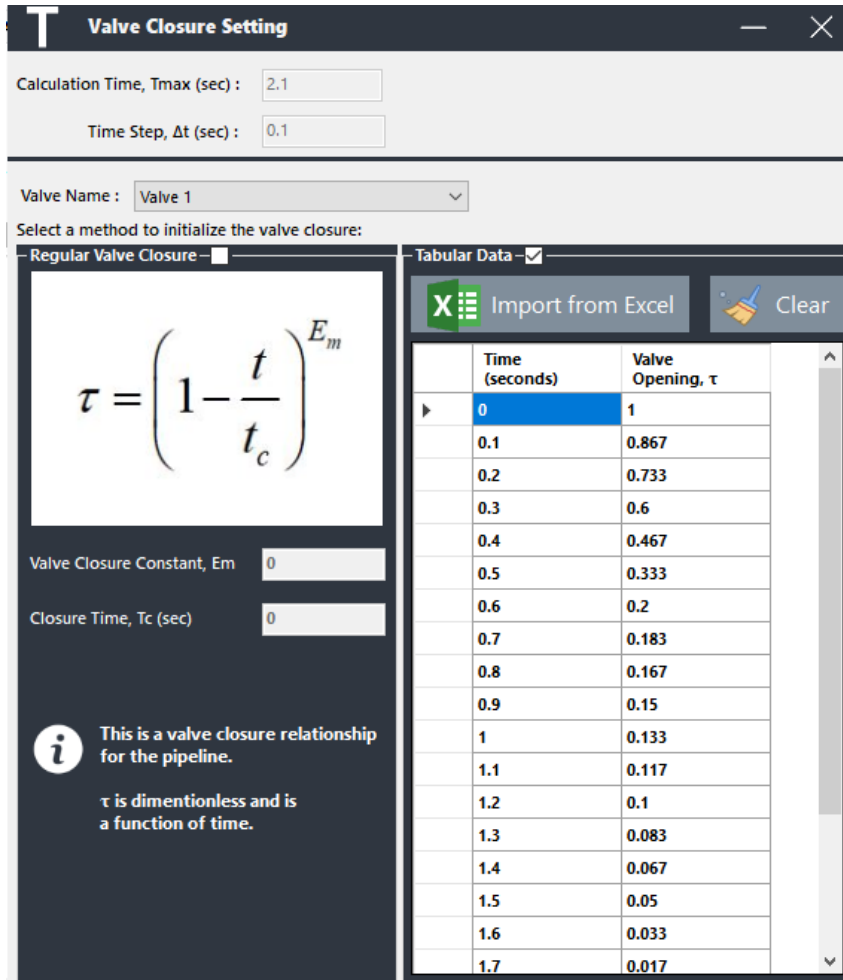


Figure 5.39 Inputs in valve closure settings panel for Case-4

Then, data about the initial conditions for the system are entered into the program, as shown in Figure 5.40. The maximum allowable time step value is calculated as 0.1 seconds to satisfy the Courant condition. Case-4 has the initial discharge value as an input instead of the value of  $C_d A_g$  or initial velocity.

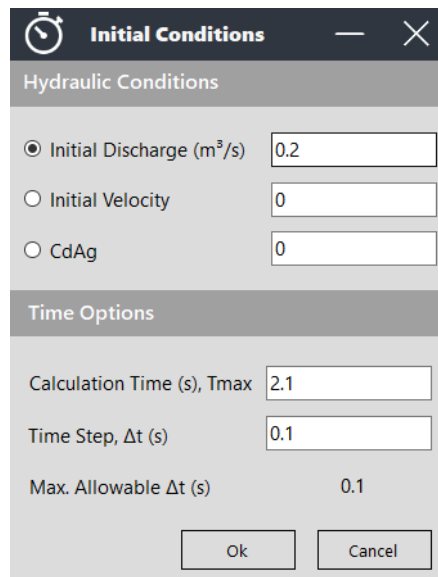


Figure 5.40 Inputs in the initial conditions panel for Case-4

After all data are entered into the proper panels of the program, transient analyses and simulations can be observed in tables, time charts, and animation charts forms. At the beginning of the calculation step, the initial reservoir head value,  $H_R$ , is computed as 289.036 m; then, the other computations are made with this initial value. The program calculated all data at each node and junction.

Even though the wave speed values for the pipes are 1200 m/s at the beginning of computation, these values are adjusted as 1170, 1207.5, and 1150 m/s for ‘Pipe 1’, ‘Pipe 2’, and ‘Pipe 3’, respectively, during the computation period. This change is made to ensure the stability of the Courant condition without affecting the results, and it is caused by the selection of grid-mesh in the software.

The obtained outputs for the upstream reservoir and valve-end are represented in tabular form, as shown in Figures 5.41 and 5.42, respectively. The obtained outputs for the discharge and head values at the valve-end of the pipeline are represented in graphical form, as shown in Figure 5.43.

Tables

Precision: 0.000

Time-Based Pipe-Based Junction-Based

Select a junction : J-1 Select side : Downstream

Export to Excel Show Table

	Time (sec)	Object Name	Side	Distance from Reservoir	Head (m)	Discharge (m <sup>3</sup> /s)	Velocity (m/s)	Pressure (KPa)
▶	0.00	J-1	Downstream	0	289.036	0.2	2.829	2834.29
	0.10	J-1	Downstream	0	289.036	0.2	2.829	2834.29
	0.20	J-1	Downstream	0	289.036	0.2	2.829	2834.29
	0.30	J-1	Downstream	0	289.036	0.2	2.829	2834.29
	0.40	J-1	Downstream	0	289.036	0.2	2.829	2834.29
	0.50	J-1	Downstream	0	289.036	0.2	2.829	2834.29
	0.60	J-1	Downstream	0	289.036	0.2	2.829	2834.29
	0.70	J-1	Downstream	0	289.036	0.2	2.829	2834.29
	0.80	J-1	Downstream	0	289.036	0.2	2.829	2834.29
	0.90	J-1	Downstream	0	289.036	0.188	2.662	2834.29
	1.00	J-1	Downstream	0	289.036	0.171	2.417	2834.29
	1.10	J-1	Downstream	0	289.036	0.144	2.041	2834.29
	1.20	J-1	Downstream	0	289.036	0.103	1.46	2834.29
	1.30	J-1	Downstream	0	289.036	0.037	0.519	2834.29
	1.40	J-1	Downstream	0	289.036	-0.074	-1.044	2834.29
	1.50	J-1	Downstream	0	289.036	-0.084	-1.19	2834.29
	1.60	J-1	Downstream	0	289.036	-0.087	-1.234	2834.29
	1.70	J-1	Downstream	0	289.036	-0.096	-1.361	2834.29
	1.80	J-1	Downstream	0	289.036	-0.101	-1.433	2834.29
	1.90	J-1	Downstream	0	289.036	-0.092	-1.301	2834.29

Figure 5.41 The view of tabular results at the upstream reservoir for Case-4

Tables

Precision: 0.000

Time-Based Pipe-Based Junction-Based

Select a pipe : Pipe 3

Export to Excel Show Table

	Time (sec)	Object Name	Node No.	Distance from Reservoir	Head (m)	Discharge (m <sup>3</sup> /s)	Velocity (m/s)	Pressure (KPa)
▶	0.00	Pipe 3	1	949	100	0.2	11.318	980.6
	0.10	Pipe 3	1	949	127.565	0.196	11.083	1250.906
	0.20	Pipe 3	1	949	167.635	0.19	10.741	1643.825
	0.30	Pipe 3	1	949	224.68	0.18	10.179	2203.212
	0.40	Pipe 3	1	949	311.411	0.165	9.327	3053.699
	0.50	Pipe 3	1	949	449.17	0.141	7.987	4404.557
	0.60	Pipe 3	1	949	668.774	0.103	5.854	6558
	0.70	Pipe 3	1	949	674.245	0.095	5.378	6611.65
	0.80	Pipe 3	1	949	651.046	0.085	4.823	6384.161
	0.90	Pipe 3	1	949	690.035	0.079	4.459	6766.484
	1.00	Pipe 3	1	949	737.276	0.072	4.087	7229.725
	1.10	Pipe 3	1	949	763.994	0.065	3.66	7491.728
	1.20	Pipe 3	1	949	789.725	0.056	3.181	7744.045
	1.30	Pipe 3	1	949	806.668	0.047	2.668	7910.183
	1.40	Pipe 3	1	949	804.883	0.038	2.151	7892.683
	1.50	Pipe 3	1	949	772.438	0.028	1.573	7574.524
	1.60	Pipe 3	1	949	685.529	0.017	0.978	6722.3
	1.70	Pipe 3	1	949	682.538	0.009	0.503	6692.964
	1.80	Pipe 3	1	949	686.131	0	0	6728.203
	1.90	Pipe 3	1	949	570.89	0	0	5598.145

Figure 5.42 The view of tabular results at the valve end for Case-4

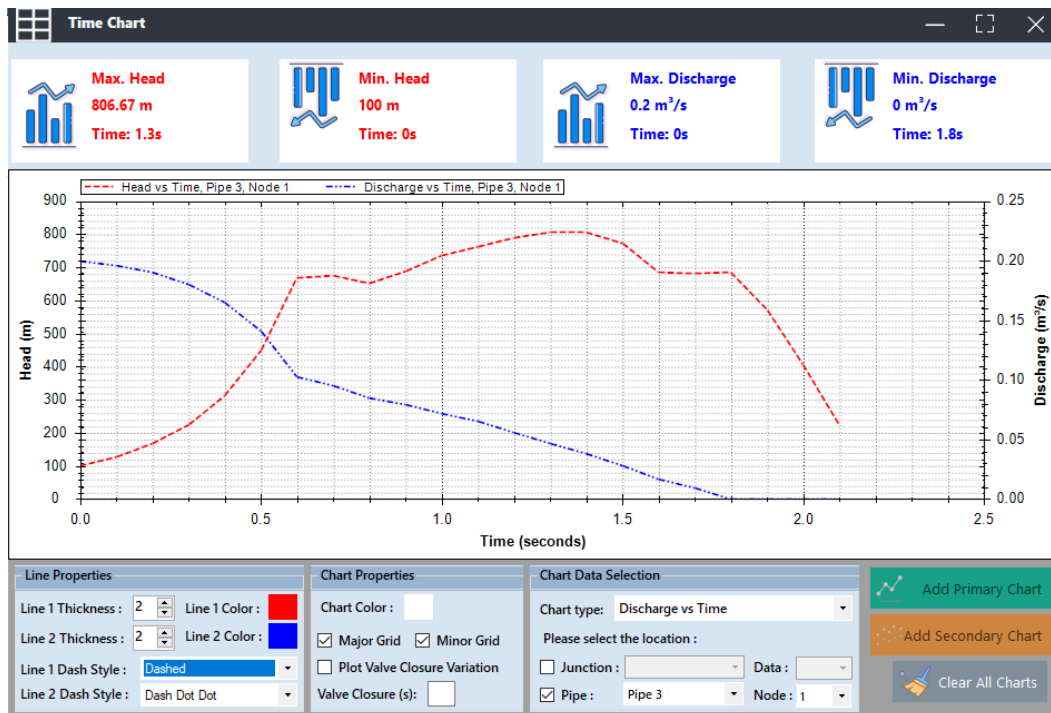


Figure 5.43 Graphical illustration of H and Q values at the valve for Case-4

After the results are obtained in both tabular and graphical form, these results are compared with the results presented by Wylie & Streeter (1978). Wylie and Streeter (1978) used the method of characteristics for this case. Head and discharge values for the end of each pipe and the reservoir sections are compared in tabular form, as shown in Table 5.10 and Table 5.11, respectively. Then, the graphical comparison is made for head values at the valve-end section and discharge values at the reservoir section, as shown in Figure 5.44 and Figure 5.45, respectively.

Table 5.10 Tabular H value comparison at the end of pipes and the reservoir for Case-4

		Head Values (m)							
		Present Study				Wylie & Streeter (1978)			
Time (sec)	$\tau$	Reservoir	Pipe 1	Pipe 2	Pipe 3	Reservoir	Pipe 1	Pipe 2	Pipe 3
0	1	289.036	279.962	190.131	100	289.04	279.96	190.13	100
0.1	0.867	289.036	279.962	190.131	127.565	289.04	279.96	190.13	127.65
0.2	0.733	289.036	279.962	209.226	167.635	289.04	279.96	209.29	167.51
0.3	0.6	289.036	279.962	237.034	224.68	289.04	279.96	236.95	224.67
0.4	0.467	289.036	279.962	280.289	311.411	289.04	279.96	280.29	311.71
0.5	0.333	289.036	279.962	346.175	449.17	289.04	279.96	346.37	448.71
0.6	0.2	289.036	290.21	451.598	668.774	289.04	290.24	451.27	668.7
0.7	0.183	289.036	305.185	621.175	674.245	289.04	305.14	621.16	673.58
0.8	0.167	289.036	328.366	647.161	651.046	289.04	328.37	646.61	651.84
0.9	0.15	289.036	363.988	667.404	690.035	289.04	364.09	667.97	690.25
1	0.133	289.036	421.548	693.863	737.276	289.04	421.37	693.87	736.11
1.1	0.117	289.036	516.216	721.432	763.994	289.04	516.21	720.75	764.86
1.2	0.1	289.036	515.864	735.794	789.725	289.04	515.51	736.44	790.15
1.3	0.083	289.036	505.186	743.12	806.668	289.04	505.57	743.16	805.23
1.4	0.067	289.036	491.15	729.193	804.883	289.04	491.17	728.44	805.76
1.5	0.05	289.036	461.823	678.413	772.438	289.04	461.26	679.15	773.19
1.6	0.033	289.036	398.229	665.758	685.529	289.04	398.87	666.19	684.02
1.7	0.017	289.036	283.421	628.911	682.538	289.04	283.49	627.78	683.85
1.8	0	289.036	282.551	597.31	686.131	289.04	282.49	598.18	686.38
1.9	0	289.036	281.722	546.232	570.89	289.04	281.68	546.49	570.22
2	0	289.036	275.36	395.326	407.334	289.04	275.5	395.07	407.59
2.1	0	289.036	260.938	165.705	221.338	289.04	260.99	165.77	221.48

Table 5.11 Tabular Q value comparison at the end of pipes and the reservoir for Case-4

		Discharge Values (m <sup>3</sup> /s)							
		Present Study				Wylie & Streeter (1978)			
Time (sec)	$\tau$	Reservoir	Pipe 1	Pipe 2	Pipe 3	Reservoir	Pipe 1	Pipe 2	Pipe 3
0	1	0.2	0.2	0.2	0.2	0.2	0.2	0.2	0.2
0.1	0.867	0.2	0.2	0.2	0.196	0.2	0.2	0.2	0.196
0.2	0.733	0.2	0.2	0.195	0.19	0.2	0.2	0.195	0.19
0.3	0.6	0.2	0.2	0.188	0.18	0.2	0.2	0.188	0.18
0.4	0.467	0.2	0.2	0.177	0.165	0.2	0.2	0.177	0.165
0.5	0.333	0.2	0.2	0.161	0.141	0.2	0.2	0.161	0.141
0.6	0.2	0.2	0.194	0.135	0.103	0.2	0.194	0.135	0.103
0.7	0.183	0.2	0.185	0.093	0.095	0.2	0.185	0.093	0.095
0.8	0.167	0.2	0.171	0.088	0.085	0.2	0.171	0.088	0.085
0.9	0.15	0.188	0.15	0.085	0.079	0.188	0.188	0.085	0.079
1	0.133	0.171	0.117	0.077	0.072	0.171	0.117	0.077	0.072
1.1	0.117	0.144	0.061	0.068	0.065	0.144	0.061	0.068	0.065
1.2	0.1	0.103	0.05	0.059	0.056	0.103	0.051	0.059	0.056
1.3	0.083	0.037	0.041	0.048	0.047	0.037	0.04	0.048	0.047
1.4	0.067	-0.074	0.023	0.035	0.038	-0.074	0.023	0.035	0.038
1.5	0.05	-0.084	0	0.018	0.028	-0.084	0.001	0.018	0.028
1.6	0.033	-0.087	-0.028	0.011	0.017	-0.088	-0.028	0.011	0.017
1.7	0.017	-0.096	-0.07	0.009	0.009	-0.095	-0.07	0.009	0.009
1.8	0	-0.101	-0.079	-0.004	0	-0.101	-0.079	-0.004	0
1.9	0	-0.092	-0.082	-0.021	0	-0.092	-0.082	-0.021	0
2	0	-0.065	-0.087	-0.026	0	-0.065	-0.087	-0.026	0
2.1	0	-0.074	-0.084	-0.036	0	-0.074	-0.083	-0.036	0

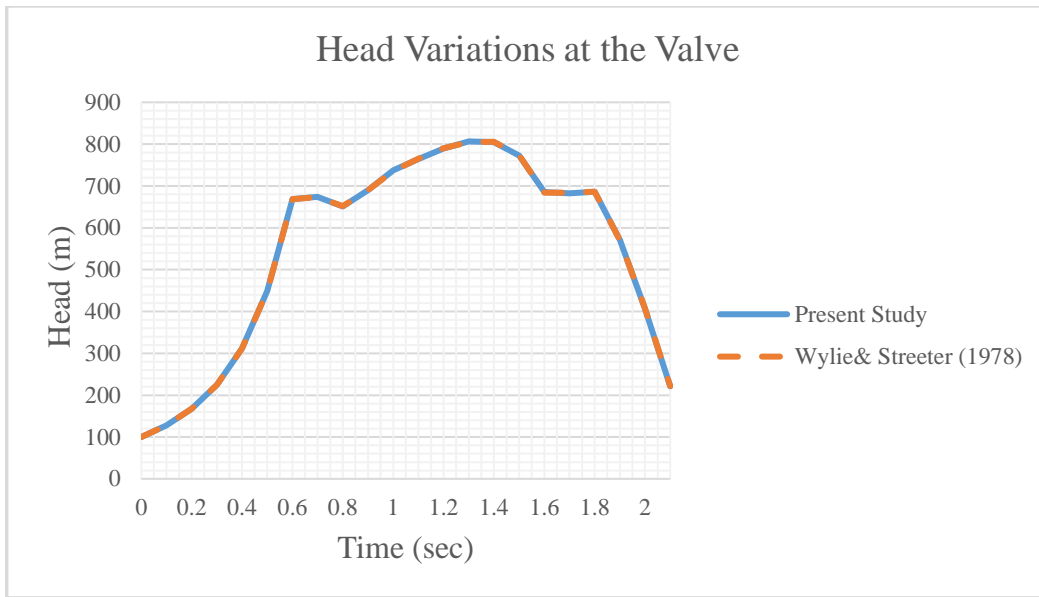


Figure 5.44 Graphical comparison for the H values at the valve-end of Case-4

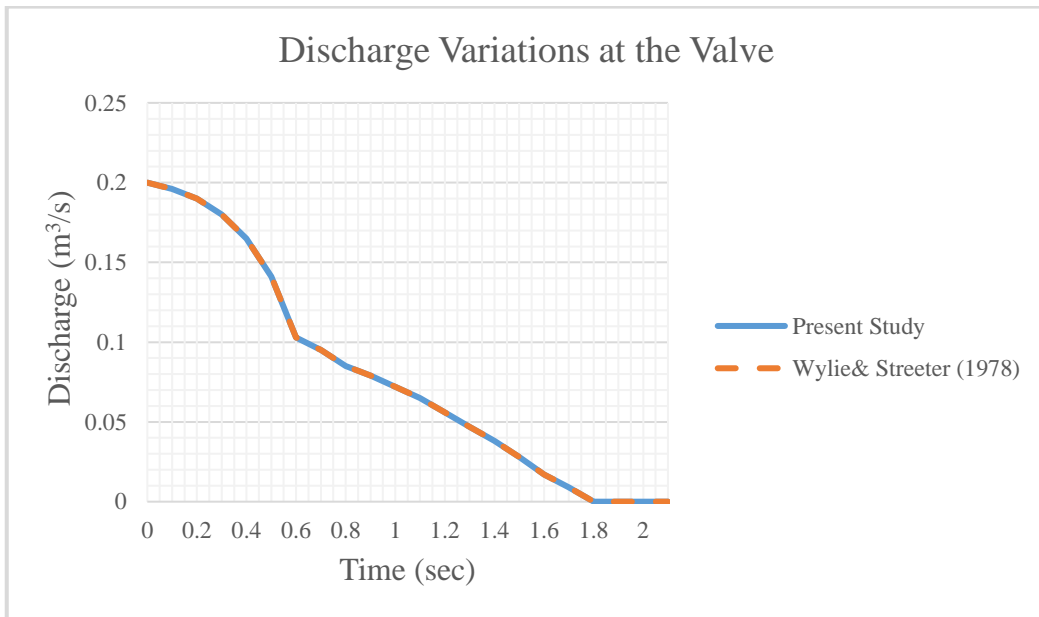


Figure 5.45 Graphical comparison for the Q values at the reservoir of Case-4

According to the comparison shown in Table 5.10, Table 5.11, Figure 5.44, and Figure 5.45, the obtained results in the presented study are highly accurate and very similar to the results presented in Wylie & Streeter (1978).



### 5.3 Verification for Surge Tanks

In order to verify the program for surge tank computations, two different cases, which contain different types of surge tanks, were used to benchmark the results calculated by the program with the results in the literature.

#### 5.3.1 Case-5: Simple Surge Tank by Cofcof (2011) Benchmark

In this section, the results of the computation for a simple surge tank are obtained and compared with the results in the literature. In the case study provided by Cofcof (2011), the hydraulic system includes a large upstream reservoir with a constant head, two pipes that refer to the energy tunnel and penstock, a surge tank, and a downstream control valve which is located at the upstream side of a turbine. The system and notations are illustrated in Figure 5.46. In this scenario, a case of a complete load rejection at the turbine at ‘t=0’ is studied, and water surface oscillation in a simple surge tank is observed with a simulation. This case is examined with the maximum and minimum initial discharge values for the hydraulic system.

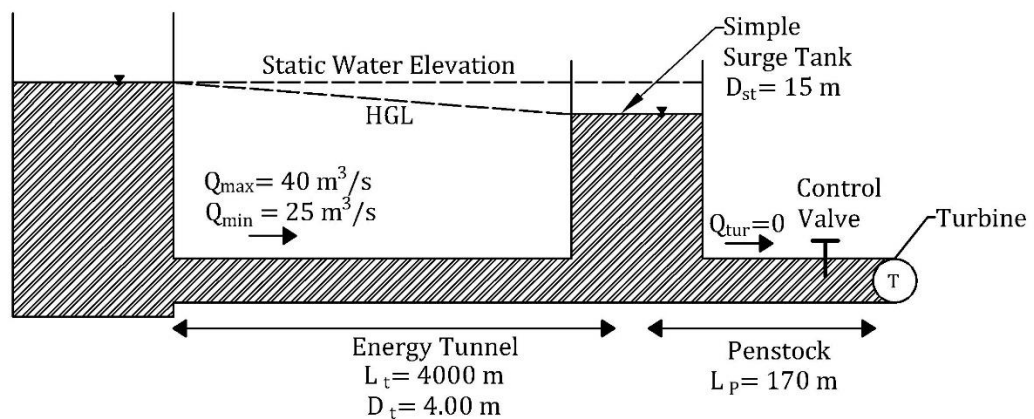


Figure 5.46 Configuration of Case-5 by Cofcof (2011)

According to Cofcof (2011), the known data for this case can be listed as:

- Water surface elevation in the reservoir,  $WSE_R = 350$  m

This also means the static water elevation is 350 m.

- Elevation of the tunnel centerline,  $WSE_R = 310$  m
- The maximum value of initial discharge through the energy tunnel for the first operation,  $Q_{t_{max}} = 40$  m<sup>3</sup>/s
- The maximum value of initial discharge through the energy tunnel for the second operation,  $Q_{t_{min}} = 25$  m<sup>3</sup>/s
- Head losses in the energy tunnel,  
 $h_f = 8.72$  m and  $h_f = 3.45$  m for  $Q_{t_{max}}$  and  $Q_{t_{min}}$  respectively
- Length of the penstock,  $L_p = 170$  m
- Length of the energy tunnel,  $L_t = 4000$  m
- Diameter of the tunnel,  $D_t = 4$  m
- Diameter of the penstock,  $D_p = 3.1$  m
- Diameter of the surge tank,  $D_{st} = 15$  m
- Turbine flow,  $Q_{turbine} = 0$  m<sup>3</sup>/s

At first, the surge tank simulator panel in the program is used to solve this case with the Runge-Kutta method. All data and properties are entered into the relevant sections as inputs in the surge tank simulator form of the program.

In addition to these given data, the simulation time is selected as 1000 seconds to observe fluctuations of the water surface in the simple surge tank properly. Then, the time increment is selected as 0.5 seconds.

From the head losses, the friction factor is calculated as 0.017 for the tunnel by using the Darcy-Weisbach head loss equation represented in Eq. (5.1).

$$h_f = f \frac{L}{D} \frac{Q^2}{2gA^2} \quad (5.1)$$

The calculated friction factor of the energy tunnel is inserted into the program instead of the Manning coefficient or beta value. Then the simulations for Case-5 with the discharge of 45 m<sup>3</sup>/s and 25 m<sup>3</sup>/s are shown in Figures 5.47 and 5.48, respectively.

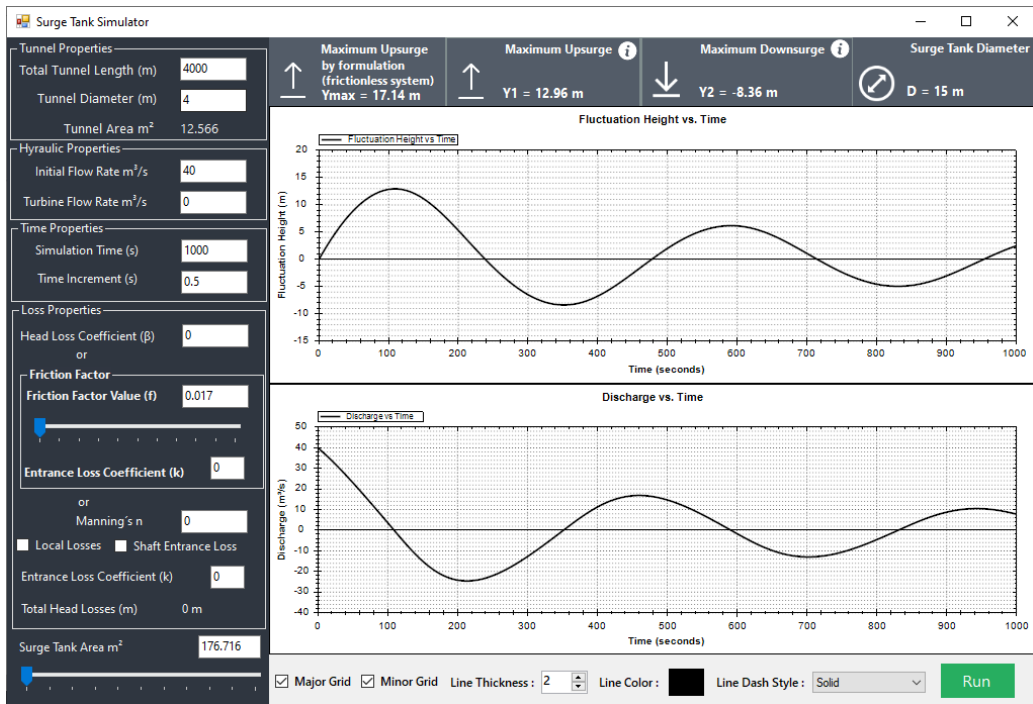


Figure 5.47 The view of the results in the surge tank simulator for Case-5  
( $Q_{\text{tunnel}}=40 \text{ m}^3/\text{s}$ )

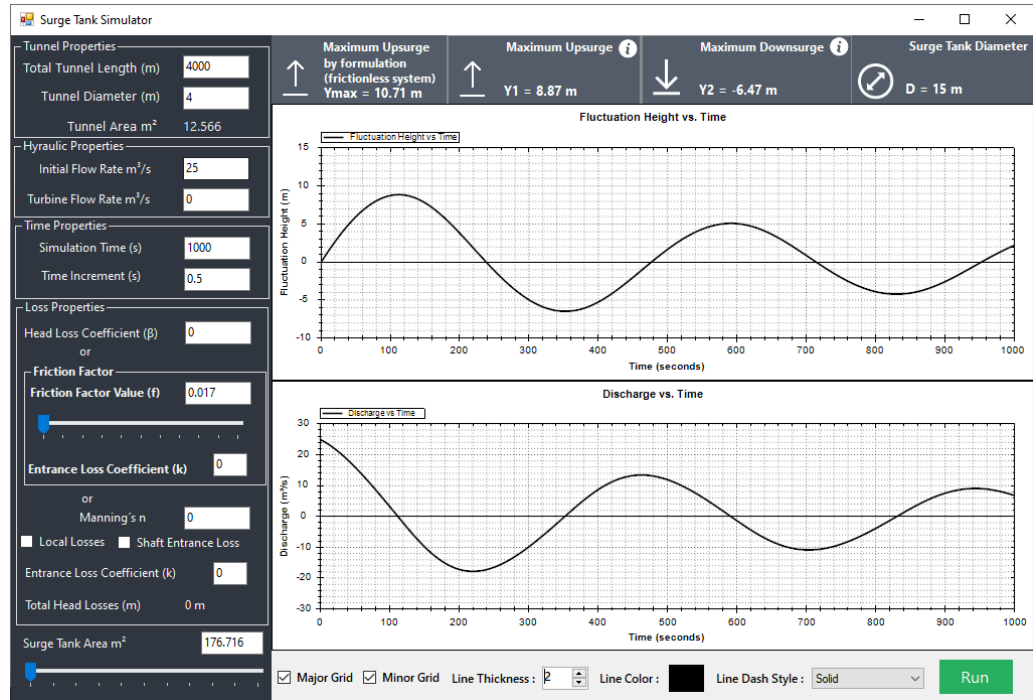


Figure 5.48 The view of the results in the surge tank simulator for Case-5  
( $Q_{\text{tunnel}}=25 \text{ m}^3/\text{s}$ )

As shown in the simulations, the maximum increase in the water level from the static water level ( $Y_1$ ) for the case with  $Q_{\text{tunnel}}=40 \text{ m}^3/\text{s}$  and  $Q_{\text{tunnel}}=25 \text{ m}^3/\text{s}$  is computed as 12.96 m and 8.87 m, respectively.

Then, to observe the  $Y_{\text{max}}$ , which is the value of the maximum increase in water level in the surge tank from the static water level in frictionless conditions, the case is simulated again. In these simulations, the friction factor values are inserted as '0', as shown in Figures 5.49 and 5.50.  $Y_{\text{max}}$  values are calculated as 17.36 m and 10.85 m for the case with  $Q_{\text{tunnel}}=40 \text{ m}^3/\text{s}$  and  $Q_{\text{tunnel}}=25 \text{ m}^3/\text{s}$ , respectively.

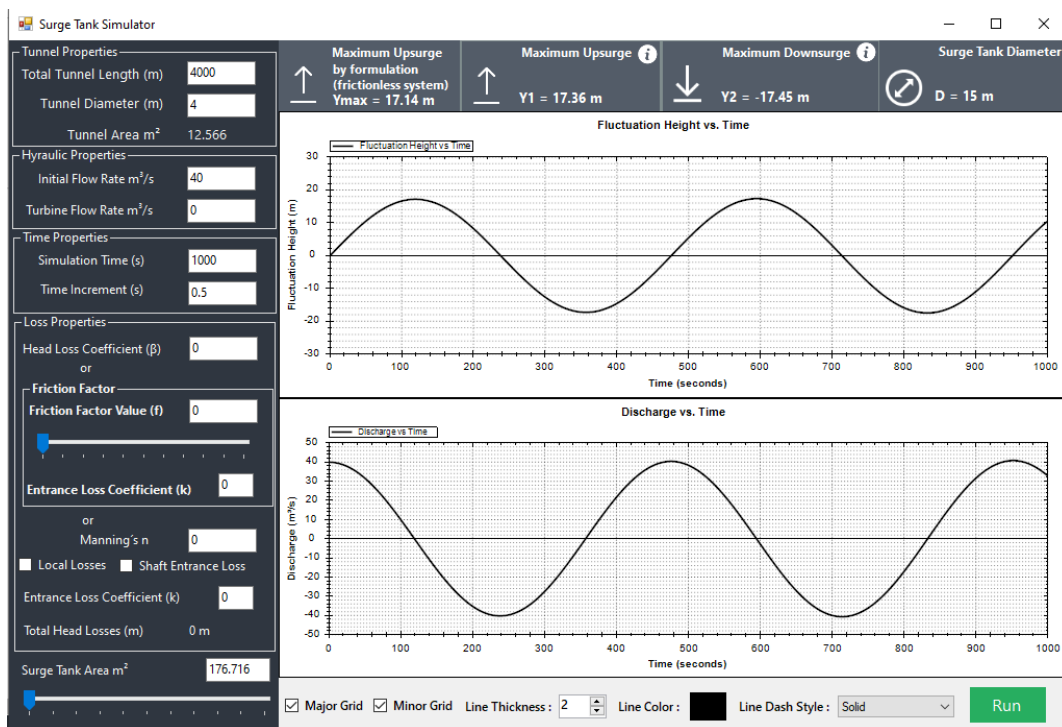


Figure 5.49 The view of the results in surge tank simulator for Case-5 ( $Q_{\text{tunnel}}=40 \text{ m}^3/\text{s}$ ) with frictionless condition

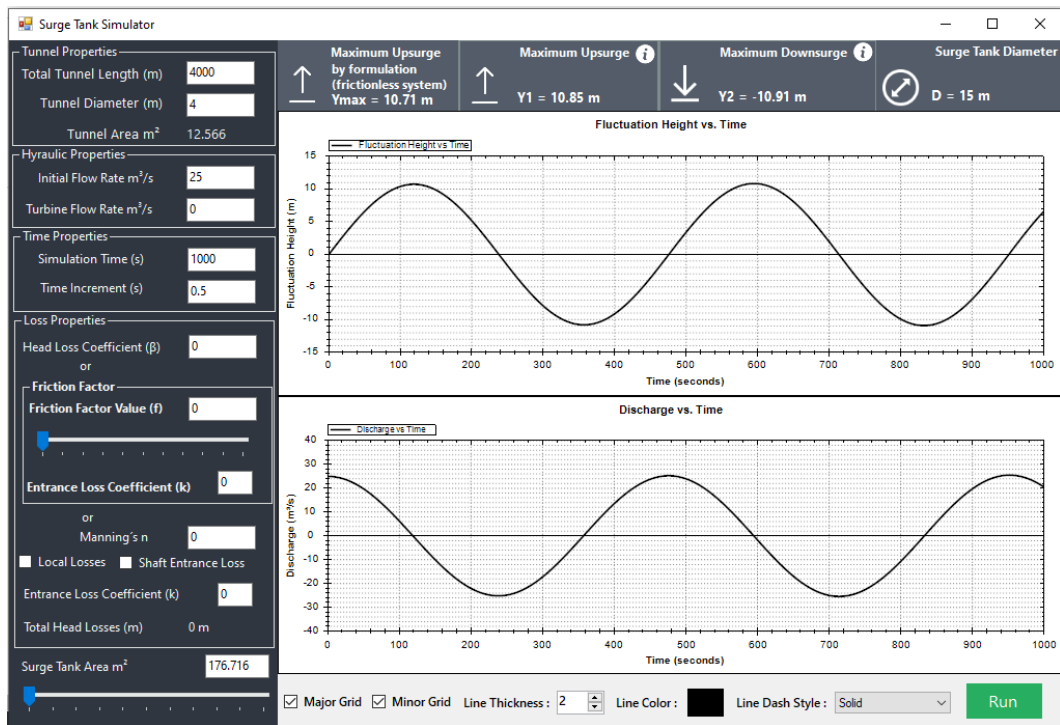


Figure 5.50 The view of the results in the surge tank simulator for Case-5 ( $Q_{\text{tunnel}}=25 \text{ m}^3/\text{s}$ ) with frictionless condition

The second solution technique is designing the model on the canvas of the program and observing the results computed with the method of characteristics. In this solution section, the elevations are used in the calculations.

In the first step, the case was visualized in the canvas of the program, as shown in Figure 5.51. Reservoir, pipes, simple surge tank, and control valve components are added to the system.

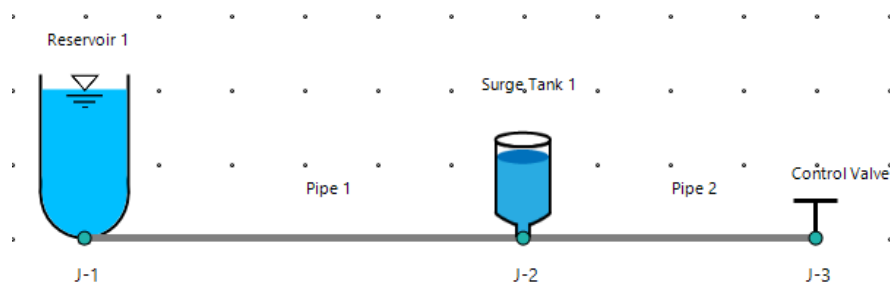


Figure 5.51 The visual design of Case-5 on canvas

Then, for the case with  $Q_{\text{tunnel}}=40 \text{ m}^3/\text{s}$ , the given properties of the upstream reservoir, Pipe 1, which refers to the energy tunnel, Pipe 2, which refers to penstock, and the surge tank are entered into relevant sections of properties panels in the program as shown in Figure 5.52, 5.53, 5.54, and 5.55 respectively. In addition, the wave speed of Pipe 1 and Pipe 2 is entered as 500 m/s.

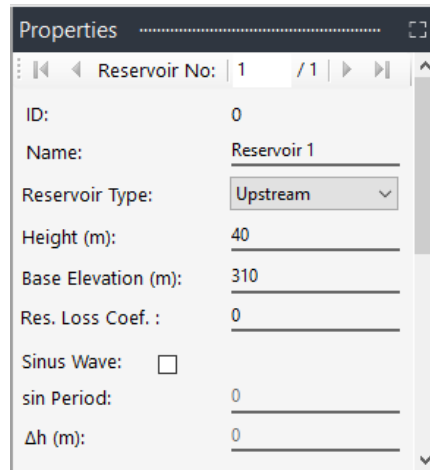


Figure 5.52 Inputs in the reservoir properties panel for the upstream reservoir of Case-5 ( $Q_{\text{tunnel}}=40 \text{ m}^3/\text{s}$ )

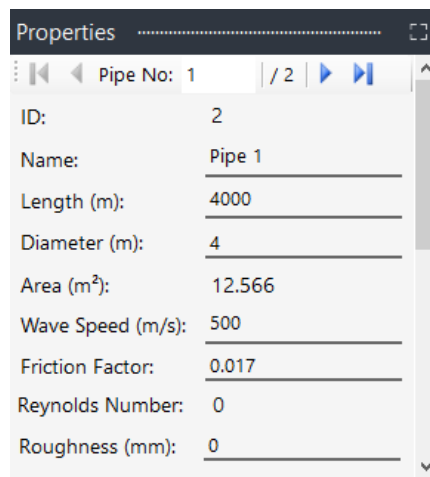


Figure 5.53 Inputs in the pipe properties panel for the first pipe of Case-5 ( $Q_{\text{tunnel}}=40 \text{ m}^3/\text{s}$ )

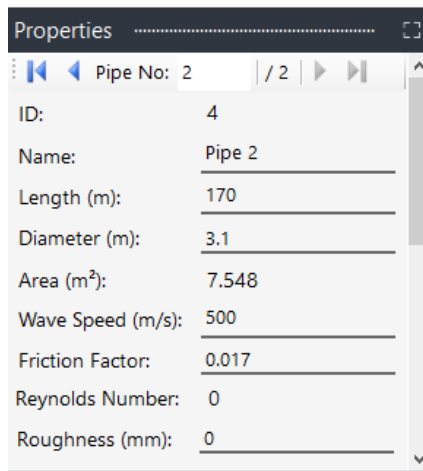


Figure 5.54 Inputs in the pipe properties panel for the second pipe of Case-5  
( $Q_{\text{tunnel}}=40 \text{ m}^3/\text{s}$ )

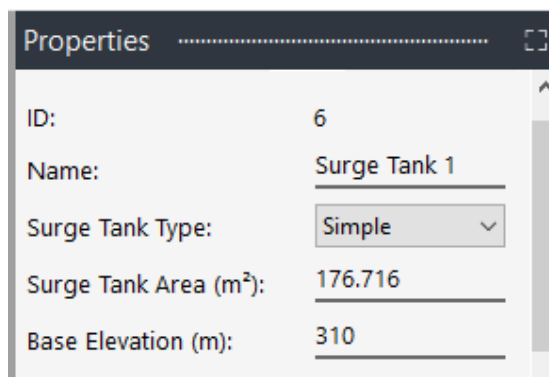


Figure 5.55 Inputs in the surge tank properties panel for the surge tank of Case-5  
( $Q_{\text{tunnel}}=40 \text{ m}^3/\text{s}$ )

In the initial conditions panel, the initial discharge given as input in Case-5, maximum time, and time step must be entered. Water surface oscillation in the surge tank cannot be observed in small time intervals properly, so the maximum time is defined as 1500 seconds to examine the oscillation in the results. The maximum allowable time step value is calculated by the program as 0.34 seconds to satisfy the Courant condition. Then this value is selected as a time step. The entered data about the initial conditions for the system is shown in Figure 5.56.

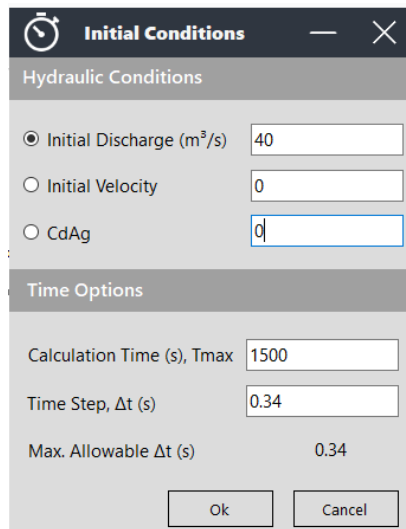


Figure 5.56 Inputs in the initial conditions panel for Case-5 ( $Q_{\text{tunnel}}=40 \text{ m}^3/\text{s}$ )

After that, all given and assumed data are entered into the proper panels of the program, transient analyses and simulations can be observed in tables, time charts, and animation charts forms. The obtained outputs for water level oscillation in the simple surge tank case which has an initial discharge of  $40 \text{ m}^3/\text{s}$ , are represented in graphical form as shown in Figure 5.57.

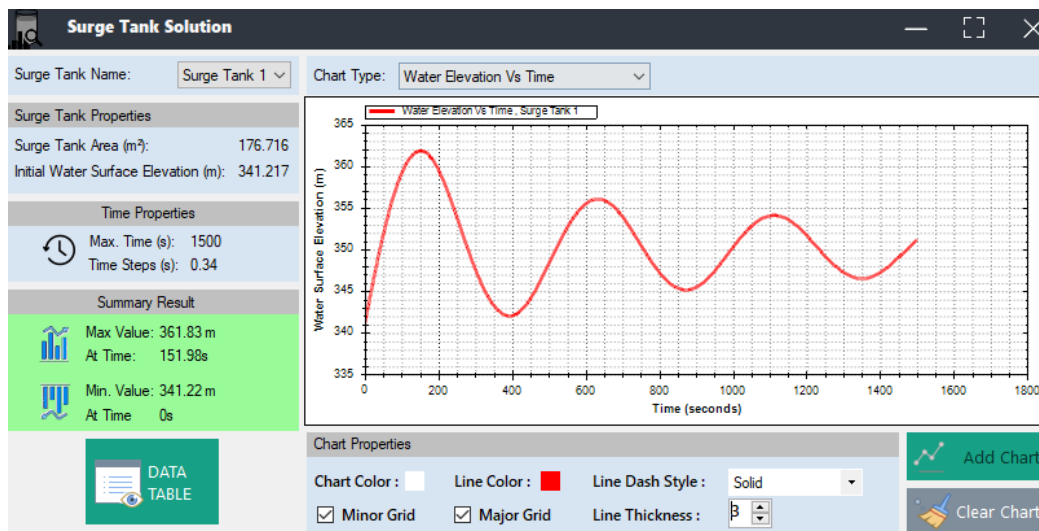


Figure 5.57 Graphical illustration of water oscillations in the surge tank for Case-5 ( $Q_{\text{tunnel}}=40 \text{ m}^3/\text{s}$ )



As shown in the graphical illustration, the maximum upsurge value is computed as 361.83 m. Then, the maximum increase in the water level from the static water level ( $Y_1$ ) for the case with  $Q_{\text{tunnel}}=40 \text{ m}^3/\text{s}$  is computed as;

$$Y_1 = 361.83 \text{ m} - 350 \text{ m} = 11.83 \text{ m}$$

Then, to observe the  $Y_{\text{max}}$ , which is the value of the maximum increase in water level in the surge tank from the static water level in frictionless conditions, the case is simulated again. In this simulation, the friction factors for the pipes are inserted as '0'. The maximum upsurge elevation of the water in the surge tank for the frictionless model is 367.16 m, as seen in Figure 5.58. So,  $Y_{\text{max}}$  values can be calculated as;

$$Y_{\text{max}} = 367.16 \text{ m} - 350 \text{ m} = 17.86 \text{ m}$$

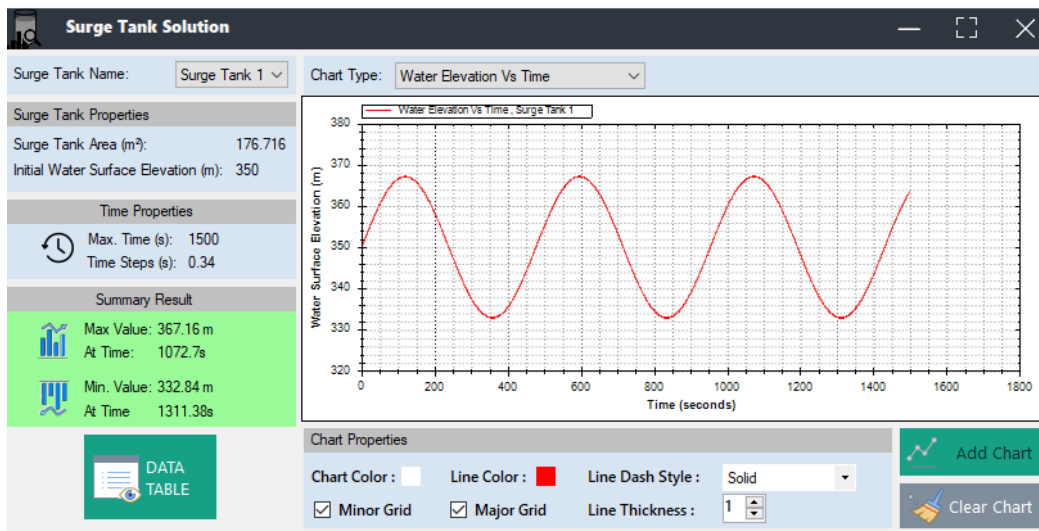


Figure 5.58 Graphical illustration of water oscillations in the surge tank for Case-5 ( $Q_{\text{tunnel}}=40 \text{ m}^3/\text{s}$ ) for frictionless condition

Then the same calculation procedures are applied for Case-5 with the initial discharge of  $25 \text{ m}^3/\text{s}$ . After these computations,  $Y_{\text{max}}$  and  $Y_1$  values for the case with  $25 \text{ m}^3/\text{s}$  are obtained as 10.72 m and 8.55 m, respectively.

Finally, all results computed by the Runge-Kutta method, which is used in the surge tank simulator panel, and the method of characteristics which is used in the main form of the program are compared with the results in Cofcof (2011) as seen in Table

5.12 and Table 5.13. It must also be mentioned that Cofcof (2011) used empirical equations to simulate this case study.

Table 5.12 Tabular comparison of  $Y_{\max}$  values for Case-5.

Initial Discharge ( $\text{m}^3/\text{s}$ )	$Y_{\max}$ (m)		
	Present Study		Cofcof (2011)
	by Runge-Kutta	by MOC	
40	17.36	17.86	17.10
25	10.85	10.72	10.76

Table 5.13 Tabular comparison of  $Y_1$  values for Case-5

Initial Discharge ( $\text{m}^3/\text{s}$ )	$Y_1$ (m)		
	Present Study		Cofcof (2011)
	by Runge-Kutta	by MOC	
40	12.96	11.83	11.8
25	8.87	8.55	Not Provided

According to the comparison, the obtained results in the present study are similar to the results presented in Cofcof (2011). The differences can be caused by the method that is used for solutions, differences in head loss calculations, variety of the selection of head loss coefficients, and the consideration of minor losses.

### 5.3.2 Case-6: Surge Tank with Standpipe by Cofcof (2011) Benchmark

In this section, the results of the computation for a surge tank with a standpipe are obtained and compared with the results in the literature. In the case study provided by Cofcof (2011), the hydraulic system includes an upstream reservoir with a constant head, two pipes that refer to the energy tunnel and penstock, a surge tank with a standpipe, and a downstream control valve that is located at the upstream side of a turbine. The system and notations are illustrated in Figure 5.59. In this scenario, a case of a complete load rejection at the turbine at 't=0' is studied and water surface oscillation in a surge tank connected to a pipeline with a standpipe is observed.

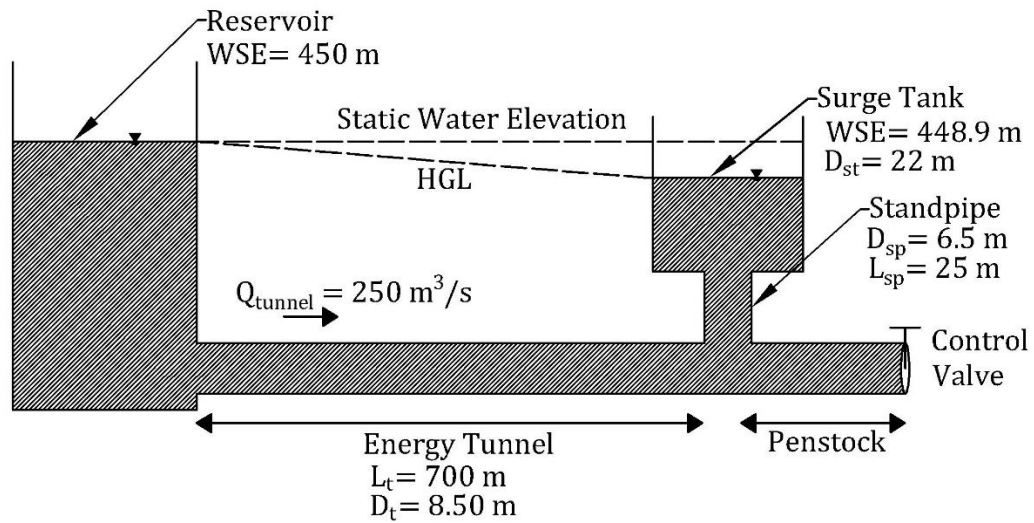


Figure 5.59 Case-6 as used by Cofcof (2011)

According to Cofcof (2011), the known data for this case can be listed as:

- Initial water surface elevation in the reservoir,  $WSE_R = 450$  m
- Elevation of the center of the tunnel,  $TCE = 398$  m
- Initial discharge through the energy tunnel,  $Q_t = 250$  m<sup>3</sup>/s
- Length of the tunnel,  $L_t = 700$  m
- Diameter of the tunnel,  $D_t = 8.5$  m
- Diameter of the surge tank,  $D_{st} = 22$  m
- Diameter of the standpipe,  $D_{sp} = 6.5$  m
- Length of the standpipe,  $L_{sp} = 25$  m
- Initial water surface elevation in the surge tank determined by head losses in the tunnel,  $WSE_{ST} = 448.9$  m
- Static water elevation,  $SWE = 450$  m

It is also known that the friction in the standpipe is neglected during the computation for Case-6.

From the known data, the height of the water surface in the reservoir is calculated as;

$$WSE_R - TCE = 450 \text{ m} - 398 \text{ m} = 52 \text{ m}$$

The base elevation of the surge tank can be calculated as;

$$BE_{ST} = TCE + \frac{D_t}{2} + L_{st} = 398 \text{ m} + 4.25 \text{ m} + 25 \text{ m} = 427.25 \text{ m}$$

The initial height of the water surface in the surge tank from the base elevation of the surge tank can be computed as;

$$WSE_{ST} - BE_{ST} = 448.9 \text{ m} - 427.25 \text{ m} = 21.65 \text{ m}$$

In the program, the computation process of water oscillation in the surge tank with a standpipe contains the method of characteristics equations. So, the friction factor of the tunnel must be entered as an input. In order to determine the friction factor, the known value of the head loss on the tunnel is used. The difference between the hydraulic grade line elevations of the surge tank and the reservoir section in the steady-state condition gives the head losses in the tunnel, which is 1.1 m. Then the friction factor of the tunnel can be obtained as 0.013 by using the Darcy-Weisbach head loss equation.

In the first step, Case-6 was visualized in the canvas of the program, as shown in Figure 5.60. Reservoir, pipes, surge tank with a standpipe, and control valve are added to the system. The second pipe is added to the system in order to provide the connection between the surge tank and downstream instant load rejection.

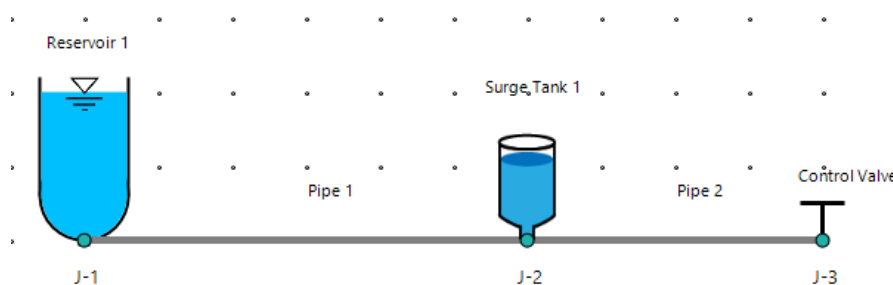


Figure 5.60 Visual design of Case-6 in canvas

Then, the given properties of the upstream reservoir, Pipe 1, Pipe 2, and the surge tank are entered into relevant sections of properties panels in the program, as shown

in Figures 5.61 through 5.64, respectively. The diameter and length of Pipe 2 are entered as 8.5 m and 10 m, respectively. In addition, the wave speed of Pipe 1 and Pipe 2 is entered as 500 m/s.

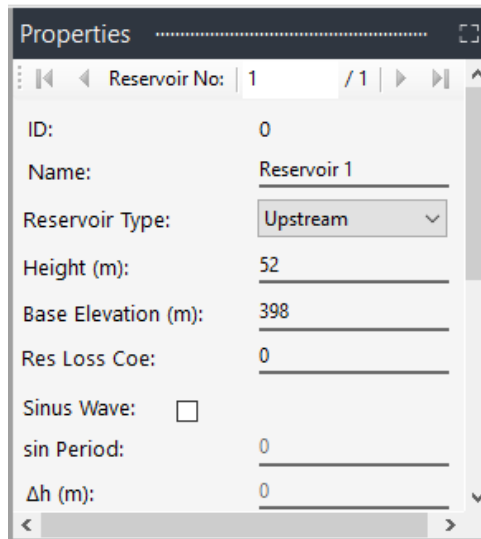


Figure 5.61 Inputs in the reservoir properties panel for the upstream reservoir of Case-6

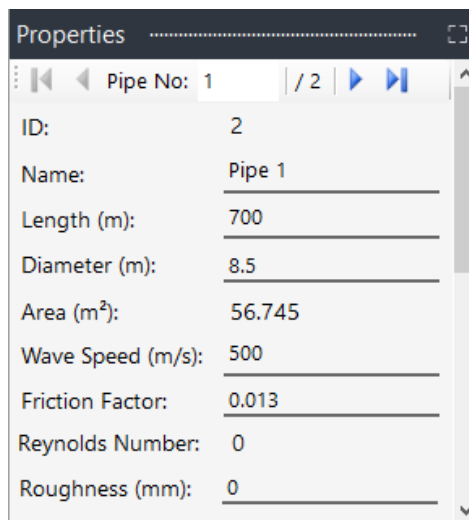


Figure 5.62 Inputs in the pipe properties panel for the 1<sup>st</sup> pipe of Case-6

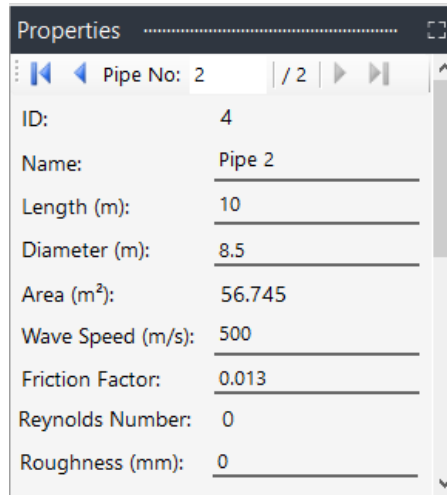


Figure 5.63 Inputs in the pipe properties panel for the 2<sup>nd</sup> pipe of Case-6

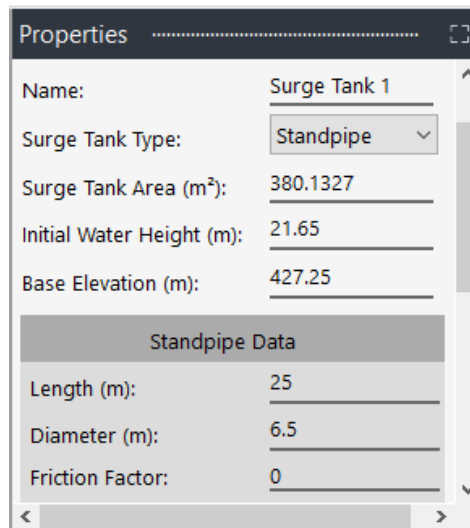


Figure 5.64 Inputs in the surge tank properties panel for Case-6

In the settings panel of initial conditions, the initial discharge is given as input; the maximum simulation time and time step must also be entered. The maximum time is defined as 300 seconds to visibly examine the oscillation in the results. The maximum allowable time step value is calculated by the program as 0.02 seconds to satisfy the Courant condition. Then this value is selected as a time step. It must also be mentioned that the maximum allowable time increment value can be increased by using the second pipe as the connection pipe. The entered data about the initial conditions for the system is shown in Figure 5.65.

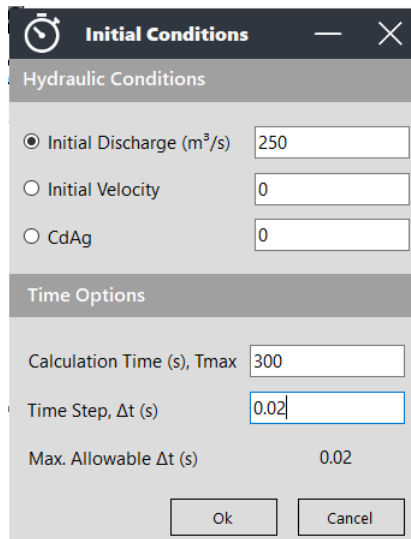


Figure 5.65 Inputs in the initial conditions panel for Case-6

After that, all given and assumed data are entered into proper panels of the program, transient analyses and simulations can be observed in tables, time charts, and animation charts forms. The obtained outputs for water level oscillation in the surge tank are represented in graphical form, as shown in Figure 5.66.

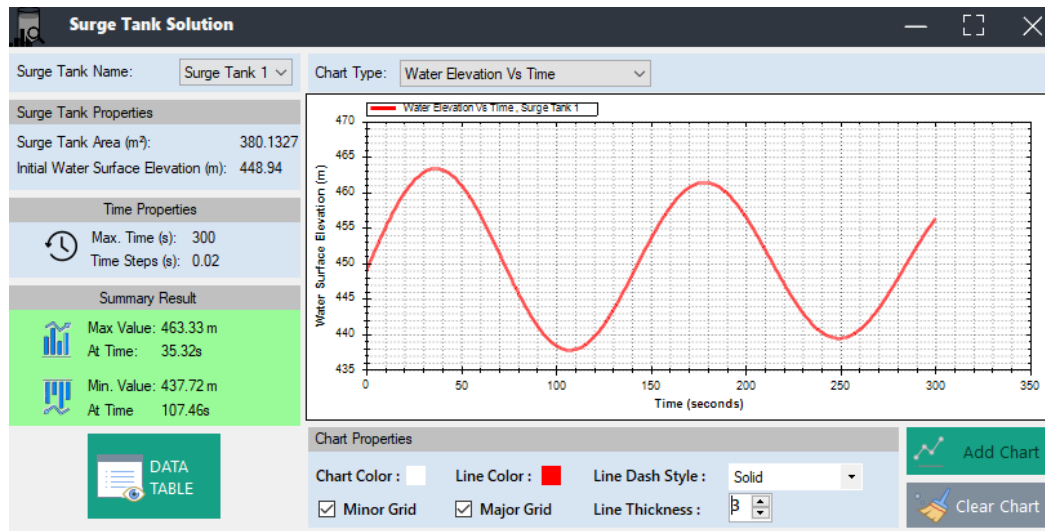


Figure 5.66 Graphical illustration of water oscillations in the surge tank for Case-6  
According to the results computed in the program, the maximum upsurge and downsurge elevations are obtained as 463.33 m and 437.72 m, respectively, as shown in Figure 5.66. In order to compare the results with the results given by Cofcof

(2011), the value of the maximum increase in water level from the static water level in frictionless conditions ( $Y_{\max}$ ), the maximum increase in water level from the static water level ( $Y_1$ ), and maximum decrease in water level from the static water level ( $Y_2$ ) in the surge tank are calculated. The maximum upsurge of the frictionless system is observed at an elevation of 464 m in a new simulation. In this simulation, all case data stay the same, but the friction factor value is adjusted as '0' for the energy tunnel. Then the results are calculated as;

$$Y_{\max} = 464.00 \text{ m} - 450 \text{ m} = 14.00 \text{ m}$$

$$Y_1 = 463.33 \text{ m} - 450.00 \text{ m} = 13.33 \text{ m}$$

$$Y_2 = 450.00 \text{ m} - 437.72 \text{ m} = 12.28 \text{ m}$$

The results of empirical solutions by Jaeger (1956) and Forcheimer (1901); graphical solutions by Parmakian (1963) for this case study are provided by Cofcof (2011). Finally, the results of those solutions and the results of the present study are compared in Table 5.14.

Table 5.14 Comparison of the results for Case-6

	EMPIRICAL SOLUTIONS		GRAPHICAL SOLUTIONS	SOLUTIONS BY MOC
	Jaeger (1956)	Forcheimer (1901)	Parmakian (1963)	Present Study
$Y_{\max}$	14.36 m	Not Provided	Not Provided	14.00 m
$Y_1$	11.97 m	Not Provided	11.00 m	13.33 m
$Y_2$	Not Provided	15.00 m	12.10 m	12.28 m

It is obvious that the obtained results in the present study are to a large degree similar to the results presented in Cofcof (2011). The small differences, which are negligible, may be attributed to the method that is used for solutions, differences in head loss calculation, and the consideration of minor losses.



## 5.4 Verification for Pump Failure

In order to verify the program for pump failure scenarios, a case study was used to compare the results calculated by the program with the results in the literature.

### 5.4.1 Case-7: Pump Failure by Wylie et al. (1993) Benchmark

A transient event can also be observed for pump failure scenarios. In this section, the developed program will be verified for pump failure situations with a case study presented by Wylie et al. (1993). In this case study, called Case-7, the hydraulic system includes an upstream reservoir, downstream reservoir, pipe, and pump with a discharge valve. The system and notations are illustrated in Figure 5.67.

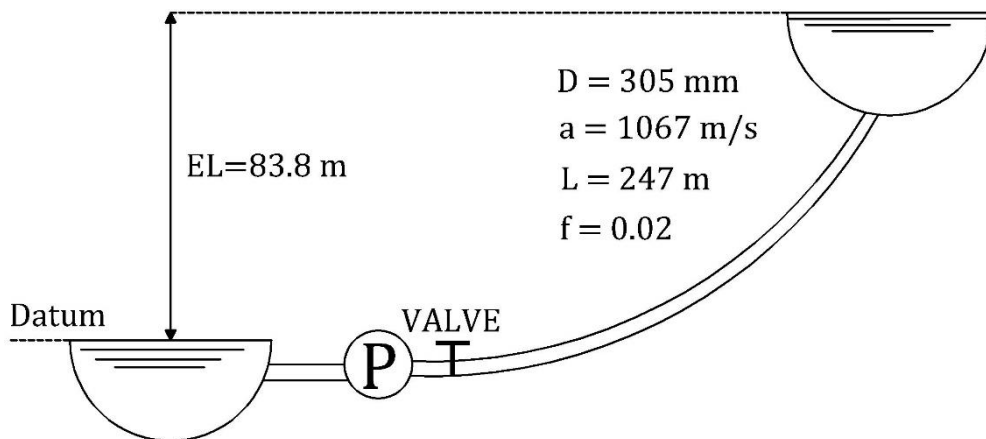


Figure 5.67 The pump failure scenario presented by Wylie et al. (1993)

In Case-7, the datum is located at the water level of the upstream reservoir. According to Wylie et al. (1993), the known data for the system can be listed as shown in Table 5.15.

In this benchmark, a pump trips at  $t=0$  due to sudden power loss. In addition, a valve at the downstream side of the pump starts to close 1.5 seconds after the pump failure occurs.

Table 5.15 Given data for Case-7 as used by Wylie et al. (1993)

DATA TYPE	VALUE	UNIT
Pipe Length (L)	427	m
Pipe Diameter (D)	305	mm
Wave Speed (a)	1067	m/s
Friction Factor of Pipe (f)	0.02	-
Elevation of Upstream Reservoir (ELL)	0	m
Elevation of Downstream Reservoir (ELR)	83.8	m
Rated Head of Pump ( $H_R$ )	94.488	m
Rated Discharge of Pump ( $Q_R$ )	0.1764	m <sup>3</sup> /s
Rated Torque of Pump ( $T_R$ )	100.926	Nm
Rated Speed of Pump ( $N_R$ )	1760	rpm
WR <sup>2</sup> Value of Pump	7.88	Nm <sup>2</sup>
Valve Loss Coefficient	0.3	-
Pump Trip Time	0	sec
Time increment (t)	0.2	sec

In the first stage, the case was visualized in the canvas of the program, as shown in Figure 5.68. In this step, the upstream reservoir, connection pipe (first pipe), pump with a discharge valve, main pipe (second pipe), and downstream reservoir components are added to the system. The main reason for using the connection pipe is that the pump component is connected next to the upstream reservoir in the case study. In the developed program, this situation can be modeled with the help of a connection pipe.

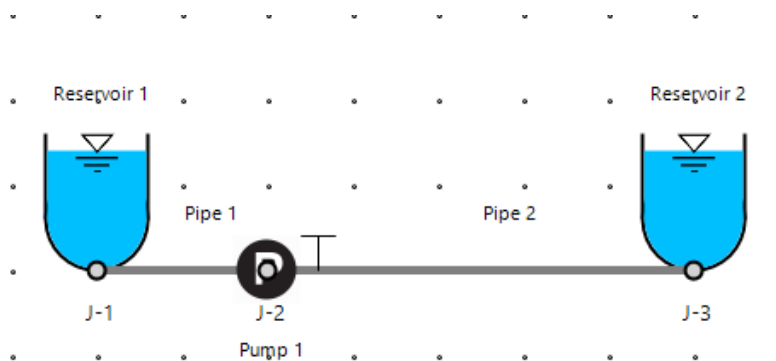


Figure 5.68 Visual design of Case-7 in canvas

Then, the properties of the upstream reservoir, connection pipe, main pipe, and downstream reservoir components are entered into relevant sections of properties panels in the program. In order to enter pump properties, at first, a pump setting is created in the pump settings panel, as shown in Figure 5.69. This dataset includes the rated values, which are given in Table 5.15, and the pump characteristics (Suter) curve. In this benchmark, the pump characteristics curve used for NS=35 rpm (SI units) has been selected. Then the whole pump and discharge valve data are entered in the pump properties panel.

Next, data about the initial conditions for the system are entered into the program. The maximum allowable time increment value is calculated as 0.4 seconds to satisfy the Courant condition. So, the time increment can be selected as 0.2 seconds. The maximum simulation time is selected as 12 seconds.

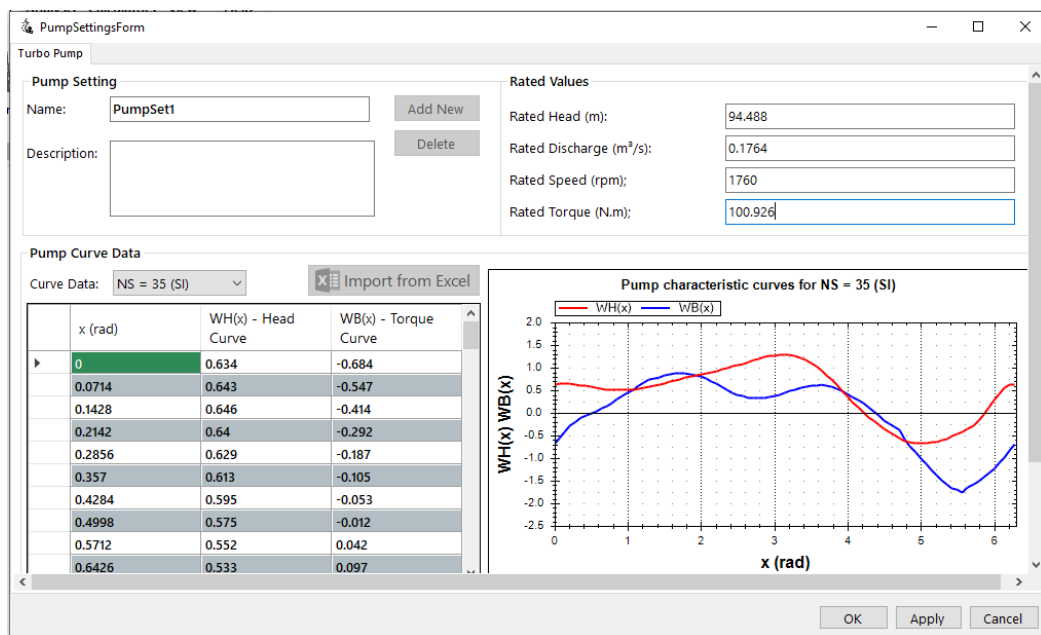


Figure 5.69 The entered inputs in the pump settings panel for Case-7

After the determination of time selections, valve closure data are defined in the valve closure settings panel for the discharge valve, as shown in Figure 5.70. According to the given data by Wylie et al. (1993), tabular closure data is used for this case study.

**T Valve Closure Setting**

Calculation Time, Tmax (sec) : 12

Time Step, Δt (sec) : 0.2

Valve Name : Right discharge valve for Pump 1

Select a method to initialize the valve closure:

Regular Valve Closure  Tabular Data

$$\tau = \left(1 - \frac{t}{t_c}\right)^{E_m}$$

Valve Closure Constant, Em : 0

Closure Time, Tc (sec) : 0

**i** This is a valve closure relationship for the pipeline.  
 $\tau$  is dimensionless and is a function of time.

Import from Excel Clear

Time	Tau
0	1
0.2	1
0.4	1
0.6	1
0.8	1
1	1
1.2	1
1.4	1
1.6	0.907
1.8	0.721
2	0.535
2.2	0.349
2.4	0.163
2.6	0.069
2.8	0.067
3	0.065
3.2	0.063
3.4	0.061

Figure 5.70 Inputs in valve closure settings panel for Case-7

After that, all data are entered into the proper panels of the program, transient analyses and simulations can be observed in tables, time charts, and animation charts forms. In the steady state calculation of the system, the initial discharge is calculated as 0.1805 m<sup>3</sup>/s. Then, with the transient analysis, the program calculated the unknowns at each node and junction.

The obtained results for just the downstream side of the pump, which is located at the second junction, are represented in tabular form, as shown in Figure 5.71. The outputs for the discharge and head values at the downstream side of 'Junction 2' are also represented in graphical form, as shown in Figure 5.72.

Time (sec)	Object Name	Side	Distance from Reservoir (m)	Head (m)	Discharge (m <sup>3</sup> /s)	Velocity (m/s)	Pressure (KPa)
0.00	J-2	Downstream	1	92.507	0.181	2.471	907.912
0.20	J-2	Downstream	1	68.933	0.165	2.254	676.547
0.40	J-2	Downstream	1	52.262	0.153	2.101	512.933
0.60	J-2	Downstream	1	39.918	0.146	1.994	391.778
0.80	J-2	Downstream	1	30.71	0.14	1.913	301.406
1.00	J-2	Downstream	1	31.268	0.111	1.519	306.881
1.20	J-2	Downstream	1	29.738	0.089	1.219	291.862
1.40	J-2	Downstream	1	27.474	0.073	0.999	269.642
1.60	J-2	Downstream	1	25.315	0.06	0.828	248.456
1.80	J-2	Downstream	1	24.679	0.033	0.456	242.212
2.00	J-2	Downstream	1	23.476	0.011	0.146	230.405
2.20	J-2	Downstream	1	22.294	-0.007	-0.096	218.805
2.40	J-2	Downstream	1	22.187	-0.021	-0.283	217.756
2.60	J-2	Downstream	1	25.373	-0.046	-0.625	249.02
2.80	J-2	Downstream	1	30.497	-0.065	-0.895	299.317
3.00	J-2	Downstream	1	35.046	-0.08	-1.101	343.962
3.20	J-2	Downstream	1	38.57	-0.091	-1.249	378.552
3.40	J-2	Downstream	1	46.45	-0.108	-1.477	455.891
3.60	J-2	Downstream	1	52.034	-0.12	-1.637	510.687
3.80	J-2	Downstream	1	56.011	-0.128	-1.751	549.727
4.00	J-2	Downstream	1	58.706	-0.134	-1.833	576.17

Figure 5.71 The view of the tabular results at the pump for Case-7

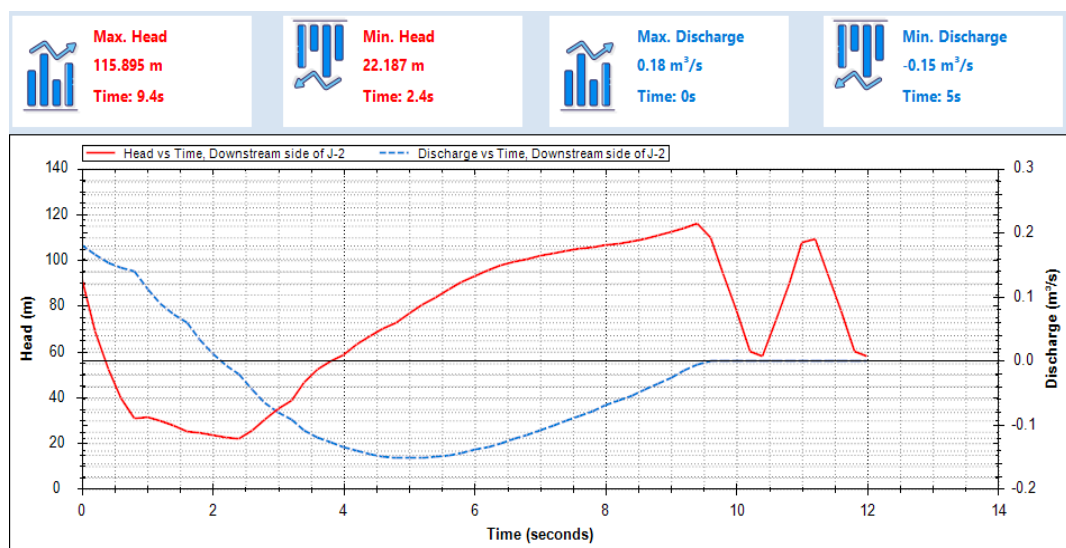


Figure 5.72 Graphical illustration of H and Q values at the downstream side of the pump for Case-7

After the results are obtained in both tabular and graphical form, these results are compared with those presented by Wylie et al. (1993). The results in the literature

are calculated by the method of the characteristics as in the developed program. Head and discharge values for the downstream reservoir and the pump sections are compared in tabular form, as shown in Table 5.16 and Table 5.17. It must be mentioned that Wylie et al. (1993) provided the head and discharge output data for the time interval of [0-4.8] and [7.6-10.8]. Then, the graphical comparison is made for head values at the pump section for [0-4.8] and [7.6-10.8] time intervals, as shown in Figure 5.73 and Figure 5.74, respectively. In addition, the graphical comparison is made for discharge values at the pump section for [0-4.8] and [7.6-10.8] time intervals, as shown in Figure 5.75 and Figure 5.76, respectively.

According to the comparison shown in Table 5.16, Table 5.17, Figure 5.73, Figure 5.74, Figure 5.75, and Figure 5.76, the obtained results in the present study are highly accurate and very similar to the results presented in Wylie et al. (1993). The calculated node number and the unit conversions may cause differences in the results. Wylie, Streeter and Suo provide that the node number is selected as four. In the developed program, the node number is calculated as two according to the time increment value. It must also be mentioned that the properties data of the case and the outputs are given in common U.S. Customary units in the literature. The data were converted to the SI units for this program. Some conversion error due to truncation of the digits is possible. The maximum difference in head and discharge values are 3 m and 0.006 m<sup>3</sup>/s, respectively. Also, the maximum difference rate is approximately %15 and %7 for discharge and head values, respectively. Still, the head and discharge values calculated in the program are generally similar to the literature results. So, the small differences may be considered negligible. Then, it can be said that the code is verified for the pump trip scenarios as well.

Table 5.16 Tabular comparison of H and Q values at the pump and downstream reservoir for the interval [0 - 4.8] sec., Case 7

		At the Pump Location				At the Downstream Reservoir			
		Wylie et al. (1993)		Present Study		Wylie et al. (1993)		Present Study	
TIME (s)	$\tau$	Q (m <sup>3</sup> /s)	H (m)	Q (m <sup>3</sup> /s)	H (m)	Q (m <sup>3</sup> /s)	H (m)	Q (m <sup>3</sup> /s)	H (m)
0	1	0.182	92.914	0.181	92.507	0.182	83.8	0.181	83.8
0.2	1	0.166	69.068	0.165	68.933	0.182	83.8	0.181	83.8
0.4	1	0.155	52.150	0.153	52.262	0.182	83.8	0.181	83.8
0.6	1	0.148	39.729	0.146	39.918	0.152	83.8	0.150	83.8
0.8	1	0.142	30.395	0.140	30.710	0.131	83.8	0.128	83.8
1	1	0.114	30.792	0.111	31.268	0.116	83.8	0.113	83.8
1.2	1	0.093	29.230	0.089	29.738	0.105	83.8	0.101	83.8
1.4	1	0.077	26.933	0.073	27.474	0.078	83.8	0.074	83.8
1.6	0.907	0.065	24.735	0.060	25.315	0.056	83.8	0.052	83.8
1.8	0.721	0.038	24.276	0.033	24.679	0.039	83.8	0.034	83.8
2	0.535	0.016	23.121	0.011	23.476	0.026	83.8	0.021	83.8
2.2	0.349	-0.001	21.858	-0.007	22.294	-0.001	83.8	-0.006	83.8
2.4	0.163	-0.015	21.282	-0.021	22.187	-0.023	83.8	-0.030	83.8
2.6	0.069	-0.040	23.658	-0.046	25.373	-0.042	83.8	-0.048	83.8
2.8	0.067	-0.059	28.031	-0.065	30.497	-0.055	83.8	-0.062	83.8
3	0.065	-0.075	32.332	-0.080	35.046	-0.079	83.8	-0.084	83.8
3.2	0.063	-0.086	35.682	-0.091	38.570	-0.095	83.8	-0.100	83.8
3.4	0.061	-0.103	43.656	-0.108	46.450	-0.107	83.8	-0.112	83.8
3.6	0.059	-0.115	49.265	-0.120	52.034	-0.115	83.8	-0.120	83.8
3.8	0.057	-0.124	53.405	-0.128	56.011	-0.127	83.8	-0.131	83.8
4	0.055	-0.130	56.219	-0.134	58.706	-0.135	83.8	-0.138	83.8
4.2	0.053	-0.139	61.331	-0.141	63.321	-0.141	83.8	-0.143	83.8
4.4	0.051	-0.144	64.975	-0.146	66.878	-0.145	83.8	-0.147	83.8
4.6	0.049	-0.147	68.081	-0.149	69.824	-0.149	83.8	-0.151	83.8
4.8	0.047	-0.149	70.931	-0.151	72.826	-0.152	83.8	-0.153	83.8

Table 5.17 Tabular comparison of the H and Q values at the pump and downstream reservoir for the interval [7.6 - 10.8] sec., Case-7

		At the Pump Location				At the Downstream Reservoir			
		Wylie et al. (1993)		Present Study		Wylie et al. (1993)		Present Study	
TIME (s)	$\tau$	Q (m <sup>3</sup> /s)	H (m)	Q (m <sup>3</sup> /s)	H (m)	Q (m <sup>3</sup> /s)	H (m)	Q (m <sup>3</sup> /s)	H (m)
7.6	0.019	-0.088	106.123	-0.086	104.866	-0.089	83.8	-0.087	83.8
7.8	0.017	-0.080	107.090	-0.078	105.635	-0.081	83.8	-0.079	83.8
8	0.015	-0.072	107.997	-0.070	106.416	-0.073	83.8	-0.071	83.8
8.2	0.013	-0.063	108.963	-0.062	107.305	-0.064	83.8	-0.063	83.8
8.4	0.011	-0.055	110.044	-0.054	108.312	-0.055	83.8	-0.054	83.8
8.6	0.009	-0.046	111.178	-0.045	109.446	-0.046	83.8	-0.046	83.8
8.8	0.007	-0.036	112.485	-0.036	110.793	-0.037	83.8	-0.037	83.8
9	0.005	-0.027	113.925	-0.026	112.282	-0.028	83.8	-0.027	83.8
9.2	0.003	-0.016	115.515	-0.016	113.960	-0.017	83.8	-0.017	83.8
9.4	0.001	-0.006	117.334	-0.006	115.895	-0.007	83.8	-0.007	83.8
9.6	0	0.000	110.550	0.000	109.570	0.004	83.8	0.004	83.8
9.8	0	0.000	94.345	0.000	94.119	0.016	83.8	0.016	83.8
10	0	0.000	77.211	0.000	77.667	0.017	83.8	0.017	83.8
10.2	0	0.000	58.971	0.000	60.031	0.007	83.8	0.007	83.8
10.4	0	0.000	57.147	0.000	58.091	-0.004	83.8	-0.004	83.8
10.6	0	0.000	73.313	0.000	73.502	-0.016	83.8	-0.016	83.8
10.8	0	0.000	90.417	0.000	89.922	-0.017	83.8	-0.017	83.8



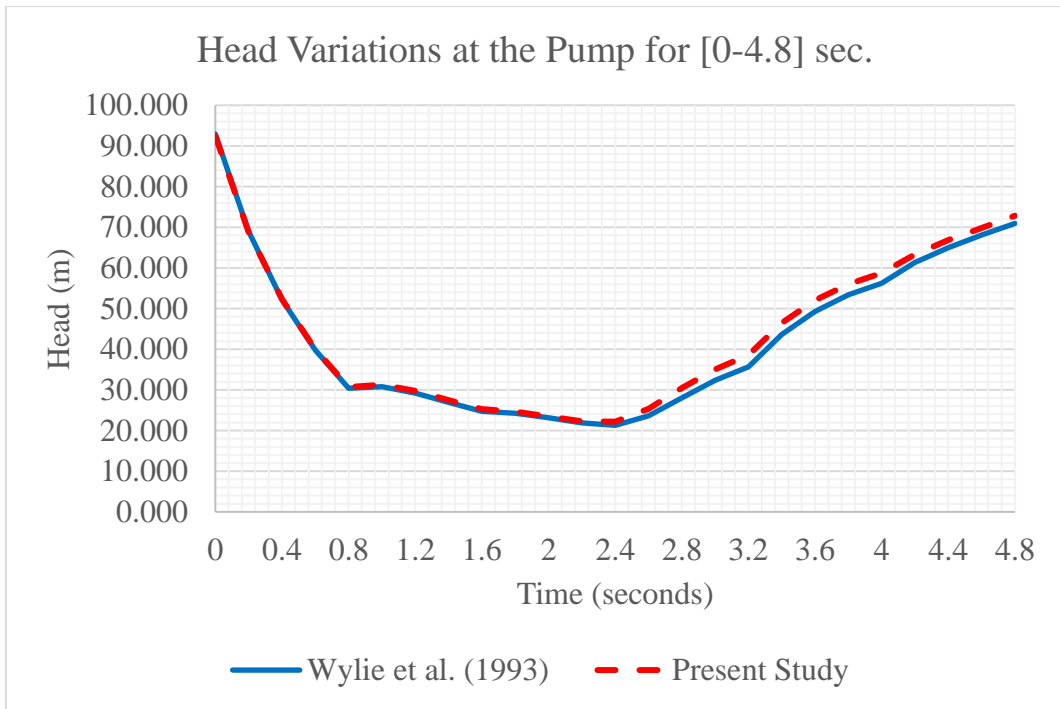


Figure 5.73 Graphical comparison of H values at the pump for [0-4.8] sec., Case-7

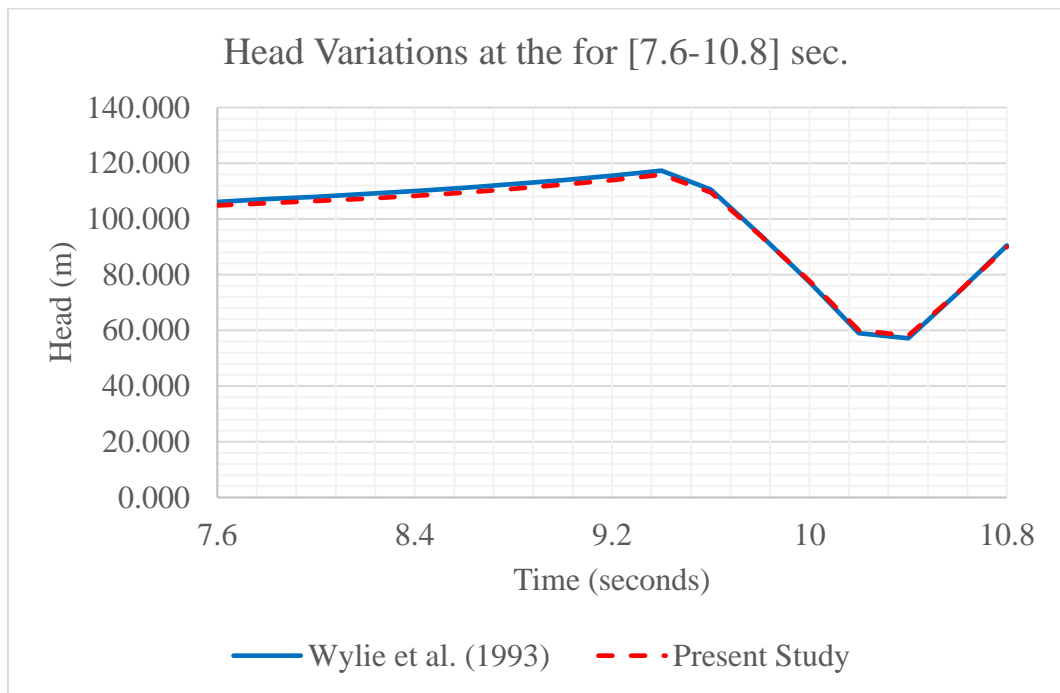


Figure 5.74 Graphical comparison of H values at the pump for [7.6-10.8] sec., Case-7

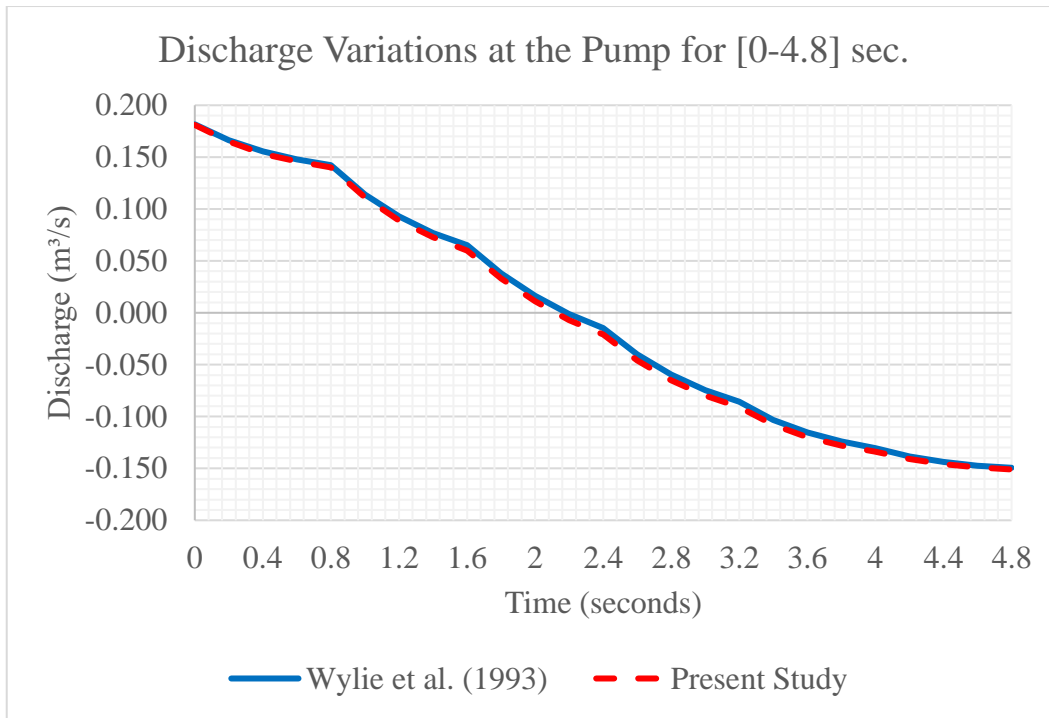


Figure 5.75 Graphical comparison of Q values at the pump for [0-4.8] sec., Case-7

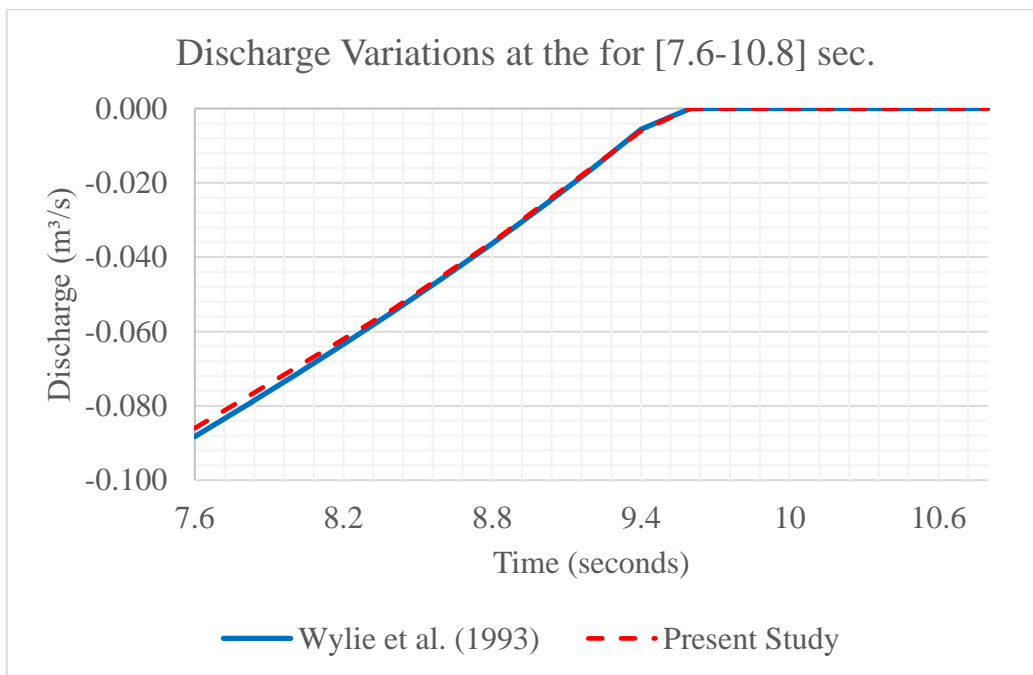


Figure 5.76 Graphical comparison of Q values at the pump for [7.6-10.8] sec., Case-7

## **CHAPTER 6**

### **DISCUSSION**

The developed program includes different features from previous studies. In this chapter, the computation time of the program will be discussed. Also, this program will be compared with the programs developed in earlier studies according to its advantages and disadvantages. The disadvantages will be presented as features that can be added in future works.

#### **6.1 Computation Time of the Program**

The software is verified for different transient flow scenarios in the previous chapter. The results for each case study were computed by running the program several times. The required times determined during these computation periods were averaged and the approximate computation time was determined for each benchmark, as shown in Table 6.1.

In Table 6.1, it can be inferred that the software can generally solve the investigated hydraulic system in a short computation time. On the other hand, the run time may increase due to the complexity of the hydraulic systems or the reduction of the time increment value. For instance, the computation time is calculated as 5.6 seconds for the surge tank with a standpipe scenario which has 0.02 seconds time increment value, even though the computation times of other scenarios are less than 1 second. This increase in time occurred with decreasing time steps may not be considered as a long time since it increases the accuracy of the calculation.

Table 6.1 The run time data of the benchmark studies

<b>Case Studies</b>	<b>Maximum Simulation Time (sec.)</b>	<b>Time Step (sec.)</b>	<b>Computer Run Time (sec.)</b>
Single Pipe Scenario by Wylie & Streeter (1978)	4.3	0.1	0.11
Single Pipe Scenario by Wood et al. (2005)	10	1	0.08
Pipes Connected in Series Scenario by Chaudhry (1979)	10	0.5	0.09
Pipes Connected in Series Scenario by Wylie & Streeter (1978)	2.1	0.1	0.08
Simple Surge Tank Scenario by Cofcof (2011)	1500	0.34	0.82
Surge Tank with a Standpipe Scenario by Cofcof (2011)	300	0.02	5.6
Pump Failure Scenario by Wylie et al. (1993)	12	0.2	0.11

The computation times of the recently developed program are not mentioned in the previous studies, so the comparison of run time for the programs is not provided in this study.

## **6.2 Advantages and Limitations of the Program**

This study includes different features and novelties that are not included in the previous works. Table 6.2 can be used to compare the developed software with the programs developed in the earlier studies by considering important features.

Table 6.2 Comparison table for features

Features	The Studies			
	Present Study	Koç (2007)	Dalgıç (2017)	Topraghghaleh (2020)
Detection of the order of objects	Yes	No	No	No
Requirements of external program	No	No	Yes	No
Topography	No	Yes	Yes	No
Steady-State Solution	Yes	Yes	No	No
Wave Speed and Friction Factor Calculator	Yes	Yes	Yes	Yes
Reynolds Number Calculator	Yes	Yes	No	No
Animation Chart	Yes	No	Yes	Yes
Solution for Pressurized Pipeline Systems	Yes	Yes	Yes	Yes
Solution for Pipes Connected in Series Systems	Yes	Yes	Yes	Yes
Solution for Branching Pipeline Systems	No	Yes	Yes	No
Solution for Parallel Pipeline Systems	No	Yes	Yes	No

As an essential novelty, the developed program can detect the order of the objects in the drawn hydraulic system. In other words, if users add a new component to any location in the system or delete an element from the system, the program will sort the system and provide a solution by considering the change in order. This feature, which is not provided in Koç (2007), Dalgıç (2017), and Topraghghaleh (2020), makes the program more user-friendly.

Since the developed program has its drawing area and various useful graphics, panels, table information input fields (data grid view), and text boxes, it can run independently without external programs such as AutoCAD and MS Excel. This feature, which is not provided in Dalgıç (2017), provides great convenience for users.

In the developed program, the steady-state solution of the system is also provided to users. Suppose the friction factor values of pipes and initial discharge value are not provided and required data are entered for a hydraulic system. In that case, the program can calculate these values for the steady-state conditions. This feature was not mentioned in the study of Dalgıç (2017) and Topraghghaleh (2020). In addition, this program contains wave speed, friction factor, and Reynolds number calculator windows. Some of these helpful windows are not provided in the recent studies, as shown in Table 6.2.

The program is designed to display the simulation results as tables, graphs, and animations. In the previous works, these simulation features are generally provided to the user. But the animation chart is not provided in Koç (2007).

Compared to the previous studies, the topography of the hydraulic system is partially provided to users. In the developed program, the base elevation and water level of the reservoirs can be entered as inputs. In addition, useful text boxes are added to the program to enter the elevation values of the junction.

The program can simulate the steady and transient flow for hydraulic systems, which include a single pipe and pipes connected in series. However, it cannot provide a

solution for parallel pipes and branch connections. These shortcomings can be stated as important limitations of the program to be added in the future.

The program can solve different transient flow scenarios containing various boundary conditions for pipes connected in series systems. These boundary conditions are upstream reservoir with constant or variable head, downstream reservoir with constant head, a valve at the downstream or in-line, downstream dead end, single centrifugal pump with or without a discharge valve, air chamber with orifice, simple surge tank and surge tank with a standpipe. The previous studies include more or fewer boundary conditions than the developed program. In order to compare these programs according to their boundary conditions, the comparison table shown in Table 6.3 can be observed.

Table 6.3 Comparison table for boundary conditions

<b>Boundary conditions</b>	<b>The Studies</b>			
	<b>Present Study</b>	<b>Koç (2007)</b>	<b>Dalgıç (2017)</b>	<b>Topraghaleh (2020)</b>
Upstream Reservoir	Yes	Yes	Yes	Yes
Downstream Reservoir	Yes	Yes	Yes	No
Downstream Valve	Yes	Yes	Yes	Yes
Valve In-line	Yes	Yes	Yes	No
Downstream Dead-end	Yes	Yes	Yes	Yes
Single Pump	Yes	Yes	Yes	Yes
Pumps Connected in Series or Parallel	No	Yes	Yes	No
Air Chamber with Orifice	Yes	Yes	Yes	No
Air Chamber with a Standpipe	No	No	Yes	No
Simple Surge Tank	Yes	Yes	Yes	Yes
Surge Tank with a Standpipe	Yes	No	Yes	No
Turbine	No	No	No	No

As shown in Table 6.3, the present study does not include air chamber with a standpipe, pumps connected in series or parallel, and turbine boundary conditions. In addition, other common boundary conditions, such as different types of valves, air valves, and different types of protection devices, are not included in the developed program.

In addition, there are several commercial computer programs to solve transient flow, such as Bentley Hammer and Wanda Transient. These programs were developed in very professional ways with great investments in a considerably long time. So, the developed program may not be considered as an equal alternative to these commercial programs at the current level. However, it is deemed that the present study is the right step in the right direction to generate an accurate and affordable local software handling fluid transient problems in pressurized pipe systems.

### **6.3 Recommendations**

The disadvantages and limitations of the program are mentioned in the previous section. As future objections, some important advice and improvements will be mentioned in this section.

The developed program can simulate steady and transient flow in pressurized pipeline systems. In future studies, solution methods for open channels can be added to the program. In addition, the ability of the complex pressurized hydraulic systems solution, such as pipe networks with branching connections or pipes connected in parallel, can be provided. Also, in the design stage of the systems, if the hydraulic system includes considerably more junctions, importing from AutoCAD option can also be added to the program. This feature can provide a more user-friendly program.

In addition, minor losses between the pipes and entrance losses are also provided in the present study. However, the verification of this feature is not provided in this thesis. In future studies, this feature can be verified with proper benchmarks.



In this stage, each elevation of the junction in the system can be entered as inputs with textboxes in junction properties panels. But this feature is not used in the calculations, and the verification of the program is not provided. For the hydraulic systems which have pipes with slopes, some improvements should be added to the program in the future.

The developed program used a quasi-steady friction model in the calculations. As an addition, various unsteady friction models can be added into the program to present more options in future works.

This program uses SI units. In order to provide a more user-friendly program, different units, such as U.S. Customary units, can be included in the program.

Lastly, additional boundary conditions, which are turbine, pumps connected in series or parallel, and other protection devices, can be added with their calculation methods to the program in future studies.



## **CHAPTER 7**

### **CONCLUSION**

In this study, a computer code has been developed that can solve different transient problems with various boundary conditions in pipe flows, as stated in its purpose. In the software program, the widely preferred method of characteristics (MOC) was used to analyze unsteady pipe flow. The applied solution and analysis process are discussed in detail in the relevant sections. The equations and solutions of some incorporated boundary conditions, which are commonly observed in transient flow examples, are used in the program. These boundary conditions can be listed as reservoir at the upstream with a constant head, reservoir at the upstream with variable head, reservoir at the downstream with a constant head, valve at the downstream, valve at an interior point, single pump, air chamber with orifice, simple surge tank, and surge tank with the standpipe.

Efforts were made to develop the computer program in such a way that it can run on any computer without requiring significant system requirements. In addition, this program can run without the use of an additional external program or application. Although it is designed as user-friendly software, a user's guide has been prepared so that this program can be used easily and more efficiently.

In this developed program, the results of calculated analyses based on various scenarios can be observed in graphical, tabular form or as graphical animation according to the selected nodes and time. The verification of the software was provided by comparing the results of some benchmark studies of the literature with those calculated by the software developed in the present study.

The software was coded to provide that the runtime of the computer for an investigated hydraulic system is as short as possible. However, it may increase due to the complexity of the hydraulic systems, or the reduction of the time increment

value in order to obtain more accurate results, or the system containing more components.

Although many features have been added to the program, it is realized that there is much room for further improvements in the future, and new additions can be applied to the code of the program. In future works about the presented topic, new boundary conditions may be added, such as different transient protection devices not included in the program, components such as turbines, different valves and the calculation methodology of more complex hydraulic pipeline systems such as pipe networks and branching pipelines. In addition, an advanced topography logic that can be used in calculations, importing from AutoCAD options for large-scale systems, different friction models used in calculations, and U.S. Customary units as an extra option can be added to the program in future studies.

Even though the program developed in the present study has many limitations compared to the expensive commercial software programs developed abroad, it may be considered as a right step in obtaining an ultimate domestic, cheap and user-friendly alternative in the near future.

## REFERENCES

- Adamkowski, A. (2001). Case Study: Lapino Powerplant Penstock Failure. *Journal of Hydraulic Engineering*, 127(7), 547–555.
- Afshar, M. H., & Rohani, M. (2008). Water hammer simulation by implicit method of characteristic. *International Journal of Pressure Vessels and Piping*, 85(12), 851–859. <https://doi.org/10.1016/J.IJPVP.2008.08.006>
- Bozkuş, Z. (2008). Water hammer Analyses of Çamlidere-Ivedik Water Treatment Plant (IWTP) Pipeline. *Teknik Dergi*, 19(2), 4409–4422. <https://www.researchgate.net/publication/228762757>
- Calamak, M., & Bozkuş, Z. (2012). Protective Measures against Waterhammer in Run of River Hydropower Plants. *Teknik Dergi*, 23(4), 6187–6202.
- Chaudhry, M. H. (1979). *Applied Hydraulic Transients* (First Edition). Van Nostrand Reinhold, Michigan University
- Chaudhry, M. H. (2014). *Applied hydraulic transients* (Third Edition) (Vol. 415). New York: Springer.
- Cofcof, Ş. (2011). *Denge Bacaları*. Dolsar Müh. Ltd. Şti.
- Dalgıç, H. (2017). *Development of a Computer Code to Analyse Fluid Transients in Pressurized Pipe Systems* [Master's Thesis]. Middle East Technical University.
- Dinçer, A. E. (2013). *Investigation of Waterhammer Problems in the Penstocks of Pumped-Storage Power Plants* [Master's Thesis]. Middle East Technical University.
- Dinçer, A. E., & Bozkuş, Z. (2016). Investigation of Waterhammer Problems in Wind-Hydro Hybrid Power Plants. *Arabian Journal for Science and Engineering*, 41(12), 4787–4798. <https://doi.org/10.1007/s13369-016-2142-2>

- Dursun, S. (2013). *Numerical Investigation of Protection Measures against Water Hammer in the Yeşilvadi Hydropower Plant* [Master's Thesis]. Middle East Technical University.
- Forchheimer, P. (1901) *Wasserbewegung durch Boden*. 45th Edition, Zeitschrift des Vereins deutscher Ingenieure, Düsseldorf.
- Ismaier, A., & Schlücker, E. (2009). Fluid dynamic interaction between water hammer and centrifugal pumps. *Nuclear Engineering and Design*, 239(12), 3151–3154. <https://doi.org/10.1016/J.NUCENGDES.2009.08.028>
- Izquierdo, J., & Iglesias, P. L. (2002). Mathematical modelling of hydraulic transients in simple systems. *Mathematical and Computer Modelling*, 35(7–8), 801–812. [https://doi.org/10.1016/S0895-7177\(02\)00051-1](https://doi.org/10.1016/S0895-7177(02)00051-1)
- Jaeger, C. (1956). *Engineering fluid mechanics* (No. 627 J34). Blackie.
- Karney, B. W. (1984). *Analysis of Fluid Transients in Large Distribution Networks*. University of British Columbia.
- Koç, G. (2007). *Simulation of Flow Transients in Liquid Pipeline Systems* [Master's Thesis]. Middle East Technical University.
- Lupa, S. I., Gagnon, M., Muntean, S., & Abdul-Nour, G. (2022). The Impact of Water Hammer on Hydraulic Power Units. In *Energies* (Vol. 15, Issue 4). MDPI. <https://doi.org/10.3390/en15041526>
- Parmakian, J. (1963). *Water Hammer Analysis*. Dover Publication, New York.
- Riasi, A., Raisee, M., & Nourbakhsh, A. (2010). Simulation of Transient Flow in Hydroelectric Power Plants Using Unsteady Friction. *Journal of Mechanical Engineering*, 56(6), 377–384.
- Saikia, M. das, & Sarma, A. K. (2006). Simulation of Water Hammer Flows with Unsteady Friction Factor. *ARP Journal of Engineering and Applied Sciences*, 1(4).

- Seleznev, V. S., Liseikin, A. v., Bryksin, A. A., & Gromyko, P. v. (2014). What caused the accident at the sayano-Shushenskaya hydroelectric power plant (SSHPP): A seismologist's point of view. In *Seismological Research Letters* (Vol. 85, Issue 4, pp. 817–824). Seismological Society of America.  
<https://doi.org/10.1785/0220130163>
- Swamee P.K., Jain A.K. (1976). Explicit equations for pipe flow problems, *J.Hydraul.Eng. ASCE*, Vol. 102, No. 5, pp. 657-664.
- Thorley, A.R.D. (1991). *Fluid Transients in Pipeline Systems*. D. & L. George Ltd Publ., Herts, UK.
- Thorley, D. (2004). *Fluid Transients in Pipeline Systems* (Second Edition). Professional Engineering Publishing Limited, London and Bury St Edmunds.
- Topraghaleh, S. H. (2020). *Software Development for Analyzing Fluid Transients In Pipelines* [Master's Thesis]. Middle East Technical University.
- Wiggert, D. C. (1984). Single Pipeline Water Hammer Program. *Michigan State University*.
- Wood, D. J., Lingireddy, S., Boulos, P. F., Karney, B. W., & McPherson, D. L. (2005). Numerical methods for modeling transient flow in distribution systems. *Journal / American Water Works Association*, 97(7), 104–115.  
<https://doi.org/10.1002/J.1551-8833.2005.TB10936.X>
- Wood, F. M. (1970). History of water-hammer. *C.E. Research Rep. No. 65*, Dept. of Civil Engineering, Queen's Univ. at Kingston, Ontario, Canada
- Wylie, E. B., & Streeter, V. L. (1967). *Hydraulic transients*. McGraw-hill.
- Wylie, E. B., & Streeter, V. L. (1978). *Fluid transients*. McGraw-Hill Int. Book Co. New York <https://doi.org/10.1115/1.3448743>
- Wylie, E. B., Streeter, V. L., & Suo, L. (1993). *Fluid transients in systems* (Vol. 1, p. 464). Englewood Cliffs, NJ: Prentice Hall.





## APPENDICES

### A. USER GUIDE

In this section, the use of the software will be explained step by step with the simulation of a sample study for users. This study is an example of a pump failure case (Wiggert, 1984). The instructions are listed as follows.

1. Open the software application.
2. The file tab appears in the opening interface of the program. Press the new project button on this tab. On the window that appears on the screen, enter the project's name, and select a location where you want to save the project.

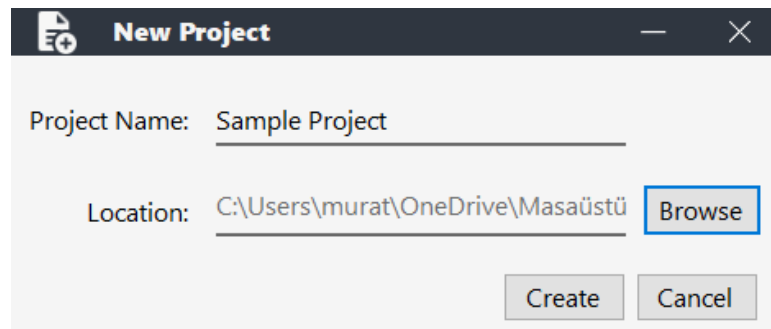


Figure A.1 New project dialog window

3. After creating the file of the project, go to the design tab. In this tab, there are buttons where you can model your hydraulic system by drawing components on the canvas area.

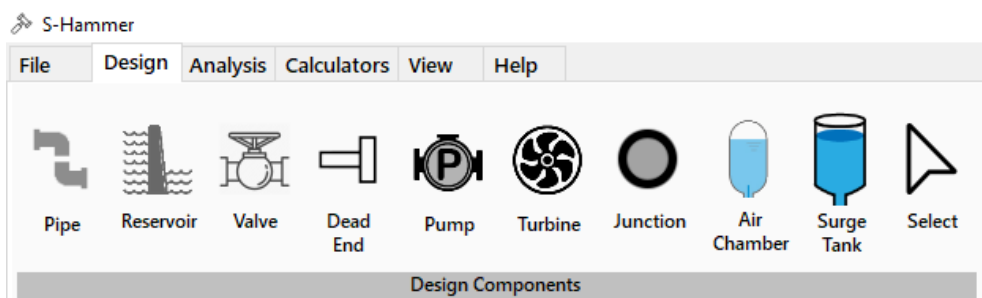


Figure A.2 The design component buttons

4. Draw your hydraulic system on canvas using the component buttons.

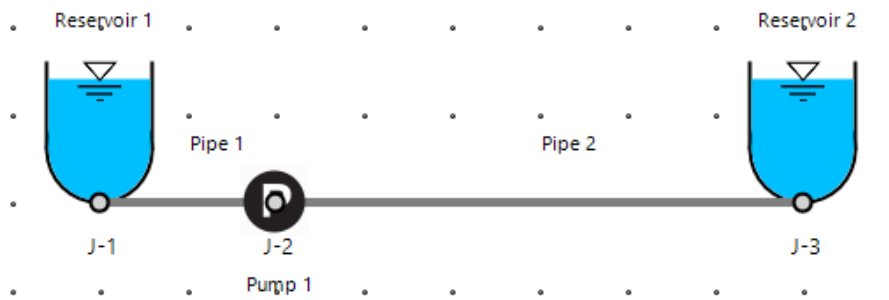


Figure A.3 A sample system drawn in the program

In the sample study, there are two pipes, a pump, and two reservoirs, which are located at the upstream and downstream ends of the system. Note that the appearance of the canvas, such as color and grid type options, can be edited with the related buttons located in the view tab.

5. Enter the properties of the reservoir and pipe components in the corresponding properties panels. The properties panels are pop-up windows that appear when an item is selected on the canvas area.

In this study, the water level elevation of the upstream reservoir was taken as a datum. So, the elevation properties of the upstream reservoir must be inserted as zero. The water height and the base elevation of the downstream reservoir are added to the system in Figure A.4.

When users add a reservoir component to the system, the reservoir type is automatically selected as “Upstream” in the reservoir properties panel. For this reason, in the properties panel of the downstream reservoir, users must select the reservoir type as “Downstream”.

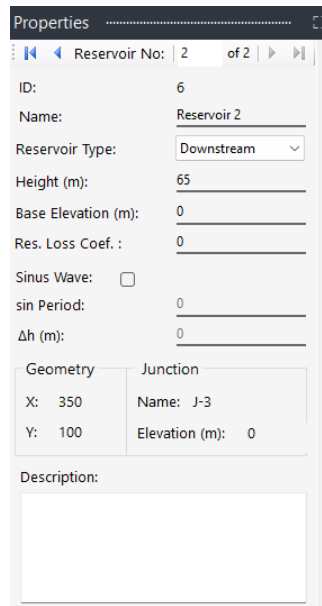


Figure A.4 Properties of the downstream reservoir

The properties of the second pipe can be entered as shown in Figure A.5. The first pipe is used as a connection pipe with a one-meter length. The other data of the first pipe can be entered as similar to the second pipe.

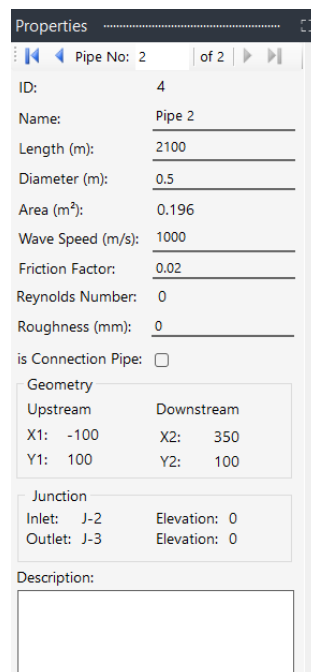


Figure A.5 Properties of the 2<sup>nd</sup> pipe

- Click on the “Pump Settings” button in the design tab. Then, click the “Add New” button to create a pump setting data set for the pump used in the system. Enter the rated head, discharge, speed, and torque values. Next, select a pump characteristics curve (Suter Curve) data. In the program, three different pump characteristics curve data are defined. Instead of choosing default pump characteristics curve data which already exist in the program, user-defined curve data can be imported from an excel file. Then, enter a name for this pump data set. After the whole data are entered or selected, and the name is defined, click on the “OK” button to save the data set.

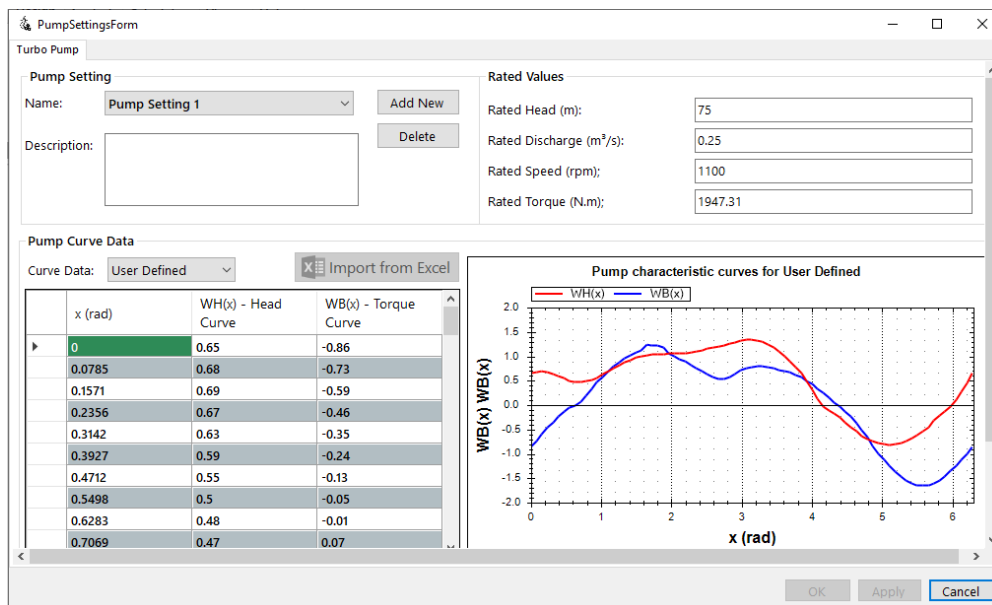


Figure A.6 Pump setting window

- Enter the properties of the pump component into the pump properties panel as shown in Figure A.7. Do not forget to select the name of the saved pump setting in the pump setting selection box which is located in the properties panel.

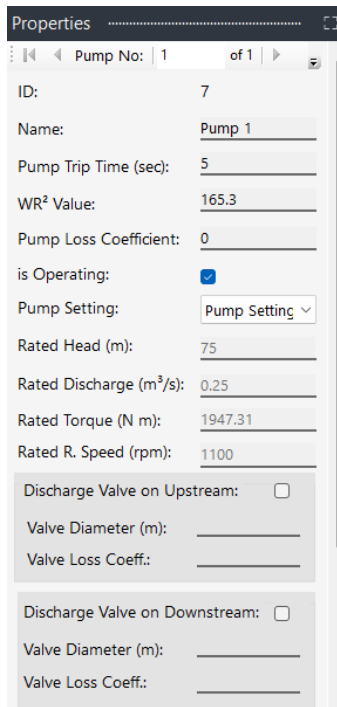


Figure A.7 Properties of the pump component

8. Click on the initial conditions button located in the design tab. Then, enter the maximum simulation time and time increment values. The time increment value must be selected as equal to or smaller than the maximum allowable time step value to satisfy the Courant condition, as shown in Figure A.8.

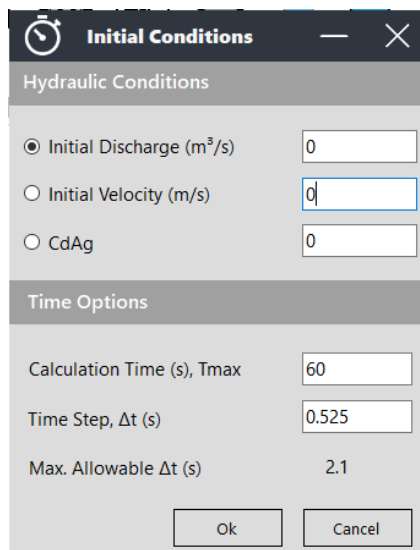


Figure A.8 Initial conditions window and selected time options for the case

It must be mentioned that if there is a valve, the closure data can be entered on the valve closure settings window located in the design tab.

- Next, go to the analysis tab and click on “Compute for Steady-State” button. After the analyses are finished, the steady-state results of the system are presented in a window as shown in Figure A.9.

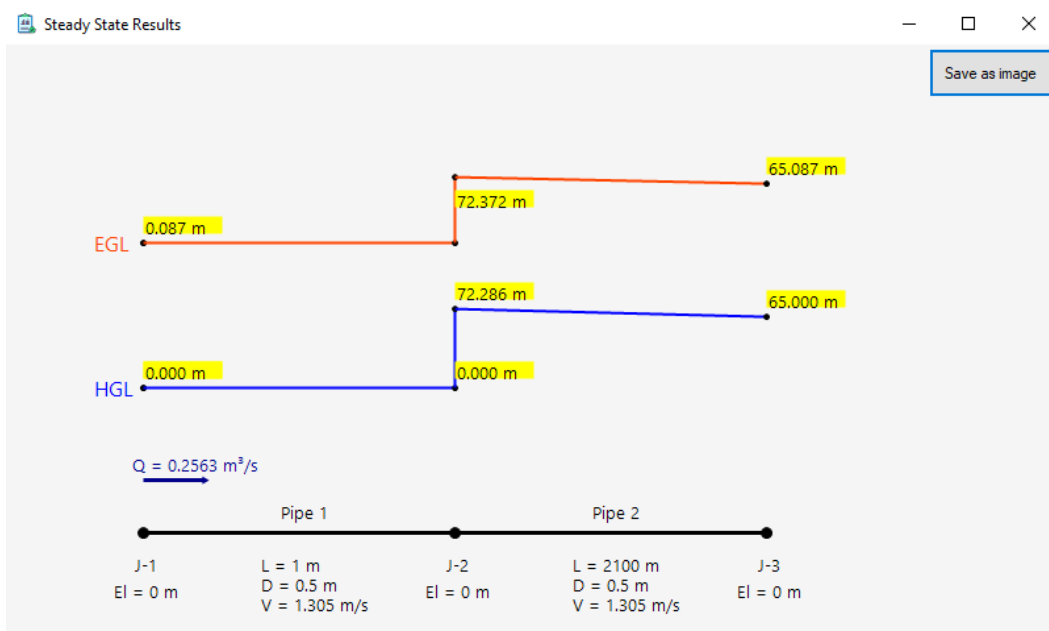


Figure A.9 The steady-state results window

- In the next step, click on “Compute for Transient” button. After the transient analyses are done, a message appears on the screen to inform the user, as shown in Figure A.10.

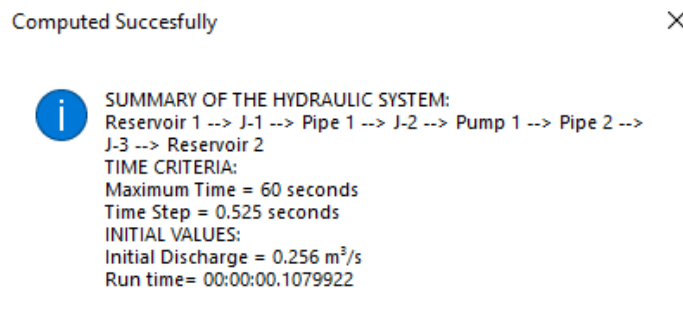


Figure A.10 The informative pop-up window

In the analysis tab, tables, time charts, and animation charts buttons become enabled after the computation process is finished.

- Click on the “Tables” button located in the analysis tab to observe the results in tabular form. First, select the tabular data type you want to observe in the window that appears. Data can be observed as time-based, pipe-based, and junction-based, as shown in Figure A.11. The “Show Table” button creates tables according to the selected data type with a precision value chosen by the user. The created tables can be exported to an excel file.

	Time (sec)	Object Name	Side	Distance from Reservoir (m)	Head (m)	Discharge (m <sup>3</sup> /s)	Velocity (m/s)	Pressure (KPa)
▶	0.00	J-2	Downstream	1	72.29	0.26	1.31	709.45
	0.53	J-2	Downstream	1	72.29	0.26	1.31	709.45
	1.05	J-2	Downstream	1	72.29	0.26	1.31	709.45
	1.58	J-2	Downstream	1	72.29	0.26	1.31	709.45
	2.10	J-2	Downstream	1	72.29	0.26	1.31	709.5
	2.63	J-2	Downstream	1	72.29	0.26	1.31	709.45
	3.15	J-2	Downstream	1	72.29	0.26	1.31	709.45
	3.68	J-2	Downstream	1	72.29	0.26	1.31	709.45
	4.20	J-2	Downstream	1	72.29	0.26	1.31	709.45
	4.73	J-2	Downstream	1	72.29	0.26	1.31	709.45
	5.25	J-2	Downstream	1	26.75	0.17	0.86	262.54
	5.78	J-2	Downstream	1	11.45	0.14	0.71	112.34
	6.30	J-2	Downstream	1	4.15	0.13	0.65	40.74
	6.83	J-2	Downstream	1	0.64	0.12	0.61	6.31
	7.35	J-2	Downstream	1	-1.2	0.12	0.61	-11.79
	7.88	J-2	Downstream	1	-2.04	0.12	0.6	-19.98
	8.40	J-2	Downstream	1	-2.68	0.12	0.61	-26.3
	8.93	J-2	Downstream	1	-3.05	0.12	0.61	-29.98
	9.45	J-2	Downstream	1	4.56	-0.03	-0.15	44.75
	9.98	J-2	Downstream	1	9.29	-0.08	-0.39	91.13
	10.50	J-2	Downstream	1	11.86	-0.1	-0.48	116.36

Figure A.11 An example for the results of the case in the tables window

- Click on the “Time Charts” button located in the analysis tab. Select the chart type, and location for the case study. The location can be selected as a pipe node or a junction. Then, click on the “Add Primary Chart” button.

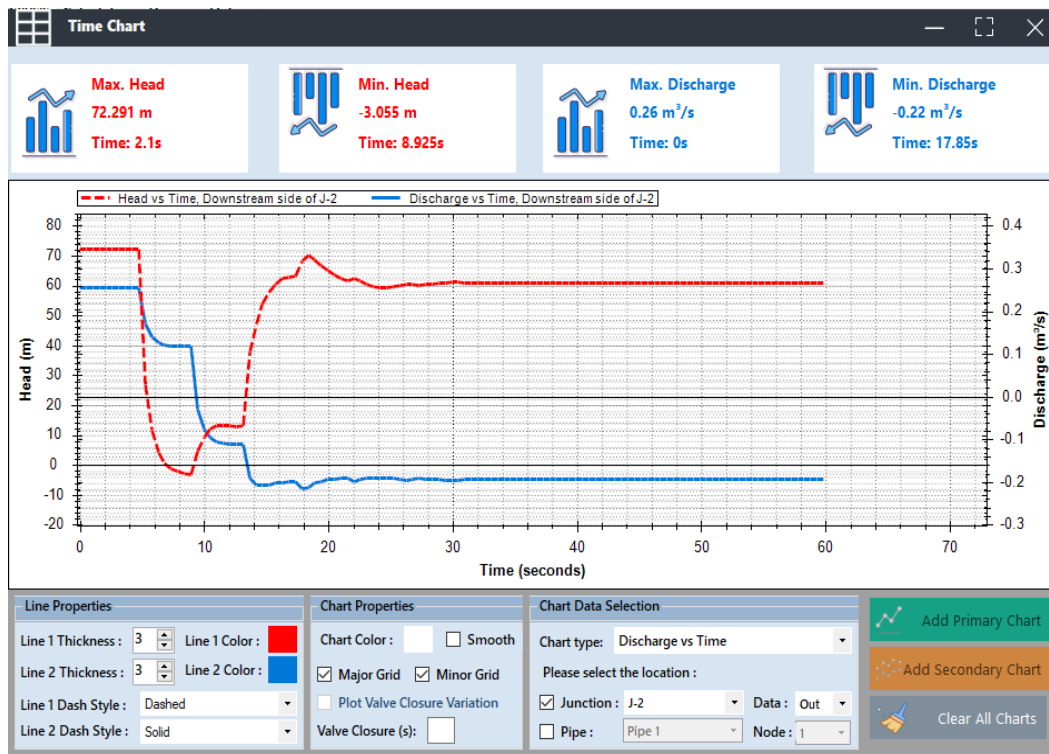


Figure A.12 An example for the results of the case in the time chart window

A different chart can be added to the drawn chart with a new y-axis by using “Add Secondary Chart” button. In addition, the visual properties can be edited for the chart and lines, as shown in Figure A.12. The color of the chart, the color of lines, the thickness, and the dash style of the lines can be changed as desired by the user.

A list of options appears when the user clicks the right button of the mouse on any area in the graphics area. This list includes useful options such as zooming, showing point values, and saving the chart as a picture.

13. Click on the “Animation Charts” button located in the analysis tab. Then add lines of the maximum envelope, minimum envelope, steady state hydraulic grad line, and pipeline profiles as shown in Figure A.13. Next, press the play button. Thus, head values that change depending on distance and time can be observed with animation. The time increment speed can be changed as desired.



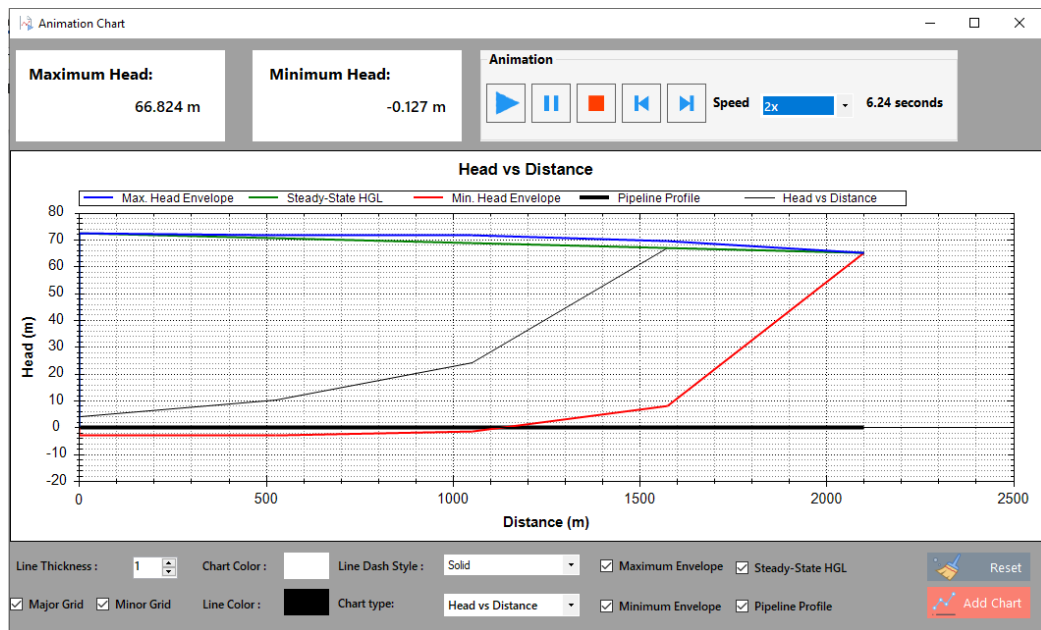


Figure A.13 Animation chart for the case study

In this window, users can observe the maximum and minimum head values on the hydraulic system for each time value. In addition, the chart type can be changed by the user. For example, users can observe the discharge values that vary depending on distance and time with the animation.

14. Lastly, in order to keep the data, the project can be saved by the user. To save the project, go to the file tab and click on the “Save” or “Save As” buttons.